Geochemical evidence for basement control of the west Cumberland haematite mineralization

Thomas J. Shepherd

GEOCHEMICAL EVIDENCE FOR BASEMENT CONTROL OF THE WEST CUMBERLAND HAEMATITE MINERALIZATION

by

THOMAS J. SHEPHERD, B.Sc.

Thesis submitted to the University of Durham for the degree of Doctory of Philosophy.

September 1973

ABSTRACT

GEOCHEMICAL EVIDENCE FOR BASEMENT CONTROL OF THE WEST CUMBERLAND HAEMATITE MINERALIZATION

T. J. SHEPHERD. 1973

A geochemical investigation of the West Cumberland metasomatic haematite deposits and related vein deposits in the central Lake District was carried out to establish the origin of the mineralizing fluids. Ore samples were analysed for a variety of major and trace elements and were found to contain a simple geochemical assemblage characterised by the abundance of arsenic and locally barium. The lack of regional variation in ore geochemistry and the equally uniform mineralogy suggests that the replacement and vein deposits are cogenetic and belong to the same metallogenic province. Minor differences which do exist can be explained by wallrock - ore fluid interactions.

In the Eskdale area the veins are associated with a particular phase of the host granite containing an abundance of free haematite. Relative trace element enrichments in the ores are matched by sympathetic depletions in the adjacent haematized granite. The implied geochemical relationship is verified by a spatial correlation between areas of mineralization and the distribution of concealed granite in the basement; as indicated by the gravity pattern. A more detailed gravity interpretation in the West Cumberland area shows that the zone of maximum mineralization in the limestones occurs directly above the faulted margin of a concealed granite shelf extending outwards from the Ennerdale granophyre.

Based on the combined geological, geochemical and fluid inclusion evidence a new model of haematite ore genesis is proposed which envisages the convective circulation of hot saline brines in the granite basement with the concomitant leaching of iron and its redeposition at higher levels as epigenetic haematite mineralization. The hypothesis is consistent with the known distribution of orebodies and the observed spatial variation for arsenic and copper in the West Cumberland orefield. Baritic ores are related to the mixing of the ore fluids with formational waters from the Permo-Triassics.

CONTENTS

ILLUSTRATIONS

1. INTRODUCTION

1.1. Research Objectives

The primary objective of the present study was to investigate the geochemical characteristics of haematite deposits in the West Cumberland orefield to determine their origin and spatial variation. As early as 1893 Kendall had successfully proved the metasomatic nature of orebodies in the Carboniferous limestones, but geologists have since been unable to define the genesis or chemistry of the ore fluids. Present theories, often based on geological observations in restricted areas, have provided a wealth of conflicting information. To avoid making the same error it was realised that the geochemistry must be interpreted in conjunction with existing evidence and that the proposed mechanism must also account for similar mineralization in the Lower Palaeozoics east of the orefield. By studying the geochemistry of ores throughout this extended area it was hoped to provide a model of the mineralization which would explain the origin, nature and extensive development of epigenetic haematite in the Lake District. This work represents the first geochemical study of the Cumbrian haematites to be undertaken and has meant a reinterpretation of certain mineralogical observations recorded by earlier investigations. To verify the geochemical hypothesis a series of two-dimensional models of the basement structure were calculated for the gravity anomaly over the West Cumberland orefield. In the following chapters the results of these investigations are presented and a new theory of ore genesis is developed which relates the spatial, temporal and chemical characteristics of the mineralization to the dynamic evolution of the basement during the late

Palaeozoic and early Mesozoic. By providing a working hypothesis it was hoped that future exploration for concealed orebodies would be based on geological criteria and less dependent on expensive pattern drilling.

1.2. Previous Theories of Mineralization

Previous theories although generally lacking in quantitative evidence are unrivalled for their variety and imagination. However, after Kendall's irrefutable proof that the majority of orebodies in the Lower Carboniferous limestones were the result of selective metasomatic replacement (Kendall 1893), theories on ore genesis have been divided into two opposing schools. The "ascensionists" supported by McDonald (1925), Dixon (1927), Trotter (1945) and Schnellmann (1947) propose ascending iron-rich fluids of deep seated magmatic origin. In contrast the "descensionists" championed by Goodchild (1889) and Smith (1924) envisage the downward movement of meteoric waters with the leaching of iron oxides from Tertiary lateritic soils or "red beds" in the N.R.S. Series. Differences within the schools are primarily differences in the chronology of faulting and mineralization, and the extent of lateral migration. The main points of these theories may be summarized as follows:

DESCENSIONISTS

Goodchild 1889

(i) Theory

Downward percolation of meteoric waters through the N.R.S. Series accompanied by selective leaching of the iron oxides with later deposition along faults and fissures in the Carboniferous limestones.

(ii) Age

Post-Triassic

(iii) Evidence

(a) Proximity of red Triassic sandstones to areas of haematization in the Carboniferous limestones.

(b) Occurrence of orebodies in limestones overlain by, or considered to have been overlain by N.R.S. series.

Smith, 1919, 1924 and 1927

(i) Theory

As for Goodchild

(ii) Age

As for Goodchild

(iii) Additional Evidence

(a) Powerful solvent action of groundwaters on chalk flints in the Lower Tertiary deposits of Kent.

(b) Disruption and dislocation of haematite flats by post-Triassic faulting in the Wyndham, Gillfoot and Clints mines.

ASCENSIONISTS

Kendall 1875, 1876, 1879, 1893, 1921 and 1929

(i) Theory

Vertical ascent of deep seated iron-rich magmatic fluids along deep faults in the western and central areas of the Lake District.

(ii) Age

Pre-Brockram

(iii) Evidence

(a) Presence of haematite deposits along faults in both the

Lower and Upper Palaeozoics.

(b) Complete chemical replacement of the limestone by haematite.

(c) Angular pebbles of haematite in the Brockram deposits of the Bigrigg opencut.

(d) Brecciation and dislocation of an orebody along a pre-Trias fault by post-Trias movement.

McDonald 1925

(i) Theory

Lateral migration of iron-rich vapours outwards from the Eskdale and Ennerdale granites during their intrusion, along a series of hypothetical radial faults into the reactive Carboniferous limestones. Also, allows for the mixing with groundwaters and recirculation along N-S and NW-SE faults.

(ii) Age

Post-Carboniferous

(iii) Additional Evidence

(a) Presence of haematite veins and disseminations throughout the exposed intrusives and along several of the inferred major channelways (e.g. Bleng River Fault).

Dixon 1927

(i) Theory

Ascent of iron-rich fluids from a deep seated unexposed magmatic source in the central Lake District along fractures in the Lowes-water Flags. Orebodies being formed where the limestones over-step the flags. Also allows for slight lateral migration by groundwater circulation.

(ii) Age

Post-Triassic

(iii) Additional Evidence

(a) The similarity between hydrothermal mineral zonation in Cornwall and the apparent partial peripheral distribution of haematite deposits around the lead-zinc veins of the central Lake District.

(b) Occurrence of economic orebodies in the Skiddaw Slate Series at Kelton Fell.

(c) Concentration of mineralization along NW-SE post-Triassic faults.

Trotter 1945

(i) Theory

Vertical ascent of iron-rich fluids from a deep-seated magmatic source in the central Lake District into a pre-denudation Brockram cover followed by downdip migration into areas underlain by Carboniferous limestones. The western limit of migration in the West Cumberland area being controlled by a lateral facies change in the Brockrams from permeable breccia-conglomerates to impervious shales.

(ii) Age

Post-Permian

(iii) Additional Evidence

(a) Association of specular haematite, fluorite, barite and chalcopyrite with the ores. (Interpreted as a typical hydrothermal assemblage).

(b) Occurrence of barites and haematite in the Brockrams and lower units of the St. Bees Sandstones south of Egremont.

(c) Apparent correlation between the westerly known limit of the West Cumberland orefield and the thickening of the St. Bees Shale.

Schnellmann 1947

(i) Theory

Vertical ascent of iron-rich hydrothermal fluids from a deep seated source into structural "highs" along faults and fissures.

(ii) Age

Post-Triassic

(iii) Additional Evidence

(a) Association of a silica - fluorite - dolomite - barite assemblage with the ores.

(b) Clustering of orebodies around an inferred anticlinal structure in the Egremont-Cleater Moor area.

It is clear that each theory refers to one or more important characteristics of the mineralization and is an adequate model when considered by its own criteria. Unfortunately no single theory appears to explain the evidence offered by alternative theories and thus exists only as a negative argument. This weakness can be attributed to four main causes:

(i) Attaching undue importance to observations in restricted areas, especially in the highly productive limestone belt.

(ii) Envisaging metallogenesis as a process unrelated to the geological evolution of the area.

(iii) Failure to recognise the possibility of spatial coincidence

between iron oxide-rich sedimentary sequences and iron oxide mineralization.

(iv) Misinterpretation of the gangue mineral assemblage.

These factors have tended to distract attention from the total environment of the mineralization and its place in the geological continuum. The author does not intend to discuss the "pros" and "cons" of individual theories and the reader is referred to the references given above. Instead it is intended to introduce relevant points into the discussion as the new theory of ore genesis is developed.

2. REGIONAL GEOLOGY

2.1. Introduction

Haematite mineralization as shown by the development of veins and metasomatic replacements of haematite, occurs throughout large areas of the western, central and southern parts of the Lake District. Unless these occurrences are dismissed as mere freaks of nature, their genesis must be related to the geological evolution of the region. The following chapter has therefore been written to provide a necessary geological framework for a new theory of mineralization which attempts to relate the genesis of the ores to the structural and geochemical nature of the basement.

2.2. General Geology

The Lake District is essentially a domed area, comprising a core of folded Ordovician-Silurian rocks surrounded by a girdle of relatively undeformed Carboniferous and Permo-Triassic sediments (Fig. 1). Passively intruded into the core are a group of post-orogenic Devonian granites surrounded by their respective thermal metamorphic aureoles.

On the western flank of the dome the peripheral rocks are strongly faulted and Triassic sandstones are brought into juxtaposition with major Ordovician elements of the core. The accepted stratigraphical succession shown in Table 1 is broken by a series of strong unconformities, each marking a prolonged period of denudation.

(i) Skiddaw Slate Series

These represent the oldest known rocks in the Lake District and consist of a thick sequence of greywackes, siltstones and pelites laid down under geosynclinal conditions and subjected to the full deformational forces of the Caledonian orogeny.

FIGURE 1

GEOLOGY OF THE LAKE DISTRICT

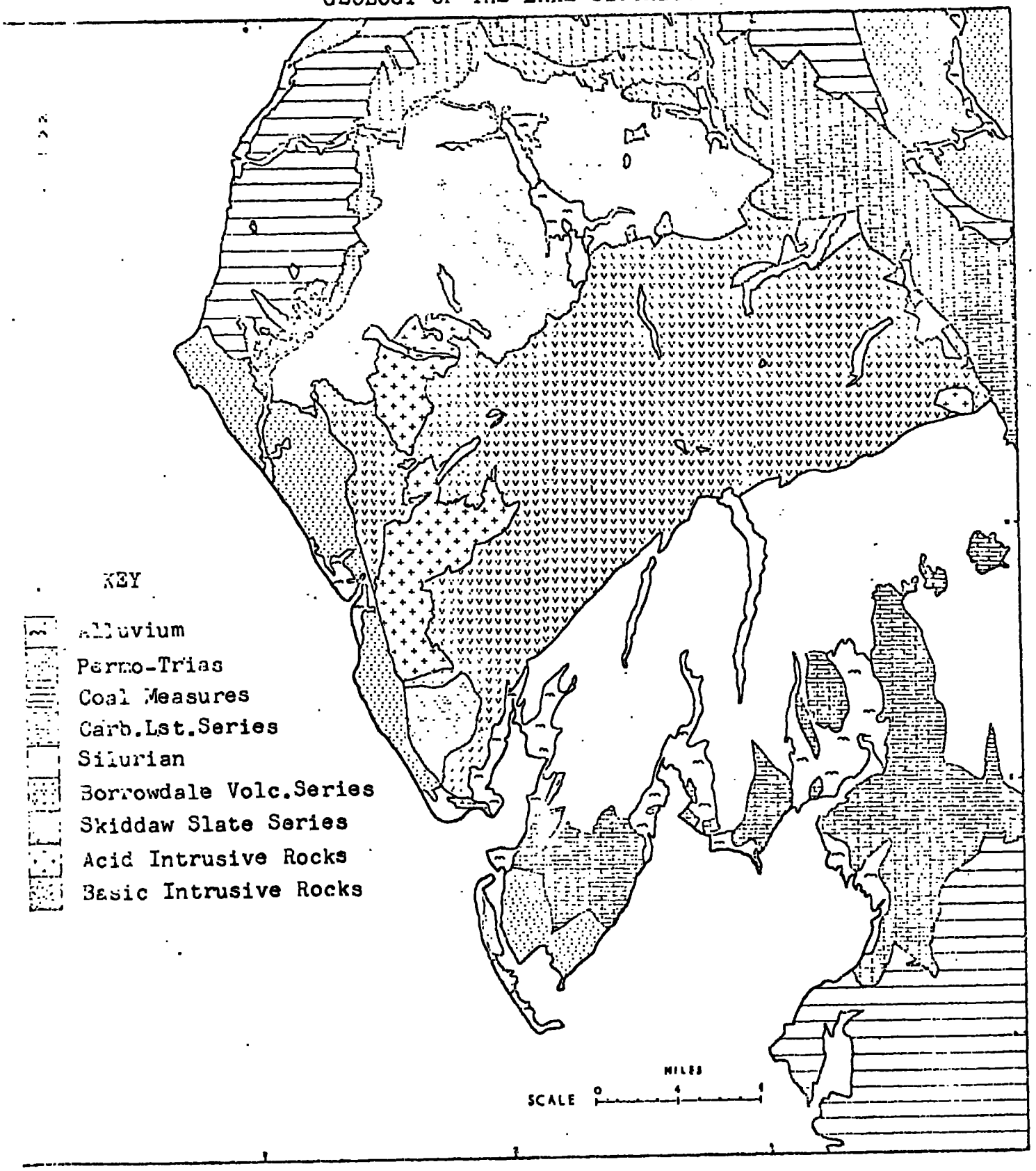

TABLE 1

GENERALISED GEOLOGICAL SUCCESSION
FOR THE LAKE DISTRICT

Period	Formation	Thickness (feet)
Permo-Triassic	(St. Bees Sandstone	+3000
	(St. Bees Shales	0-250
	(Magnesian Limestone	0-18
	(Brockrams	0-450
	Unconformity	
Upper Carboniferous	(Coal Measure Series	
	(Millstone Grit Series	50-200
Lower Carboniferous	(Hensingham Group	60-1600
	(Carboniferous Limestone Group	700
	Unconformity	
*		
Silurian	(Ludlow Series	12000
	(Wenlock Series	1000
	(Llandovery Series	250
Upper Ordovician	(Ashgill Series	100
	(Coniston Limestone Series	150-1100
	Unconformity	
Lower Ordovician	Borrowdale Volcanic Series	
	Skiddaw Slate Series	+2500

(* Devonian absent from the succession except in the Ullswater area - ? Mell Fell Conglomerate.)

(ii) Borrowdale Volcanic Series

The Borrowdale Volcanic Series lie directly above the Skiddaw Slate Series and constitute a volcanic pile of calc-alkaline lavas and tuffs; the junction between the two remaining a controversial stratigraphical problem (i.e. conformable or unconformable).

(iii) Upper Ordovician and Silurian Sediments

These rest with classic unconformity on the Borrowdale volcanics and pass lithologically from shallow water limestones and shales of a shelf facies, upwards into deeper water mudstones siltstones, and shales of a geosynclinal turbidite facies.

(iv) Carboniferous Limestone Group

Forming the innermost zone of the Upper Palaeozoic girdle, the Lower Carboniferous rocks lie discordantly on Ordovician-Silurian strata and in the Ullswater-Haweswater area can be seen to overstep all three units of the core. The lowermost beds, known as the Carboniferous Limestone Series, consist of a regular alternating succession of limestones and shales. Seven massive limestones have been identified and are numbered one to seven in downward sequence.

(v) Hensingham Group

Originally included in the younger Millstone Grit Series they are now known to contain a Lower Carboniferous limestone fauna and have been separated accordingly. Predominantly sandstones and shale with subordinate limestone they are best developed in the Whitehaven area and pass without break into the Millstone Grit Series.

(vi) Millstone Grit Series and Coal Measures

The Millstone Grit Series comprising flaggy sandstones, coarse

feldspathic grits and shales is succeeded conformably by the Coal Measures, a thick alternating sequence of shales, fireclays, productive coal seams and sandstones.

(viii) Brockram, Magnesian Limestone and St. Bees Shales

These may be grouped together because collectively they form the base of the Permo-Triassic succession. The Brockrams are coarse breccia-conglomerates and provide the type basal facies for most of the region. In West Cumberland however they pass laterally westwards into the Magnesian Limestone and St. Bees Shales; a lithological transition related to the proximity of the area to the margin of a deep Permo-Triassic basin now concealed beneath the eastern Irish Sea. Elsewhere the Brockrams are succeeded by their lateral equivalents. At Egremont the Brockrams rest directly on Borrowdale volcanics, having completely transgressed the intervening Carboniferous succession.

(viii) St. Bees Sandstone

This formation follows on from the St. Bees Shales without break and consists of a series of well bedded red sandstones of unknown thickness (+ 3000 ft.). The red coloration is due to the presence of finely divided intergranular haematite and is considered by some geologists as a possible source of iron for the local haematite deposits (Goodchild 1889 and Smith 1924).

(ix) Igneous Rocks

Excluding dykes and other minor intrusives, igneous intrusions are found only in the Lower Palaeozoic core of the dome. The five largest intrusions are the Shap, Skiddaw and Eskdale granites, the Ennerdale granophyre and the Carrock Fell gabbro complex. Of these, the granite

intrusives were passively emplaced during the early Devonian, and post-date the late Silurian deformation of the Caledonian orogeny. Thermal metamorphism is greatest around the Skiddaw granite but areas of static hornfels and contact alteration have been mapped around each of the other intrusions. Epidotization (calcium metasomatism) is also well developed in areas where Borrowdale volcanics form the country rocks.

For a more detailed description of the regional geology, papers by Mitchell (1956) and Hollingsworth (1955) provide excellent precis.

2.3. Structure

The dominant structural element of the Lake District is a complex Caledonian anticline "Lake District Anticline" trending NE-SW through Buttermere and Skiddaw. It was formed during the late Silurian and divides the outcrop of the Borrowdale volcanics into northern and southern zones. Within this structure the tight isoclinal folds of the Skiddaw Slate Series contrast sharply with the more open folds of the Borrowdale Volcanic Series. Some workers attribute this feature to differential competancy of the strata during a single phase of deformation (Soper 1970) whilst others assert that the Skiddaw slates underwent polyphase deformation prior to the deposition of the volcanics (Simpson 1968).

Caledonian faults are difficult to recognise because there is little stratigraphic evidence to provide a pre-Hercynian time marker. Firman (1960) and Clark (1963) both working independently agree that Caledonian faulting in the Lake District is represented by conjugate sets of high angle NW and NE trending wrench faults which suffered later vertical movement.

The ensuing Hercynian orogeny produced only minor flexuring of the strata and was essentially a period of block movement accompanied by

strong faulting. New fault patterns were established but many earlier lines of weakness were reactivated. Moseley (1967) records a similarity in trend between joints and faults in the Carboniferous and Triassic sediments and suggests that post-Caledonian structures in the north of England share a common inheritance.

The girdle of Carboniferous/Permo-Triassic sediments is disrupted by a multitude of pre-Triassic and post-Triassic faults. The former set is best developed in West Cumberland where it is represented by a series of NE-SW structures throwing Coal Measures against Lower Carboniferous limestones. Although more widespread the second set is characterised by a series of major NW-SE faults which parallel the margins of the main Permo-Triassic basins. In West Cumberland the largest of these faults is the Boundary Fault which throws Triassic sandstones against the Skiddaw Slate Series and Eskdale Granite.

2.4. Eskdale and Ennerdale Intrusives

In view of their suspected role in the genesis and distribution of the haematite ores a separate section has been included to describe their main features more fully. The Eskdale granite and Ennerdale granophyre form the largest of the exposed Devonian intrusives and cover an area of 84 square miles (Fig. 1). Both are composite bodies in which the individual units are petrologically dissimilar but petrogenetically related. This relationship is clearly demonstrated by the nature of the regional gravity pattern, the details of which are described in chapter 6 and appendix I. They are also extensively mineralized and compared to other Lower Palaeozoic strata carrying a greater number of discrete vein

deposits. Parts of the Eskdale granite, especially along the Eskdale valley, are pervaded by a network of haematite veinlets and disseminations, and almost every joint plane is coated with haematite.

Recent work by Clark (1963), Firman (1953) and Oliver (1961) has done much to clarify the geological setting of the intrusives and their observations have provided additional evidence in support of the present study.

2.4.1. Petrology of the Intrusives

(i) Eskdale granite

The Eskdale granite is a stock-like body, intruded into the Borrowdale Volcanic Series and surrounded by a narrow thermal metamorphic aureole. According to Simpson (1934) three types of granite can be recognised: a Pink type, a Green type and a Grey type. The Pink type occupies the northern area of the intrusive and is a coarse-grained muscovite - biotite granite. The Green type is confined to patches within the Pink and has a slightly higher content of biotite and orthoclase. Contrary to Simpson's classification the Survey do not recognise this distinction and consider the Green to be merely a local variation of the Pink. The Grey type occupies the southern area of the granite and is a medium-grained granodiorite containing a higher percentage of biotite and plagioclase.

Late stage alteration is represented by deuteric sericitization, chloritization and minor greisenization, and effects most of the granite. Feldspar seriticization is ubiquitous, especially in areas of the Pink granite, where the degree of alteration varies from a few flakes of sericite along cleavage planes to completely sericitized masses. Chloritization of the biotites is also widespread and in the Pink variety very little of the original

dark brown biotite now remains. Both processes were accompanied by a redistribution of the iron and an explusion of included iron oxides into intergranular areas.

The author believes however that in general the iron was not completely lost from the system but precipitated locally as haematite in microfractures, fissures, joints and faults in adjacent areas of granite. This would account for the close association between areas of haematized granite and areas of strong alteration. The end product of complete alteration is probably represented by the equigranular quartz-sericite rock at Water Crag where the iron has been removed beyond the zone of alteration:

biotite		chlorite		sericite
feldspar	⟶	feldspar	⟶	quartz
quartz		sericite		muscovite
		quartz		

Griesenization is restricted to the immediate vicinity of Devoke Water and here the granite has been partially converted to a quartz-topaz rock with minor fluorite. Apart from the fluorite occurrences at Beckfoot Quarry, fluorine pneumatolysis is very localised. (c.f. restricted distribution of fluorite in the West Cumberland orefield.) At present there is no evidence for the age of the deuteric alteration orgreisenization and one can only presume that they were a manifestation of the final consolidation of the granite.

(ii) Ennerdale granophyre

The Ennerdale granophyre is intruded into the Lower Palaeozoics along the NE-SW Skiddaw slate - Borrowdale volcanic junction but is elongated north-south. Although not completely unroofed, the exposed

sections show that 80% of the mass consists of granophyre and subordinate porphyritic microgranite. Petrographically the granophyre consists of feldspar phenocrysts in a fine-grained micrographic quartz-feldspar matrix with irregular clots of biotite and iron oxides. Deuteric alteration is weaker than in the Eskdale granite.

Irrespective of the controversial field evidence, K-Ar age dating indicates that both the Ennerdale and Eskdale intrusives were emplaced in a relatively short space of time (Brown et al. 1964).

2.4.2. Thermal Metamorphism of the Country Rocks

Surrounding the intrusions there are aureoles of thermal metamorphism which vary from a few hundred feet to several miles in width. The effect on the country rocks is greatest in the Borrowdale Volcanic Series where there is a conspicuous development of biotite and wispy amphibole. On the eastern side of the granite the biotite aureole is only 600-900 feet wide but this gradually increases to 2 miles in the northeast and is completely continuous between Burnmoor Tarn and the Wasdale Head inlier. Around the eastern and southern margins of the granophyre the biotite zone is over 1 mile in width and though not proven probably merges with the granite aureole.

In contrast the Skiddaw slates adjacent to the intrusives are converted into felsitic hornfels, passing outwards into hardened unlaminated slates. On the western side of the granophyre the aureole is 3 miles in width but elsewhere is limited to several hundred yards. Clark attributes this difference to structural anisotropism related to the strike of the Caledonian cleavage. However, a more realistic explanation

for the observed variation in width is provided by the concealed extensions of the granophyre and granite.

2.4.3. Metasomatism of the Country Rocks

Superimposed and extending beyond the biotite aureole various workers have recognised a zone of epidotization in the Borrowdale volcanics which decreases outwards from the igneous contacts. In the Gosforth area, Rose (1937) records widespread epidotization of the andesite lavas between the Boundary Fault and the granophyre. Similarly, Firman (1953) describes strong epidote metasomatism in the Border End, Kepple Crag, Harter Fell and Wrynose areas. Further north, Oliver (1961) describes a system of interpenetrating epidosite veins and porphyritic masses within an extensive region of epidotization in the Scafell-Esk Pike-Long Pike area which he interpretes as a genetic link with the Eskdale granite. Elsewhere similar alteration has always been regarded as lava autometasomatism because of an absence of local igneous bodies. Unpublished work by Fitton (pers. comm. 1970) indicates that the zone of epidotization extends even into the Langdale and Grasmere areas. This is entirely consistent with the inferred position of the concealed Eskdale granite as defined by the granite bouguer anomaly. Figure 2 shows the recorded distribution of epidote metasomatism together with the occurrence of haematite veins superimposed upon the simplified bouguer anomaly for the central Lake District. The marked geometrical similarity between these three patterns suggests that the basement granites are an important factor in the genesis of the haematite mineralization.

As a final comment, the author believes that the calcium metasomatism is related to the sericitization of the plagioclase feldspars in the granite by the reaction:

$$\text{Albite-Oligoclase} \longrightarrow \text{Sericite} + (Ca^{++})\uparrow$$

FIGURE 2

SIMPLIFIED GRAVITY PATTERN AND HAEMATITE VEIN DISTRIBUTION FOR THE LAKE DISTRICT

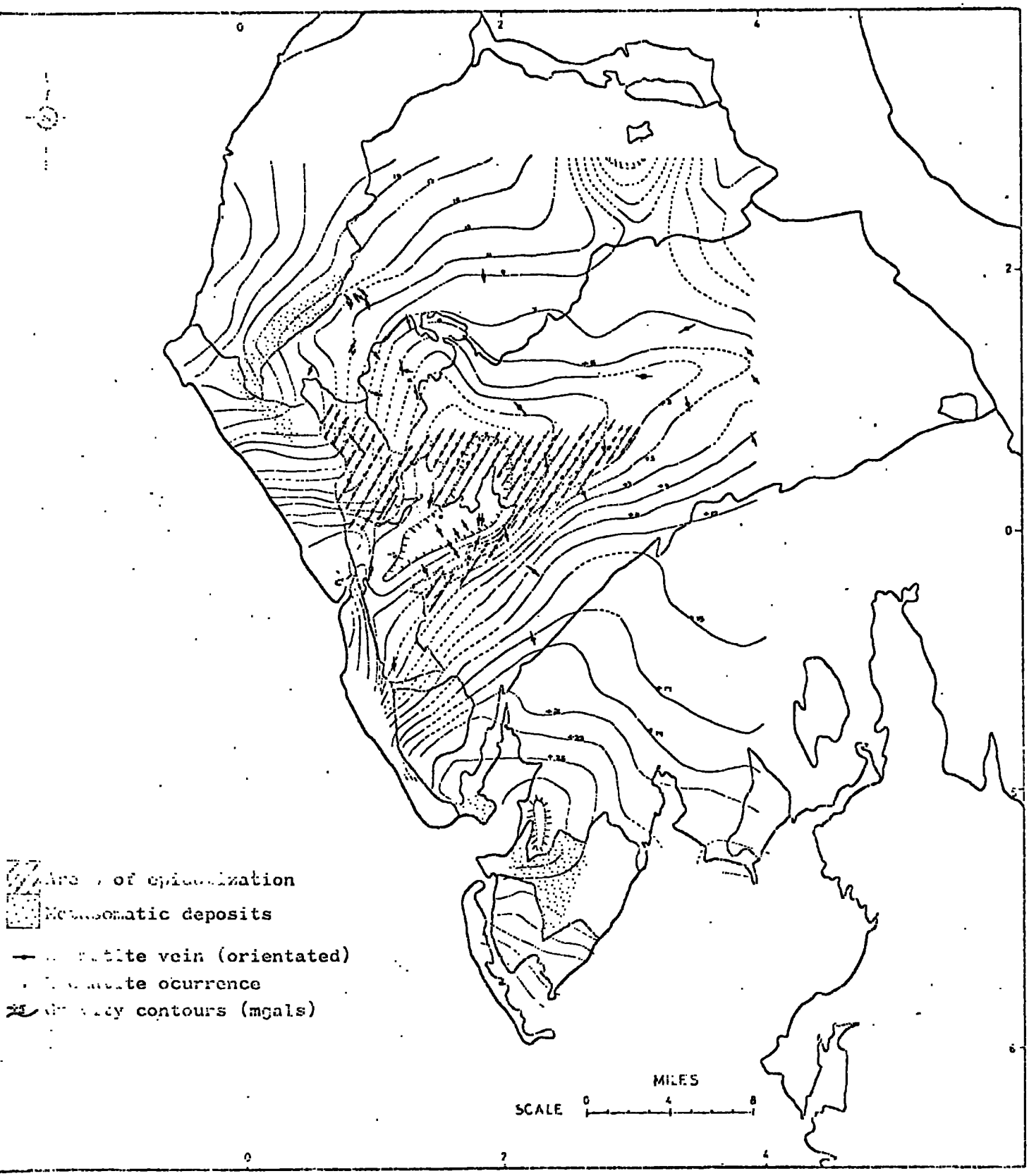

3. GENERAL DESCRIPTION OF THE CUMBRIAN HAEMATITE PROVINCE

3.1. Introduction

Confined to a narrow zone along the western side of the Lake District are a series of ore deposits which have already produced an estimated 150 million tons of high grade, low phosphorus iron ore. The zone extends from Lamplugh in the north to Stank in the south, a distance of 33 miles (Fig. 2). It is coincident with the girdle of Lower Carboniferous sediments and is recognised by a development of large metasomatic replacements of haematite in the limestone of the above succession, especially in West Cumberland and Millom-Furness. In the central section of this zone the limestones are concealed beneath a thick cover of Permo-Triassic sediments and because only traces of haematite have been found some geologists consider this section to be barren. However, until the controls of mineralization are more fully understood isolated deep drilling will prove ineffective in locating orebodies in the underlying limestones.

Although the West Cumberland and Millon-Furness orefields account for 98% of the recorded output they are merely the western sector of an extensive area of epigenetic haematite mineral ization extending eastwards across the central Lake District. The eastern section of this province is represented by widely scattered vein deposits in the Lower Palaeozoics, particularly the late orogenic Devonian intrusives. The observed mineralogical and geochemical similarities between these veins and the replacements deposits further west suggests they are probably cogenetic. Throughout the province, structural and stratigraphic

discontinuities have provided the main channelways for the mineralizing fluids. The metasomatic orebodies represent a special case in which the process of ore deposition was also controlled by the chemistry of the wallrocks.

This hypothesis is carefully examined in the present study and the term "Cumbrian Haematite Province" has been chosen to describe this greater region. (N. B. Unless otherwise stated, "mineralization" will be used synonomously with "haematite mineralization" in later chapters)

3.2. Distribution of Mineralization in the Carboniferous Limestone Zone

As shown in Figure 3 , the West Cumberland orefield occupies the northern section of the limestone zone and is divided into two parts: an "exposed" section from Lamplugh to Bigrigg in which the limestones run to outcrop, and a "concealed" section from Bigrigg to Calder Bridge in which the limestones are concealed beneath a cover of Permo-Triassic sediments (Figure 3). Orebodies are developed along NW-SE post-Triassic faults and NE-SW pre-Triassic faults, both sets predating the main phase of mineralization. Along the northeastern margin of the orefield are a series of vein deposits in the Skiddaw Slate Series which provide the closest spatial link between Lower Palaeozoic veins and Carboniferous replacement deposits.

The Millom-Furness orefield occupies the southern end of the limestone zone and forms a "V" shaped area around the flanks of the southwest pitching High Haume Anticline. The Lower Carboniferous limestones re-emerge from beneath the Permo-Triassics at Kirksanton, pass under the Duddon estuary and swing northeastwards around the nose of the anticline into the Ulverston area (Fig. 4). Orebodies north of the

FIGURE 3

GEOLOGICAL MAP OF THE WEST CUMBERLAND OREFIELD

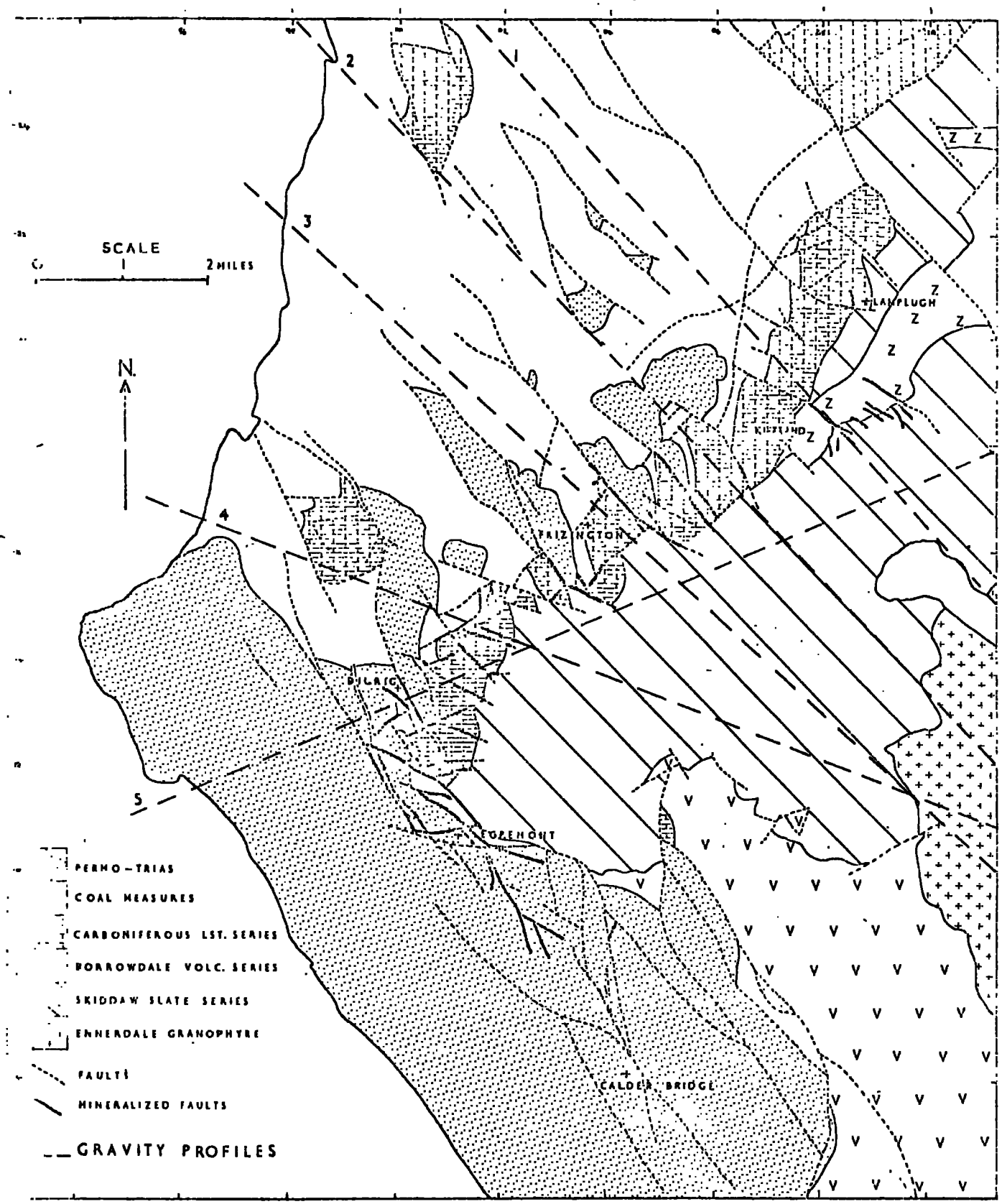

FIGURE 4

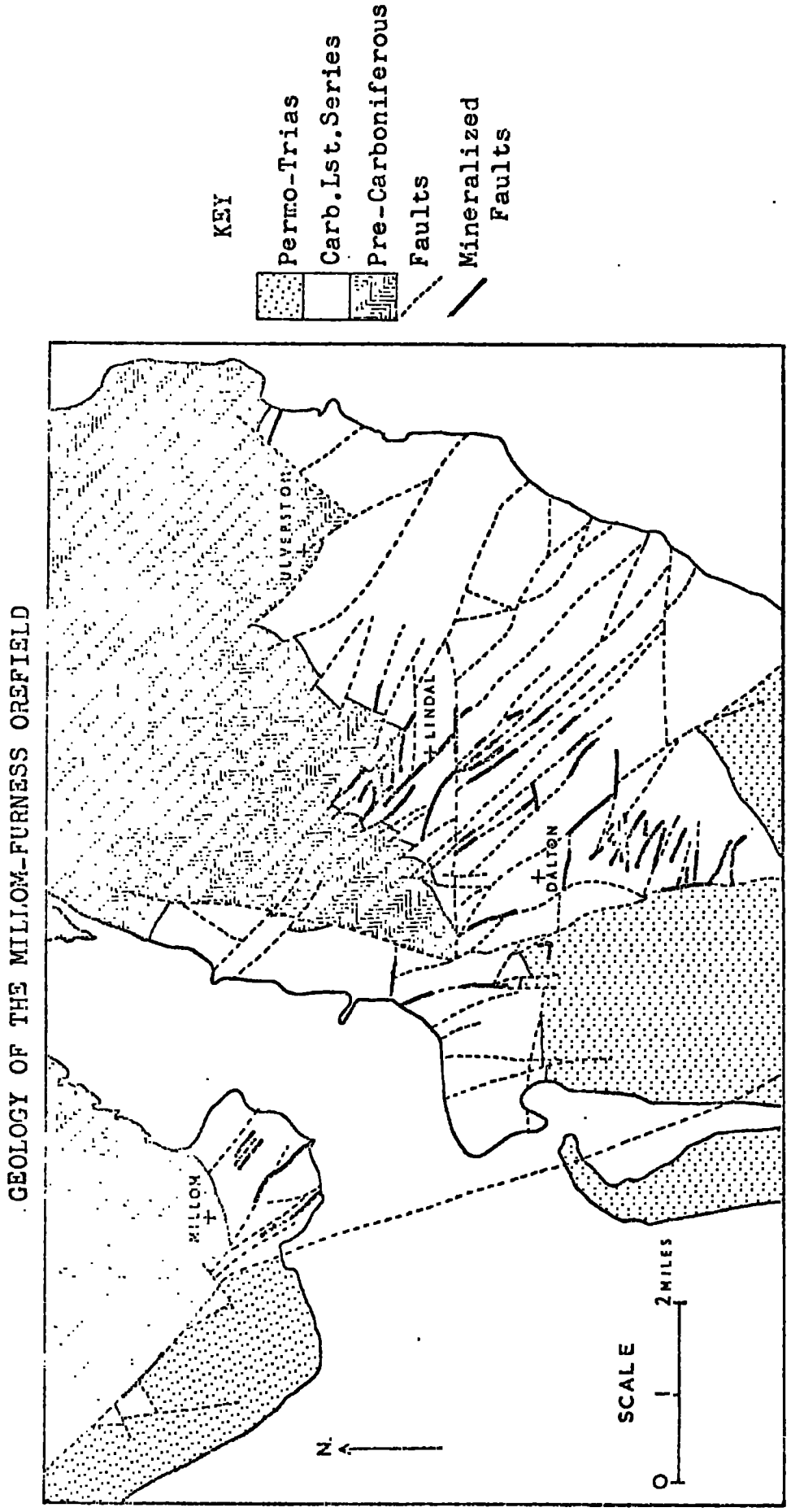

GEOLOGY OF THE MILLOM-FURNESS OREFIELD

estuary (i.e. Kirksanton to Millom) occur along small post-Triassic faults paralleling the great NW-SE trending Boundary Fault. This trend is preserved south of the estuary but as the limestone outcrop turns north an increasing number of orebodies occur along E-W post-Triassic faults. The area of mineralization is bounded to the southeast by the Urswick Syncline which runs NE-SW through Little Urswick, and to southwest by the trough of Permo-Triassic sediments west of the Yarlside Fault (a dislocated branch of the Boundary Fault). Northeast of Lindal the mineralization gradually weakens and the outermost deposit is probably represented by the Plumpton orebody.

3.3. Distribution of Mineralization in the Lower Palaeozoic areas

The extensive region of mineralization east of the limestone zone is roughly triangular shaped; the base of the triangle lying between Bootle and Mockerkin with an apex in the Brothers Water area. This encloses both the Eskdale and Ennerdale intrusives and most of the southern tract of Borrowdale volcanics in the central Lake District. Scattered throughout this area are numerous vein deposits. Mineralization is best developed in the Skiddaw Slate Series at Kelton Fell and in the Eskdale granite along the Esk valley where there are minor vein complexes.

3.4. Types of Orebody

Four main types may be recognised:

(i) Veins (sensu stricto)

These are mineralized faults and fissures in which the ore minerals fill open breccias and dilation cavities. Veins in the Loweswater Flags and Eskdale granite are typical of this

type of orebody. In general however faults in the Skiddaw Slate Series do not carry productive oreshoots because their fault planes are relatively tight structures and often filled with an impervious comminuted slate gouge.

(ii) Flats

These are flat or tabular in shape and show a strong lithological control. They are formed by the complete replacement of a favourable limestone horizon and frequently enclose undisturbed lenses of non-carbonate material. In Furness the specificity of replacement is most pronounced and only certain limestones are replaced.

The margins of such orebodies may be sharp or transitional and locally the ore may even change horizon within the same orebody. The exact mechanism of metasomatism is unknown but is undoubtedly related to the complex physiochemical conditions prevailing at the site of deposition. Flats are closely associated with faults which appear to have acted as feeders for the mineralizing fluids. The largest flat discovered was the "Hodbarrow Flat" (Millom-Furness) which averaged 60 feet in thickness and covered a surface area of $3\frac{3}{4}$ million square feet.

(iii) Vein-like bodies

In contrast to veins sensu stricto these are formed by the metasomatism of carbonate wallrocks along faults in the Carboniferous Limestone Series. The zone of replacement is narrow and orebodies are either vertical or subvertical in form.

Although highly irregular in cross section, maximum dimensions occasionally exceed 2000 feet in strike length, 100 feet in thickness and 500 feet in depth.

Transitional between types 2 and 3 there are many intermediate forms with unusual local names (e.g. guts, ginnels, stoops and pipes).

(iv) Sops

This special type of orebody is peculiar to the flanks of the High Haume Anticline, Furness, and is considered to be secondary in origin (Dunham and Rose, 1941). The haematite forms one of several layers of different material lining the inside of large solution hollows in the limestone. Because of their doubtful primary origin they were excluded from the sampling programme.

3.5. Ore types

The ores occur in three main forms:

(i) Massive ore - compact, massive, brownish red to bluish grey haematite containing macroscopic vugs filled with silica or calcite

(ii) Botryoidal ore - dense, finely banded, colloform haematite.

(iii) Specular ore - aggregates of interlocking specularite crystals.

The replacement orebodies consist almost entirely of massive ore with smaller amounts of botryoidal ore, whilst the Lower Palaeozoic vein deposits are predominantly of botryoidal ore. The massive ore described from veins deposits in the Lower Palaeozoics is only morphological massive and when examined microscopically is seen to be a partially recrystalized finely banded botryoidal ore. Similarly, other varieties referred to in the literature are either mixtures of the three end members or their weathered equivalents.

3.6 Mineralogy

The ores are almost entirely monomineralic and contain only minor amounts of gangue minerals; the most abundant being quartz, calcite and locally barite. Occasionally the barite content of the ore exceeds 10% by weight and drastically reduces its market value (e.g. Haile Moor Mine, West Cumberland). In restricted areas there are also smaller quantities of fluorite, dolomite, siderite, manganite and pyrite.

3.7 Conclusions

Although there are few productive orebodies outside the limestone zone, the veins and haematized shatter belts of the Lower Palaeozoics are equally as important in defining the region of iron metallogenesis. By considering metasomation as a limiting case, the economic bias imposed by the West Cumberland and Millom-Furness orefields no longer obscures the significant patterns of mineralization.

4. REPLACEMENTS DEPOSITS OF THE WEST CUMBERLAND OREFIELD

4.1. Introduction

The West Cumberland orefield occupies the northern section of the highly productive western zone referred to in chapter 3. Although not coextensive with the adjacent Millom-Furness orefield, both areas are characterised by a development of metasomatic replacements of haematite in the Carboniferous Limestone Series. As a result the distribution of orebodies is defined by the arcuate outcrop of limestones around the western flank of the central Lake District (Fig. 3).

Between Lamplugh and Bigrigg the limestones are well exposed but further south the outcrop turns sharply southeastwards beneath a cover of Permo-Triassic sediments.

Active mining is now restricted to two adjacent mines in the concealed section of the orefield south of Egremont. These are the Beckermet Mine (sometimes known as the "Winscales" Mine) and the Haile Moor Mine, both of which are owned and operated by the British Steel Corporation. Most of the mines in the exposed section of the orefield closed down soon after the 1914-18 war due to a fall in the price of iron ore, in response to an increasing flow of cheaper imported ore. Other factors were also responsible for the declining production but it is doubtful whether the deeper levels of the exposed orefield have ever been tested as systematically as in the concealed section.

4.2. Structure

Except for the regional westerly tilt imposed by the Tertiary doming

of the Lake District, the Upper Palaeozoics show little evidence of folding and the area is dominated by normal faulting and associated block movements. North of Bigrigg the limestones strike NE-SW and dip gently to the NW beneath a thin cover of Upper Carboniferous sediments. The limestones rest unconformably on a basement of strongly folded Skiddaw slates; the junction being frequently faulted and rarely seen. Further west the limestones reappear in the Hensingham and Distington inliers before passing beneath the main Whitehaven-Workington coalfield. South of Bigrigg the outcrop swings southeast around the nose of the Buttermere anticline and is concealed by a thick formation of Permo-Triassic sediments which also dip to the SW. The limestones are not exposed again until Kirksanton, 19 miles further south. In the concealed section of the orefield the Hensingham and higher Carboniferous groups are absent; having been removed during pre-Permian denudation. The contact is marked by a strong unconformity which between Nethertown and Ullcoats can be seen to transgress lower and lower members of the Carboniferous Limestone Group until at Ullcoats it finally overlaps the Lower Palaeozoic basement (Fig. 5).

South of Hale Moor the Skiddaw Slate Series are replaced by the Borrowdale Volcanic Series and isopachytes for the limestones indicate that Permo-Triassics rest directly on volcanics in the Calder Bridge area (Fig. 6). This appears to place an effective limit on the distribution of metasomatic orebodies but since borehole data is so meagre (i.e. holes west of the inferred Gosforth Fault have failed to penetrate the Permian sequence) the zone between Calder Bridge and Kirksanton cannot be said to have been thoroughly tested.

FIGURE 6

STRUCTURAL MAP OF THE WEST CUMBERLAND OREFIELD

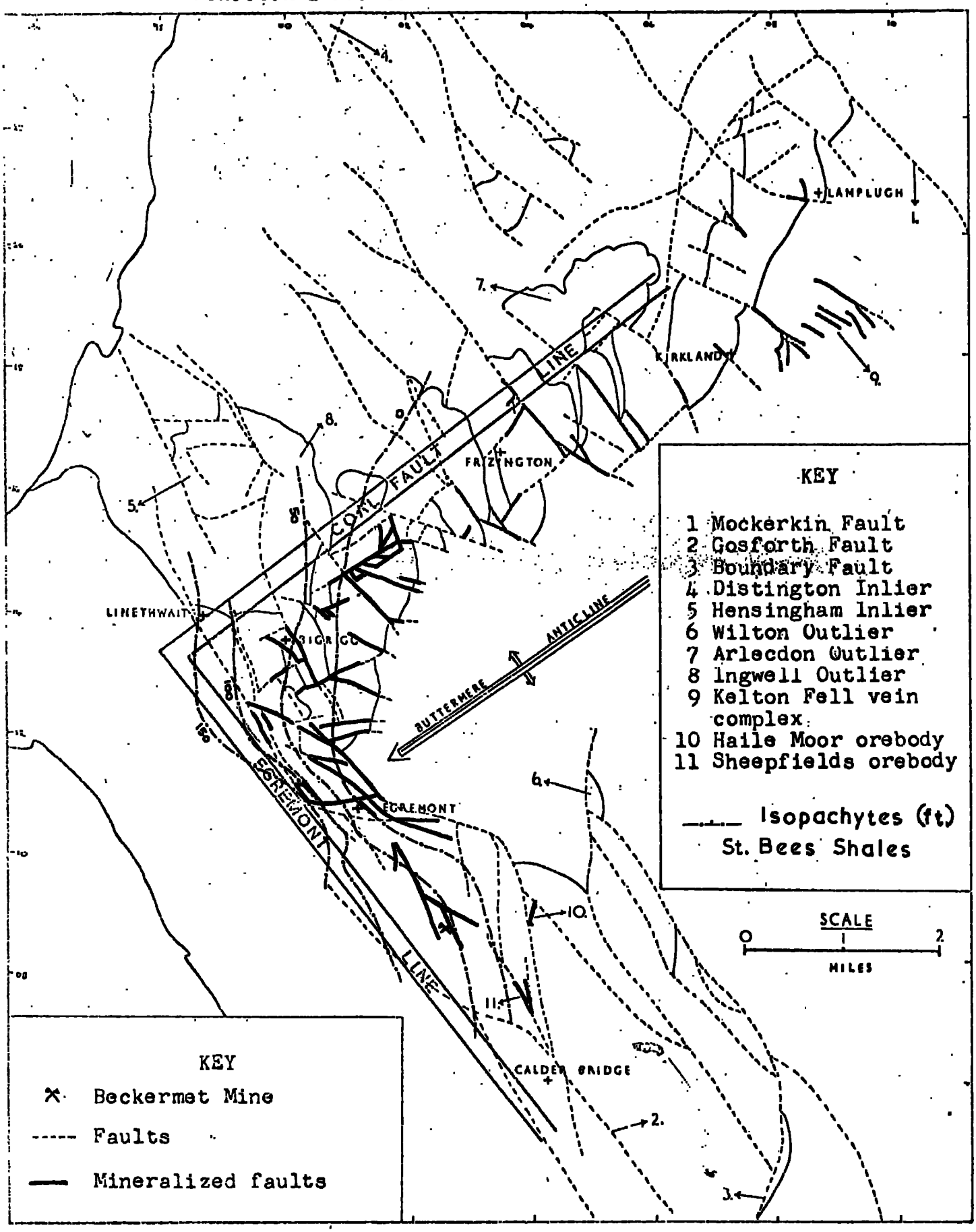

4.2.1. Folding:

Apart from the Hensingham and Distington half domes, the only significant folds are minor NE and NW flexures in the Coal Measures. These are probably related to differential block movement in the basement rather than regional orogenic compression. The apparent swing of the limestones around the Buttermere anticline suggesting post-Hercynian folding along this axis is due to post-Triassic tilting of the strata along NW-SE faults downthrowing to the SW.

4.22. Faulting:

Though many of the faults show more than one period of normal movement they can be classified according to the age of their main displacement:

(i) Pre-Triassic faults

(ii) Post-Triassic faults

The latter set determine the tectonic fabric of the area and dissect the limestone outcrop into a series of dextrally displaced "en echelon" strips.

(i) Pre-Triassic Faults

These are best illustrated by the NE-SW "Coal Faults", so called because they bring Coal Measures against Carboniferous limestones (e.g. St. Johns Church Fault, Cleator Moor Fault and the St. John Pitt Fault). They emerge from beneath the Permo-Triassic cover at Woodend and can be traced through Rowrah to Mockerkin. Identification of individual members is difficult due to repeated lateral shifting by post-Triassic NW-SE cross-faults. Other members of the set are responsible for disrupting the Carboniferous/Skiddaw unconformity. They all downthrow to the NW and displacements

occasionally exceed 1700 feet. Pre-Triassic faulting appears to have been confined to NE-SW lines in the exposed section of the orefield north of Bigrigg. Evidence of related inter-Carboniferous movement is given by the unconformity at the base of the Whitehaven Sandstone and the pre-Whitehaven movement on the Yeathouse and Henry Pit Faults. (N.B. Minor N-S pre-Triassic faults have also been recognised in the Beckermet area: pers. comm. Greenwood 1970.)

(ii) Post-Triassic Faults

These are developed throughout the Lake District but are most prominent in West Cumberland where they occur as a series of NW-SE faults. As described above, they dissect the northern section of limestones and produce a series of tectonic troughs in which are preserved remnants of the original Permo-Triassic cover. From Bigrigg to Lamplugh the downthrow is to the NE but south of Bigrigg the Permo-Triassic cover is stepped down along a series of closely spaced faults downthrowing to the SW. Where the two subsets overlap, opposite the nose of the Buttermere anticline, there is a complex zone of post-Triassic NW-SE and W-E faults which downthrow to the SW, NE, S. and N.

In addition many post-Triassic faults show a component of pre-Triassic movement:

(a) Salter Fault: pre-Brockram hollow along the line of the fault; differential thickness of the Hensingham Group on either side of the fault.

(b) Rowrah Fault: similar pre-Brockram hollow; greater displacement on the Carboniferous than the Brockrams.

(c) Yeathouse Fault: pre-Whitehaven Sandstone and post-Triassic movements.

(d) Haile Moor Fault: greater displacement on the Carboniferous than the Brockrams.

The possibility of post-Triassic reactivation illustrates the inadequacy of the bipartite classification but since not all NW-SE faults were initiated before the Permian it provides a convenient method for interpreting fault patterns. However, later movement along older lines of weakness may be more general than is presently realised. Simpson for example records a Caledonian dextral transcurrent displacement of $\frac{1}{4}$ mile on the post-Triassic Mockerkin Fault in the Loweswater Flags. Whether this indicates that the structural evolution of the Lake District during the Hercynian and Tertiary was pre-determined by a Caledonian fabric in the basement remains a topic for future research. In view of this possibility it is reasonable to assume that the granite batholith has responded as a single unit to subsequent earth movements except along its margins. Pre-Triassic faults in the Beckermet area also show a third period of movement which displaces cross-cutting post-Triassic faults (pers. comm. Greenwood 1971). Unfortunately there is no precise way of dating post-Triassic events since there are no younger rocks in the area.

4.3. Lower Carboniferous and Lower Permo-Triassic Formations

With only minor differences the general geological description given in chapter 2 also applies to the West Cumberland orefield.

4.3.1. Lower Carboniferous Limestone Series

This formation consists of the Carboniferous Limestone Group, with seven thick limestones separated by shales and sandstones of varying thickness, and of the overlying Hensingham Group.

	Lamplugh-Egremont	Beckermet
Hensingham Group	60-150 ft	Absent
1st Limestone	30-60 ft	"
Sandstones and shales	10-14 ft	"
2nd Limestone	14-24 ft	"
Orebank Sandstones and shales	40-60 ft	"
3rd Limestone	10-16 ft	"
Thin Shales	-	"
4th Limestone	235-310 ft	"
Shales and sandstones	14-24 ft	210-230 ft
5th Limestone	50-70 ft	
6th Limestone	54-70 ft	
Shales	-	
7th Limestone	40-182 ft	

4.3.2. Lower Permo-Triassic Formations

Throughout the area the Brockrams provide the type basal facies of the Permian. Lithologically they are a series of dark-red to purple breccia-conglomerates which vary from 0-400 feet in thickness. This variation, for uneroded sections, is a direct function of a lateral facies change across the margin of the Permo-Triassic basin (Fig. 7).

On passing westwards the Brockrams thin rapidly and pass laterally into the St. Bees Shales and Magnesian Limestone; their accepted offshore equivalents. Isopachytes for the St. Bees Shales are shown in Figure 6.

The Permo-Triassic formations outcrop as a broad coastal belt extending from Barrowmouth to the Duddon Estuary. The beds dip gently to the SW but because of step faulting along NW-SE post-Triassic, the succession thickens rapidly across the strike. Recent gravity work (Bott 1964) suggests that this belt is merely the feather end of a huge wedge of sediments whose centre lies several miles offshore. Isolated outliers of

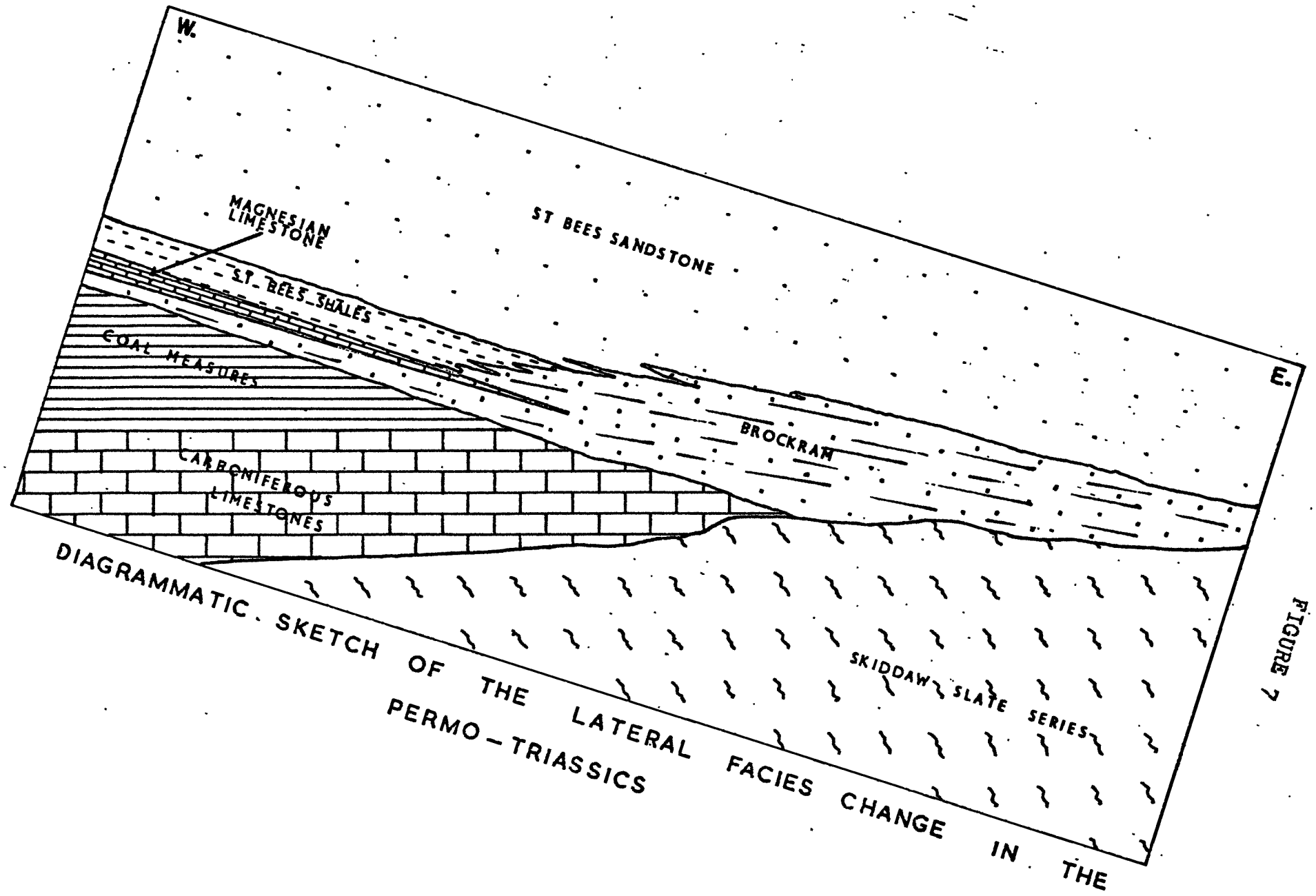

FIGURE 7

DIAGRAMMATIC SKETCH OF THE LATERAL FACIES CHANGE IN THE PERMO-TRIASSICS

Lower Permo-Triassics are also found in the northern section of the orefield in structural troughs adjacent to major NW-SE faults (e.g. the Bigrigg, Ingwell and Arlecdon outliers).

4.4. Distribution of Orebodies

The northernmost orebody occurs ½ mile south of Havercroft but drilling in Snary Beck has proved ory joints in the 4th Limestone and this must be taken as the northern limit of known mineralization (Fig. 3). The northwestern boundary is marked by the line of prominent NE-SW Coal Faults since very little ore has been found on the downthrow side of these structures. This is partly confirmed by the complete absence of mineralization in the Hensingham inlier even though the truncating fault structure is ore-bearing 1 mile to the southeast. Further south the boundaries are less well defined due to the problem of locating orebodies beneath the thick cover of unmineralized and drift covered Permo-Triassic sediments. Even so the theoretical distribution of orebodies is controlled by the distribution of replaceable carbonate formations beneath the cover (Fig. 6). Thus the zero isopachyte for the Carboniferous Limestone Series provides an approximate southern limit to the orefield; data reliability accepted. At present the southernmost workings of the Beckermet Mine are in the Sheepfields area, 1½ miles north of Calder Bridge. To the southwest orebodies are confined to an area east of a series of major post-Triassic faults trending NW-SE through Linethwaite, Pallaflat and Orgill. As expected the eastern margin is defined by the Carboniferous/Skiddaw junction and vein-like replacements pinch out on entering the Lower Palaeozic basement. Of special significance, later referred to in chapter 6, is a complete lack of mineralization in the Wilton outlier, 2 miles east

of Egremont. This is a small outlier of Carboniferous limestones preseved in a faulted trough between Skiddaw Slates and Borrowdale Volcanics.

4.5. Structural Control of Mineralization

The distribution of orebodies clearly indicates the role of both pre-Triassic and post-Triassic faults in providing channelways for the mineralizing fluids. South of Egremont and north of Frizington the NW-SE post-Triassic faults were favoured whilst in the intervening zone the fluids appear to have preferred the NE-SW pre-Triassic Coal Faults. Vein-like bodies are well developed along many of the mineralized faults but where bedding planes and joint systems offered suitable lateral channelways the limestones carry extensive flats. A fine example of lateral migration along a stratigraphic discontinuity is given by the much quoted "cascading" flats of the Helder and Gillfoot Park Mines (Fig. 8). Although the Skiddaw Slates Series beneath the orefield are haematized along ore-bearing faults no deposit has yet been found which is a vertical equivalent of a replacement orebody in the overlying limestones. Similar haematization of the Skiddaw slates occurs along faults on the eastern margin of the orefield but neither fault nor haematite staining can be traced very far beyond the Carboniferous boundary. Locally the lowermost Brockram breccias are mineralized and limestone fragments are replaced by haematite to form low grade "gravel" ores (e.g. at Orebank House, Bigrigg). In general however unless the Brockrams rest directly on the Lower Carboniferous Limestones Series replacement ores are confined to the latter horizons. The only known exception is a

FIGURE 8

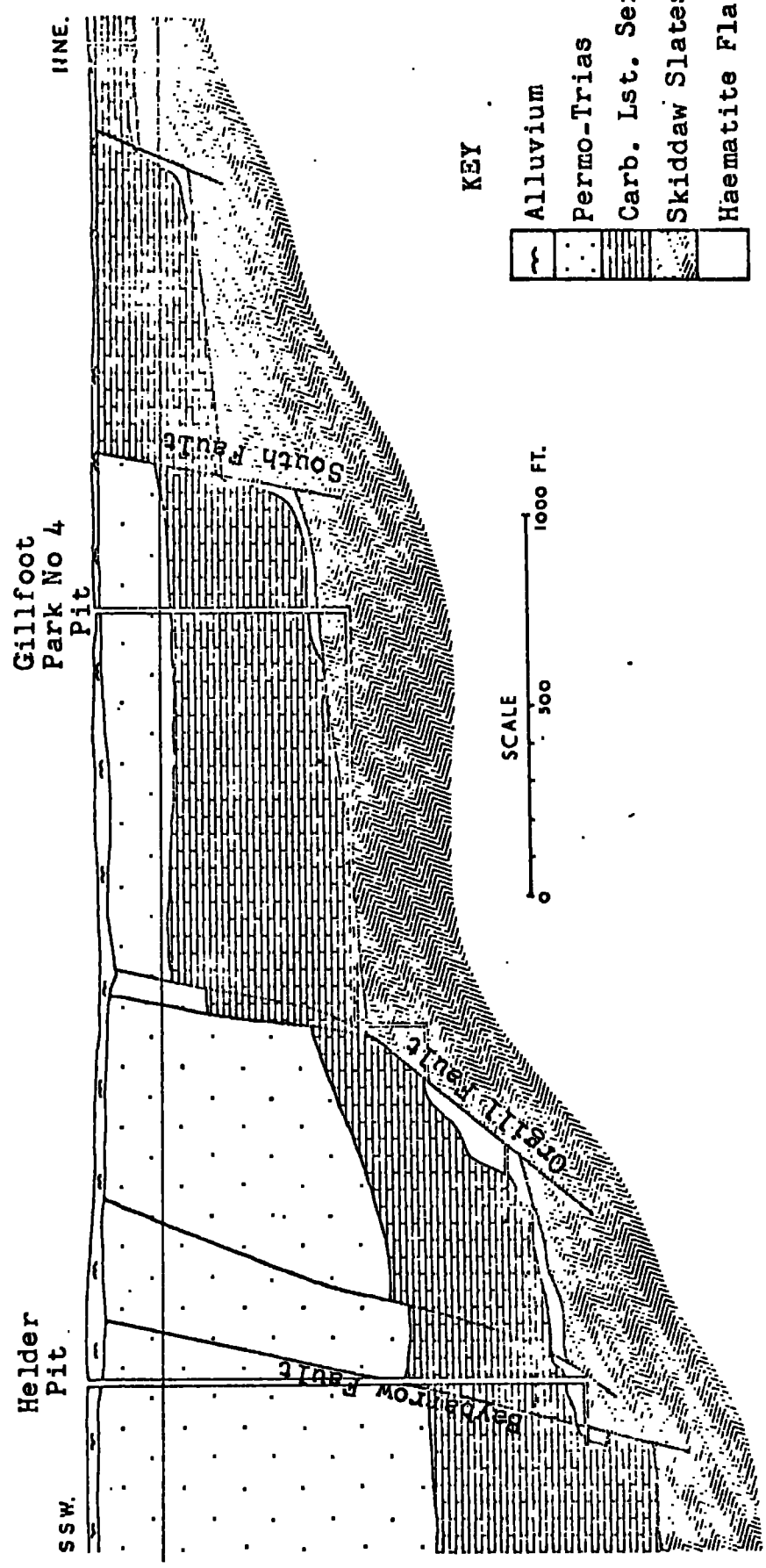

SECTION THROUGH THE "Cascading Flats" OF THE HELDER AND GILLFOOT PARK MINES, EGREMONT

small orebody in the Upper Carboniferous Coal Measures at Millyeat, ¾ mile NW of Frizington, where a thin bed of Spirobis limestone has been replaced by haematite.

4.6. Types of Orebody and varieties of Ore

The orebodies occur in two main forms "vein-like bodies" and "flats", both of which are the result of complete metasomatic replacement of limestone. Veins (sensu stricto) are not represented, and as mentioned above, do not occur as basement extensions of replacement orebodies at higher levels. Unlike the competent Loweswater Flags at Kelton Fell, the Skiddaw slates beneath the orefield are relatively incompetent and probably inhibited vein formation.

The process of replacement produces two principal varieties of ore; massive ore and botryoidal ore. The first is a "volume - volume" substitution of limestone by haematite whereas the second variety forms as a crustiform layering in open spaces within the massive ore.

(i) Massive Ore

Massive ore is found throughout the entire orefield and constitutes at least 95% of the ore mined. It varies little in bulk composition except around the margins of the orebodies where it often grades into unaltered limestone. Quartz is an integral of the ore and occurs both as a delicate intergrowth with the haematite and as a filling of variable sized macroscopic vugs. The distribution and frequency of vugs and the size of the haematite crystals determines the colour and texture of the ore.

The problem of selecting uncontaminated massive ore for analysis was resolved by applying a statistical discrimination technique to the geochemical data which identified anomalous samples. Several specimens

rejected by this method were subsequently found to contain minor inclusions of botryoidal ore.

(ii) Botryoidal Ore

A variety much sought after by lapidarists, it is almost stoichiometric haematite and develops as a crustiform-reniform deposit in cavities and channelways in the massive ore. Microscopically it is finely banded and very similar to the reniform aggregates produced by the recrystallization of interfering spherulites as described by Grigorev (1967). It also occurs in vuggy massive ore as a thin skin separating quartz overgrowths from the enclosing host. At the quartz contact like botryoidal ore shows a progressive conversion to a quartz-specularite intergrowth, which suggests a certain degree of instability in the presence of silica rich fluids. This may explain why the best specimens are often enclosed by carbonate gangue or isolated in premineralization solution cavities.

4.7. Gangue Minerals

As mentioned in the previous chapter the gangue mineral assemblage is relatively simple and comprises the following minerals in order of decreasing abundance: quartz, calcite, barite, dolomite, siderite, manganite, fluorite and pyrite.

(i) Quartz and Calcite

Both are invariable constituents of the ores and have a ubiquitous distribution. Where replacement has affected sandy limestones or calcareous sandstones the quartz content of the ore increases proportionally and variations in silica are thought to be related to the nature of the original wallrock (chap. 9). In contrast, calcite does not form an inter-

growth with the haematite and occurs in veinlets, veins and pipe-like bodies within the ore. Its occurrence strongly suggests redeposition of calcium carbonate moving away from the metasomatic front.

(ii) Barite

The distribution of barite is more localised and occupies two distinct environments. A pale blue-green variety is found in vugs in orebodies along the NE-SW Coal Faults and can be traced sporadically from Frizington to Bigrigg. The other variety is intimately associated with the ore and occurs as bladed masses of white or pink barites. (The pink colouration being due to finely divided haematite.) Its distribution indicates a relationship with orebodies having a Brockram roof or in close proximity to faulted troughs of Permo-Triassic sediments (e.g. Haile Moor, Ullcoats and Bigrigg).

(iii) Siderite and Dolomite

No coherent distribution has been observed for these minerals except to note that they are more abundant in the Lamplugh, Eskett and Yeathouse areas.

(iv) Manganite

Manganite is found in small quantities throughout the northern section of the orefield but in the Bigrigg area it attains its best development where it occurs in large masses together with barite on the fringes of the orebodies.

(v) Fluorite

The presence of fluorite as a gangue mineral has been interpreted by many to indicate an unequivocal magmatic origin for the ores. It is most abundant in the Florence Mine where it occurs as small euhedral crystals in vugs in the main orebody, but has also been recorded at Bigrigg, Cleator

Moor and Frizington. Trotter (1945) reporting work by Phemister and Templeman describes other fluorite occurrences in sandstones between the 1st and 2nd Limestones where it cements and replaces grains of calcite and quartz, and along faults in the volcanic basement beneath the Beckermet area. In each case it postdates the associated haematite and although the time interval may have been small fluorite cannot be used to support a particular theory of ore genesis. Though purely speculative there are two possible sources for the fluorite:

a. A remobilisation of fluorite from areas of fluorine pneumatolysis in the granite basement.

b. A release of fluorite from anhydrite beds in the Lower Carboniferous Limestone Series (Llewellyn et al 1968). Fluorite has not yet been identified in the Cumberland anhydrites but the association fluorite-anhydrite is not uncommon. (Dearman pers. comm. 1972).

Neither source adequately accounts for the observed distribution of fluorite but neither is there sufficient evidence to equate the sandstone occurrences with those in the Florence orebody or basement volcanics.

(vi) Pyrite

In restricted sections of the Beckermet Mine irregular cavities in the massive ore are lined with tiny pyrite crystals which are clearly later than the associated quartz or barite growths. Further work needs to be carried out before they can be related to the late stage fluorite mineralization.

4.8. Galena-Chalcopyrite Veins

As for fluorite, the presence of galena and chalcopyrite in the orefield

has created much discussion regarding the genetic relationship between sulphide and haematite (Dixon 1928). Numerous base metal veins occur in the Lower Palaeozoics east of the limestone belt but at three localities sulphides are actually found in association with haematite. (Smith 1924 and 1928, Trotter 1945). In the Crowgarth, Eskett and Crossgill Mines discontinuous lenses of chalcopyrite, malachite and barite have been found which lie partly within the orebodies. At Crossgill stringers of galena have also been found. The present work suggests that the adjacent faults have acted as channelways for two pulses of mineralizing fluids; an early copper-lead phase followed by a later iron phase. Conflicting observations by Trotter at the Crowgarth Mine can now be reinterpreted as the complete replacement of the limestone wallrocks around a pre-existing chalcopyrite vein. The abundance of botryoidal ore in the immediate area provides further proof that the haematite ore was deposited along a well developed open channelway. Thus the combined evidence supports a pre-haematite age for the sulphide mineralization.

4.9. Age of Mineralization

Recent workers with the exception of Kendall agree in regarding the mineralization as post-Triassic in age. The development of orebodies along post-Triassic faults, the sub-economic haematite impregnations in the St. Bees Sandstones and the conversion of matrix and pebbles in Brockrams into haematite are strong factors in favour of this assertion. Against this view are the observations of Kendall who records brecciated orebodies on the Salter Hall Fault and polished haematite blocks in the Brockrams further south. Even Smith briefly mentions the brecciation and slickensiding of orebodies in the Kirkland and Lamplugh areas.

4.10. Detailed Description of Mines

Detailed accounts of the mines and methods of mining have been deliberately excluded from the thesis. The author considers that since the sampling was stratigraphically uncontrolled such information adds little to the present study. There is doubt also whether the special survey memoir (Smith 1924) contains an accurate description of the abandoned workings. Kendall's review of the memoir (Kendall 1920) is far from complementary and points out several serious errors and omissions for the Salter and Eskett Park Mines. His specific criticisms are confined to the above mines but he refers to a general discrepancy between the memoir and existing mine plans.

5. VEIN DEPOSITS IN THE LOWER PALAEOZOICS

5.1. Introduction

East of the West Cumberland orefield the Cumbrian Haematite Province continues across the central Lake District as a broad triangular shaped belt with its apex in the Brothers Water area. Its position is defined by the occurrence of haematite veins (sensu stricto) in the Lower Palaeozoics; 45 of the larger veins having been worked intermittently during the past two hundred years. There are also innumerable uneconomic mineralized structures and areas of haematite staining which help to define the region of iron metallogenesis. Figure 2 shows the distribution of these veins and indicates the inferred boundaries of the province. The southern boundary, despite a paucity of veins in the Dunnerdale area, is fixed by the Ordovician-Silurian unconformity. The deep trough of Silurian sediments to the south is conspicuous by its lack of haematization and virtually isolates the main area of mineralization from the Millom-Furness orefield further south. Continuity with the north is maintained only in the extreme west along a narrow coastal corridor through Black Combe. Even so there is a five mile section of untested ground between the Kinmont orebody in the Eskdale Granite and the Kirksanton orebody in Lower Carboniferous limestones, near Whitcham. Tectonically the Millom-Furness orefield and adjacent deposits occupy a structural "high" south of the trough but it is not known whether the province continues beneath the intervening tract. The northern boundary is better defined and runs ESE from Mockerkin through Loweswater and Thirlmere to Brothers Water.

Since oreshoots are best developed along open channelways the

probability of oreshoot formation is greatest for veins in competent strata. This factor probably explains why there is a relative abundance of productive veins in the competent Eskdale granite and Loweswater Flags, and a wide-spread development of unproductive haematized faults in the less competent Borrowdale Volcanic Series and Skiddaw Slate Series.

Vein orientation analysis, using weighted strike length means, reveals three preferred directions at 00^{o}, 312^{o} and 335^{o}. The second set refers to veins in the Skiddaw slates at Kelton Fell whilst the first and third sets refer to veins in the Eskdale-Ennerdale complex and adjacent volcanics.

All mining has now ceased, the last mine to close being the Kelton Fell Mine in 1917. A complete list of known veins together with grid references and geological details are given in Appendix II. For most mines very little information is available and the special Survey memoir (Smith 1924) provides a unique collation of such data. Samples were collected from each of the recorded localities but only material from vein complexes in the Eskdale Valley and Kelton Fell areas proved geochemically suitable.

5.2. Veins in the Skiddaw Slate Series

Mineralized faults in the Skiddaw Slate Series are characterised by diffuse zones of haematized wallrock on either side of the fault plane and do not generally carry oreshoots. The highly productive vein complexes at Kelton Fell and Knockmurton Fell are therefore anomalous and deserve closer consideration.

The veins are developed along a series of NW-SE and N-S faults and fissures where they cross the junction of the Loweswater Flags with the Kirkstile Slates. Oreshoots are clustered at this horizon but many

extend northwards into the flags. The veins hade consistently to the NE and thus behave in a similar manner to NW-SE post-Triassic faults in the adjacent limestone belt.

In 1910-13 a level drift was driven southwards from the Cockran Vein to Kirkland where it intersected an 18 inch vein near Priest How. According to Smith (1924) the latter vein trends NNW-SSE in the slates and lies beneath 90 feet of limestones. If this account is correct, it provides the only conclusive evidence for a spatial correlation between replacement deposits in the Carboniferous limestones and vein deposits in the Lower Palaeozoics.

The haematite occurs mainly as a primary deposit in open channelways and apart from slight haematization of slate fragments there is little sign of large scale metasomatic replacement. Typical botryoidal encrustations are frequently encountered but the hard blue ore forming the bulk of the oreshoots is pseudo-massive haematite and contains relic botryoidal textures. Gangue minerals are subordinate and except for minor amounts of quartz and calcite the ore is practically pure haematite. Several veins have been worked to a depth of 500 feet and "cut offs" were determined by vein width and the inclusion of slate riders. Smaller veins have also been tried at Grassmoor and Eel Crags.

In the Kink Beck area, 3 miles NE of Egremont, the Skiddaw Slate Series are riddled with haematized fissures and at Thwaites the slates are smashed and haematized along a N-S belt 1300 feet wide and over 1 mile long.

5.3. Veins in the Eskdale-Ennerdale Intrusives

As described in chapter 2, the Eskdale granite is extensively

mineralized and except for areas of pervasive haematization the haematite veins are formed along a series of NNW-SSE and N-S faults (i.e. subsets 00° and 335° of the vein orientation analysis). The Ennerdale granophyre, although mineralized to a lesser degree, shows many of the same characteristics but differs in that the mineralization is concentrated around the margins of the intrusive. Firman (1960) believes that the largest veins occupy reactivated Caledonian wrench faults which underwent vertical movement prior to mineralization. The ore occurs as a typical fissure filling and is predominantly botryoidal with smaller amounts of pseudo-massive and specularite haematite. As in the Skiddaw veins, gangue minerals are subordinate and represented by minor amounts of quartz, calcite and dolomite. In general the oreshoots are well defined but in some veins the ore is intergrown with the granite wallrocks.

(i) Eskdale Granite

The main area of mineralization is located in the Eskdale valley, east of Eskdale Green, where there are a series of strong veins which cross the valley almost at right angles. Mining is confined to the well exposed valley slopes and there is no record of veins having been followed beneath the River Esk. The most extensive workings are in the Nab Gill Mine which worked a NNW-SSE vein in the hillside above Boot. Smaller mines worked similar veins in the Great Barrow, Stanley Gill, Birker Moor, Dalegarth, Blea Tarn, Eskdale Green and Brantrake areas. Beyond this zone the only other productive veins are at Middle Kinmont and Chapel Hill.

(ii) Ennerdale Granophyre

The largest mine occurs at Crag Fell and exploited a group of small

N-S, NW-SE and WNW-ESE veins along the slate/granophyre contact. Further east there is the Iron Crag Mine, a short lived venture which is known to have yielded 400 tons in 1882. The majority of veins however are not found within the intrusive but along numerous peripheral faults which dislocate the contact. Trials have been made at the following localities: Red Gill, Sourmilk Gill, Clews Gill and Scale Force.

5.4. Veins in the Borrowdale Volcanic Series

Economically these have never been important but their distribution is useful in defining the extent and nature of the Cumbrian Haematite Province. Small mines were developed on veins in the Dunnerdale, Green Hole, Tongue Gill, Red Tarn and Stainton Ground areas.

5.5. Conclusions

Haematite orebodies east of the limestone belt occur as widely scattered vein deposits in the Lower Palaeozoics. The veins are preferentially developed along reactivated Caledonian faults trending 00°, 312° and 335°. Mineralization is greatest in the Eskdale granite but economically the vein complex in the Skiddaw Slates Series at Kelton Fell records the highest output.

The ores consist mainly of pseudo-massive haematite except in the granite where there is a higher proportion of botryoidal ore. Regionally the orebodies show many structural and mineralogical similarities and are almost monomineralic. These features suggest the orefluids were saturated only with respect to haematite and were probably derived from a common source.

6. STRUCTURAL RELATIONSHIP BETWEEN BASEMENT AND MINERALIZATION

6.1. Regional Evidence

A general comparison between the distribution of haematite mineralization and the Bouguer gravity field for the Lake District reveals a marked similarity in patterns (Fig. 2). The latter appears as a huge negative anomaly enclosing almost the entire region and comprising a series of interconnected "lows" coincident with the known Devonian intrusives. The largest of these "lows" is associated with the Eskdale-Ennerdale complex and has a minima of -6.77 mgals. In outline the anomaly is pear-shaped, having a centre over the exposed Eskdale granite and an elongation eastwards towards the Shap granite. The Ennerdale granophyre is completely contained within the Eskdale centre and has no subsidiary "low" of its own which suggests that it is an integral part of the intrusive complex and not a laccolithic body as described by Rastall (1906).

To the west the anomaly is marked by a steep gradient along the line of the Bounday Fault but north of Gosforth the gradient opens out into a broad plateau for several miles west of the granophyre. In contrast the eastern boundaries are less prominent and show no correlation with fault zones. If the Eskdale "low" is due to a mass deficiency in the upper crust caused by the granite-granophyre complex, then the shape of the anomaly defines the area of concealed "granite" in the basement. As shown in Figure 2 the presence of a concealed "granite" ridge beneath the Bouguer elongation is inferred by the distribution of epidozation in the Borrowdale volcanics. (Chap. 2).

From these observations it is evident that the Cumbrian Haematite

Province is underlain by an area of "granite" petrogenetically equivalent to the Eskdale-Ennerdale complex. The implied spatial relationship between granite and mineralization is typical of other European orefields but the associated lack of haematization in the coextensive Shap and Skiddaw intrusives suggests that the Eskdale granite has acted as more than a structural "high" for the ascending ore fluids. Although not proven vein complexes similar to those at the centre of the anomaly may also continue eastwards along the crest of the "granite" ridge. However since the Eskdale veins also straddle the projected extension of the Hardknott shatter belt (a fundamental line of weakness traceable from Langdale to Hardknott) mineralization may be confined to areas where the "granite" basement is penetrated by deep fault structures.

6.2. Evidence in the West Cumberland orefield

The apparent influence of the basement on the distribution of haematite initiated a detailed interpretation of the Bouguer anomaly over the West Cumberland orefield; the results of which are described in Appendix I. Briefly the investigation proved the existence of a "granite" shelf (Ennerdale Shelf) extending 4-5 miles west of the granophyre beneath a shallow cover of Palaeozoic sediments and bounded by steep well defined margins. The northwestern margin (Coal Fault Line) strikes N 65°E and underlies the exposed section of the orefield whilst the southwestern margin (Egremont Line) strikes E 44°S and coincides with the area of concealed mineralization south of Bigrigg (Fig. 6). During the Hercynian and later earth movements these margins probably acted as major lines of weakness, allowing the granites to move as a single block along marginal dislocations. The intense faulting now seen in the over-

lying sediments is thought to be a direct consequence of this inherent weakness. Perhaps more relevant, the Ennerdale Shelf provides a temporal link between the processes of mineralization and faulting:

(i) The orientation and localisation of faults can now be related to lines of weakness in the basement. This is especially true for the Coal Faults which do not conform to the generally accepted Hercynian pattern.

(ii) Periodic readjustment at the edge of the shelf provides a simple dynamic model for generating several phases of complementary faulting in the overlying cover (c. f. the inter-Carboniferous, pre-Triassic and post-Triassic faults). In each phase the driving force may have been either orogenic movement or isostatic uplift of the Lake District in response to sedimentary loading in the adjacent Irish Sea Basin.

(iii) The system of NE-SW faults downthrowing to the NW can now be explained by pre-Triassic movement on the Coal Fault Line. Similarly post-Triassic uplift along the Egremont Line with slight pivoting in the Linethwaite intersection area would create a system of NW-SE faults downthrowing in both directions (c. f. the post-Triassic faults north and south of Bigrigg).

(iv) The development of high level fault zones above lines of major dislocation in the basement provides a perfect network of channelways for ascending ore fluids. This latter point was perhaps the most critical factor in determining the development of the West Cumberland orefield and offers an explanation of faulting and mineralization in an area beyond the exposed Eskdale granite. If one also assumes that the mineralizing fluids originated along tectonically disturbed zones in the "granite" basement,

particularly the faulted western margin of the shelf, then the distribution of haematite occurrences should reflect this control. Several lines of evidence now suggest this assumption to be correct:

(i) Metasomatic replacements of haematite are confined to narrow zones immediately above the Coal Fault and Egremont Lines.

(ii) Mineralization is absent in the Hensingham inlier and Wilton outlier, both of which are located just outside the marginal zone of the shelf.

These observations indicate a minimum degree of lateral migration along structures at right angles to the margins. Unlike the St. Bees Shale hypothesis, the "granite" source theory provides a better explanation of the known distribution of orebodies especially in areas underlain by more than 100 feet of shale.

Secondly in considering the chronology of mineralization there is no reason why there should not have been a minor phase of haematite remobilisation along the Coal Fault Line before the main period of post-Triassic faulting. This would account for the controversial brecciation of orebodies on pre-Triassic faults in the Frizington-Lamplugh area and the occurrence of rounded haematite pebbles in the Brockrams (Kendall 1893 and 1929).

7. SAMPLING AND ANALYTICAL TECHNIQUES

7.1. Sampling

The main purpose of the sampling programme was to provide suitable material for geochemical analysis such that the resulting data could be applied to the following problems:

(i) The genetic relationship between haematite deposits in the Carboniferous limestones and those in the Lower Palaeozoics. (i.e. the concept of a Cumbrian Metallogenic Province for haematite)

(ii) The geochemistry of the replacement ores.

(iii) The origin and nature of the mineralizing fluids. (i.e. to resolve the "ascensionist vs. descensionist" controversy).

7.1.1. Limitations

Excluding the Beckermet and Haile Moor Mines, sampling was virtually uncontrolled and predetermined by the availability of samples on waste dumps adjacent to abandoned mine shafts. As a consequence sampling was heavily biased to the more productive Carboniferous limestone belt. This meant that geochemical patterns for the replacement deposits could not be confidently extrapolated to include widely scattered vein deposits in the Lower Palaeozoics. Furthermore, it was necessary to assume that the samples were representative of the original orebodies. This assumption was later verified by statistical tests which showed that the samples belonged to a small number of homogeneous populations.

7.1.2. Details of the Sampling

Work began in the Egremont-Cleator Moor zone and gradually extended outwards to include all documented haematite occurrences in the

western and central Lake District. Time did not permit as detailed a survey of the Millom-Furness district, further south, and only sufficient material was collected to provide a basis for geochemical comparison. At each locality samples of the various ore types and gangue minerals were collected and their relative abundances noted.

Subsequent to the realisation that the greater part of the Cumbrian Haematite Province was underlain by "granite" it was decided to test the implied hypothesis of a geochemical association between the basement and the mineralization. Since the Eskdale and Ennerdale intrusives were clearly surface expressions of this basement they were sampled and analysed accordingly. Of the 16 Eskdale samples, 10 were classified as Pink granite, 2 as Grey granite and 4 as haematized Pink granite. Four of the original 8 Ennerdale samples were later rejected as atypical of the main granophyric phase.

Appendix II provides a complete summary of the sampling programme (i.e. grid references, sample numbers, nature of sample, etc.

7.2. Analytical Techniques

In addition to studying the geochemical variation of major and minor ore constituents (Fe, Si, Ca, Mg, Mn, Al), a group of 11 trace elements were selected for quantitative analysis (As, Ba, Cu, Ni, Pb, Rb, Sr, Ti, Y, Zn, Zr). It was considered that these would provide more diagnostic information on the nature of the mineralizing fluids because of their more definitive geochemical environments.

X-ray fluorescence spectrometry was chosen as the principal method of analysis because it provided a rapid, high precision, multi-element

method ideally suited to the project requirements.

Thermometric examination of the fluid inclusions in non-opaque gangue minerals was carried out on a heating-freezing stage attached to a Leitz microscope.

7.2.1. X-ray Fluorescence Analysis (X.R.F. Analysis)

The basic theory and techniques of X.R.F. analysis are well established and need not be reiterated. Of the many texts available those by Leibhafsky (1960), Norish and Chappell (1967) and Adler (1966) proved particularly instructive. Samples were analysed against physico-chemically similar standards on a Phillips 1212 spectrograph. The instrumental conditions used are listed in tables 2 and 3.

7.2.1.1. Sample Preparation

Haematite ores were sorted into five main classes:

(i) Massive ores

(ii) Botryoidal ores

(iii) Specular ores

(iv) Marginal ores - intergrowths of ore and wallrock

(v) Mixed ores - physical mixtures of the above.

Duplicate samples of massive and botryoidal ore from each locality were washed and dried to remove particulate surface contamination, and then finely ground in a Tema disc mill to minimise grain size and mineral heterogeneity errors. For trace element work the resultant minus 240 mesh material was supported directly on mylar film and analysed as a powder, whilst for major and minor elements the powders were compressed into 1" diameter briquettes. Several drops of mowoil, an inert polyvinyl cement, were added to assist in binding. The decision to use a twofold method of sample preparation was taken to ensure:

(i) A maximum degree of compatability between standards

TABLE 2

INSTRUMENTAL CONDITIONS FOR HAEMATITE ORE ANALYSIS

Element	Counting Statistics	mA	KV	Crystal	Counter	Collinator
Si	3×10^5 counts	16	60	P.E.T.	Flow	Coarse
Al	3×10^5	32	60	"	"	"
Fe	3×10^4	4	40	LiF	"	"
Mg	3×10^4	40	50	Gypsum	"	"
Ca	10^6	8	60	P.E.T.	"	"
Ti	10^6	16	60	P.E.T.	"	"
Mn	20 secs	32	60	LiF	"	"
		(Cr tube)				
Ba	40 secs	24	80	LiF	Scint.	Coarse
Zr	40	24	80	"	"	"
Y	40	24	80	"	"	"
Sr	40	24	80	"	"	"
Rb	40	24	80	"	"	"
Pb	100	32	60	"	"	"
Zn	100	32	60	"	"	"
Cu	100	32	60	"	"	"
Ni	100	32	60	"	"	"
As	100	32	60	"	"	"
		(W tube)				

TABLE 3

INSTRUMENTAL CONDITIONS FOR SILICATE ANALYSIS

Element	Counting Statistics	mA	KV	Crystal	Counter	Collimator
Si	10^5 counts	16	40	P.E.T.	Flow	Coarse
Al	10^5	40	50	"	"	"
Fe	10^5	8	20	LiF	"	"
Mg	10^4	40	50	Gypsum	"	"
Ca	10^5	8	20	LiF	"	"
Na	10^4	40	50	Gypsum	"	"
K	10^5	8	40	LiF	"	"
Ti	10^5	8	40	LiF	"	"
		(Cr tube)				
Ba	20 secs	24	80	LiF	Scint.	Coarse
Zr	40	24	80	"	"	"
Y	40	24	80	"	"	"
Sr	40	24	80	"	"	"
Rb	40	24	80	"	"	"
Zn	100	32	60	"	"	"
Cu	100	32	60	"	"	"
Ni	100	32	60	"	"	"
Pb	100	32	60	"	"	"
As	40	32	60	"	"	"
		(W tube)				

(ii) To avoid redistribution of the trace element spike

(iii) To reduce attenuation of long wavelength radiation by the mylar support.

Silicate samples were prepared in a similar manner.

7.2.1.2. Analytical Standards

A lack of suitable ore standards made it necessary to prepare a series of artificial standards using high-purity ferric oxide:

Series "A" - a set of Fe-Si standards containing varying proportions of Fe_2O_3 and SiO_2 (briquettes).

Series "B" - a set of Ca-Mg-Al-Mn standards made by diluting a $CaCO_3$, MgO, Al_2O_3, MnO_2 master mix with a 90% Fe_2O_3: 10% SiO_2 base briquettes).

Series "C"- a set of trace element standards made by spiking spectroscopically pure Fe_2O_3 with various compounds:

(a) subset "C-a" As, Ba, Cu, Ni, Rb, Sr, Ti Zn

(b) subset "C-b" Y, Zr.

(c) subset "C-c" Pb

Because of possible remobilisation of the spike by mowoil, trace element standards were used in the powder form. An absence of major variation in the bulk chemistry of the ores greatly facilitated the preparation of the standards since they could be matched by simple Fe_2O_3 - SiO_2 mixtures. Silicate standards presented no problem and silicate unknowns were analysed against a series of departmental research standards which included several International Standards (e.g. G.1, G.2, G.S.P. 1, etc.)

7.2.1.3. Background, Line Interference and Matrix Effects

To determine the background beneath the peaks, weighted means were calculated from the background counts taken on either side of the peak position. These were then checked against the corresponding values for Fe_2O_3 blanks to examine the errors introduced by tube contamination and linear interpolation on non-linear backgrounds. Copper, nickel and zinc impurities in the tungsten target were significant at the 3σ level and appropriate adjustments were made to the working curves (Cu, Ni, Zn).

Spectral interference from higher order lines was eliminated by using pulse height discrimination in conjunction with the analysing crystal. This technique simultaneously reduced the background contribution from scattered primary X-rays, thus improving the signal-to-noise ratio. Energy filtering does not however differentiate lines of equal energy and for the overlaps. As $K\alpha$/Pb $L\alpha$, Y $K\alpha$/Rb $K\beta$ and Zr $K\alpha$/Sr $K\beta$ it was necessary to measure the interference directly on single element standards.

In a haematite matrix 28% Pb appears as As $K\alpha$, 7% Sr appears as Zr $K\alpha$ and 17% Rb appears as Y $K\alpha$. For the lighter silicate matrix the interference are slightly higher and 37% Pb appeas as As $K\alpha$, and approximately 15-20% of Sr and Rb appear as Zr $K\alpha$ and Y $K\alpha$ respectively.

Deviations from the linear relationship between concentration and fluorescence intensity due to matrix effects were minimised by choosing standards physiochemically similar to the unknowns. This ensured a constant mass absorption coefficient and avoided the need for a heavy absorber or internal standard. Recalculation of the analyses using a matrix correction computer programme resulted in over-compensation

for total iron; values frequently exceeding the stoichio-metric composition for haematite. In view of this descrepancy, subsequent data evaluation methods used only the uncorrected analyses.

7.2.1.4. Analytical Sensitivity and Precision.

XRF spectrometry is subject to several different sources of error, the most important of which are:

(i) Power supply drift

(ii) Goniometer drift

(iii) Sample Preparation

(iv) Mass absorption effects

(v) Counting statistics

The first two are functions of machine instability and were monitored by running standards before and after each batch of unknowns. Errors attributed to sample preparation and matrix effects were dealt with as described above. Compared to conventional chemical methods, the fifth source of error is unique to XRF analysis since it involves the counting of discrete quanta. Variations in N, the number of X-ray photons detected in a given time, are described by a Poisson distribution. For values of $N>50$, this approximates to a Normal distribution for which the standard deviation $\sigma = \sqrt{N}$. Thus the probability of the true mean N lying between certain limits can be defined in terms of the standard deviation.

In accordance with established procedures an element was considered present if the peak counts were greater than three times the square root of the background counts beneath the peak (i.e. $N_{PK} > 3 \cdot \sqrt{N_{Bgd}}$). By adopting a 3σ significance level the following minimum detection limits were calculated:

As 8ppm, Bi 15 ppm, Ba 15ppm, Cd 10ppm, Cu 10ppm, Mn 17 ppm, Ni 8 ppm, Pb 8ppm, Rb 4ppm, Sr 8ppm, Ti 8 ppm, Y 4ppm, Zn 4ppm, Zr 6 ppm.

An estimate of the precision is given by the correlation coefficients for the best fit linear regression lines for the standard working curves:

As 0.998, Ba 0.996, Cu 0.998, Mn 0.995, Ni 0.996, Pb 0.997, Rb 0.997, Sr 0.998, Ti 0.996, Y 0.998, Zn 0.998, Zr 0.998.

7.2.2. Thermometric Analysis of Fluid Inclusions

Fluid inclusions were used to determine the temperature and salinity of fluid responsible for the deposition of the gangue minerals associated with the ores. The temperatures were estimated by determining the filling temperatures of two phase liquid-vapour inclusions on a heating stage (i.e. the disappearance of the vapour bubble during heating) Salinites, expressed as wt.% equivalent NaCl, were estimated by measuring the depression of freezing point for the inclusion liquids on a freezing stage (i.e. the temperature at which the last ice crystal melts). The equipment used was designed and built by Sawkins in 1965, and fitted onto a Leitz microscope. For details of the theory, assumptions and history of fluid inclusion analysis the reader is referred to Ingerson (1947), Smith (1953), Sorby (1858), Roedder (1962, 1971) and Yermakov (1965).

7.2.2.1. Equipment

(i) Heating Stage

The heating stage as shown in figure 9 comprised a central brass tube surrounded by a nichrome heating coil and insulated by annular

FIGURE 9

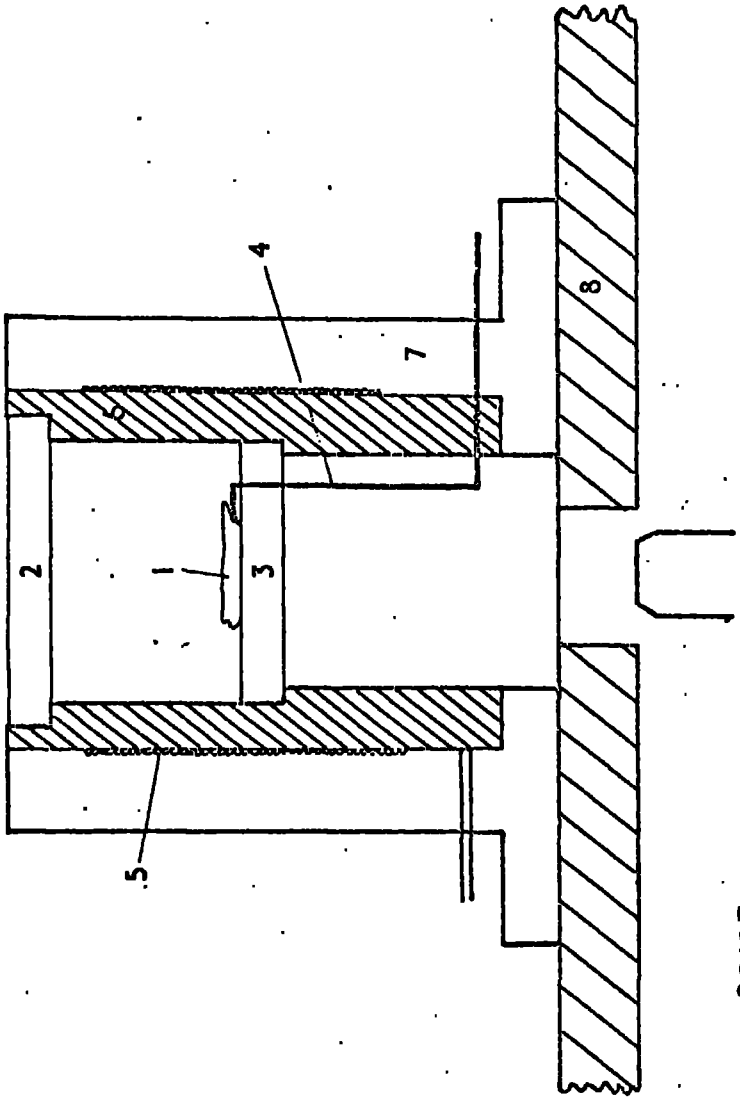

DIAGRAMMATIC SKETCH OF THE HEATING STAGE

sections of asbestos. Samples were placed on a fixed quartz plate to ensure thermal insulation. A 6 amp variac transformer controlled the heating and temperatures were measured using a chromel-alumel thermocouple in contact with the mineral sample. The e.m.f. developed at the thermocouple junction was compared to an ice water junction and the resulting signal displayed on a multi-range Phillips chart recorder.

(ii) Freezing stage

The basic feature of the freezing stage (Figure 10) was a tuffnol cube containing an aluminium tube with an hexagonal outer surface and circular inner surface. Around the outer surface were six thermo-modules which when actuated by a D. C. current transferred heat from the aluminium/module interface to the opposite interface where it was dissipated by a flow of circulated chilled water. Two 4 mm thick quartz plates complete the cell; the lower plate being firmly sealed to the inner surface of the tube. Using an acetone filling as a thermal medium, temperatures as low as -20°C could be attained. A similar thermocouple to that in the heating stage was used to measure the temperature.

7.2.2.2. Sample Preparation

Samples were mounted in cold setting Araldite resin and given a standard metallographic polish. Approximately 2mm thick slices were then removed and the sawn surfaces polished to produce double-sided polished sections. The thickness of individual samples was determined solely by their transparency and for milky quartz or calcite crystals it was sometimes necessary to reduce this value to 1 mm to permit optical examination of the inclusions. Areas of primary inclusions (i.e. those formed contemporaneously with the enclosing crystal host) were located, marked and broken away from the section.

FIGURE 10

DIAGRAMMATIC SKETCH OF THE FREEZING STAGE.

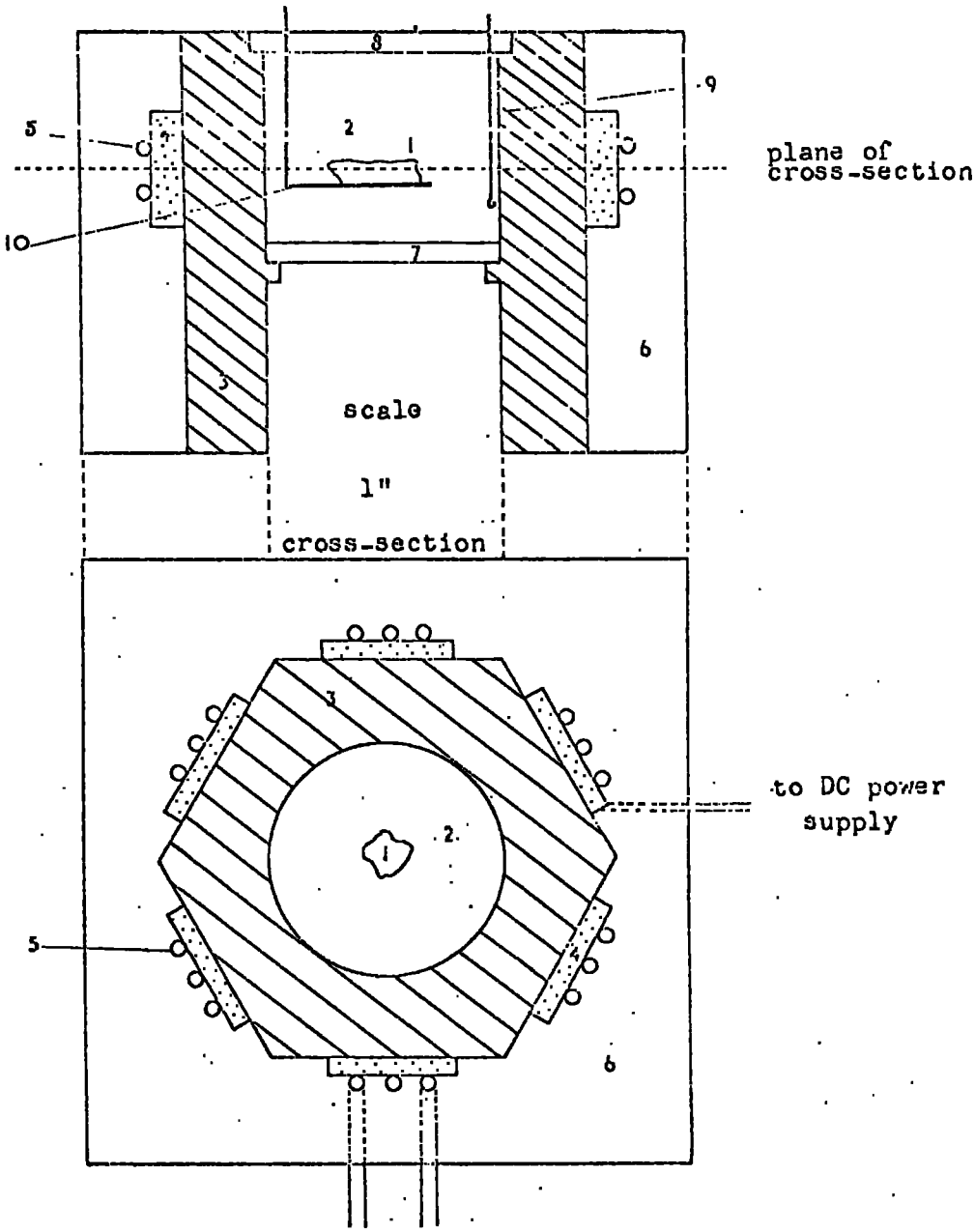

1 specimen
2 acetone filled chamber
3 inner aluminium jacket
4 thermomodules
5 cooling water
6 tuffnol cube
7 lower quartz plate
8 upper quartz plate
9 thermocouple
10 speciman holder

7.2.2.3. Heating Method.

The selected mineral fragments were loaded into the cell in contact with the thermocouple and covered by the upper quartz window. Heating rates were reduced to 1° - 2°C/Min. on approaching the homogenization point to keep thermal gradients in the cell to a minimum and to prevent thermal lag within the specimen.

7.2.2.4. Freezing Method

The inclusions were first frozen in a dry ice-acetone mixture (- 78.5°C) and then quickly transferred to the precooled acetone filled chamber on the stage (- 20°C). By controlling the power input to the thermo-modules the temperature of the chamber was gradually raised until the last ice crystal in the inclusion had melted. The wt. % equivalent NaCl corresponding to the observed depression of freezing point was then calculated from the phase diagram for the system NaCl - H_2O (Figure 11).

7.2.2.5. Discussion

Calibration of the thermocouple was carried out at regular intervals by observing the melting point of known substances loaded into short lengths ofcapillary tubing. The following organic compounds were found to be suitable:

Acetoxime	61°C
8 - hydroxyquinoline	73°C
Sucrose octa acetate	82°C
m-Nitrophenol	95°C
Resourcinol	110°C
Benzoic acid	122°C
Urea	132°C
α Benzoinoxime	152°C
Succinic acid	186°C

Accuracy was estimated to be $\pm$ 2°C

FIGURE 11

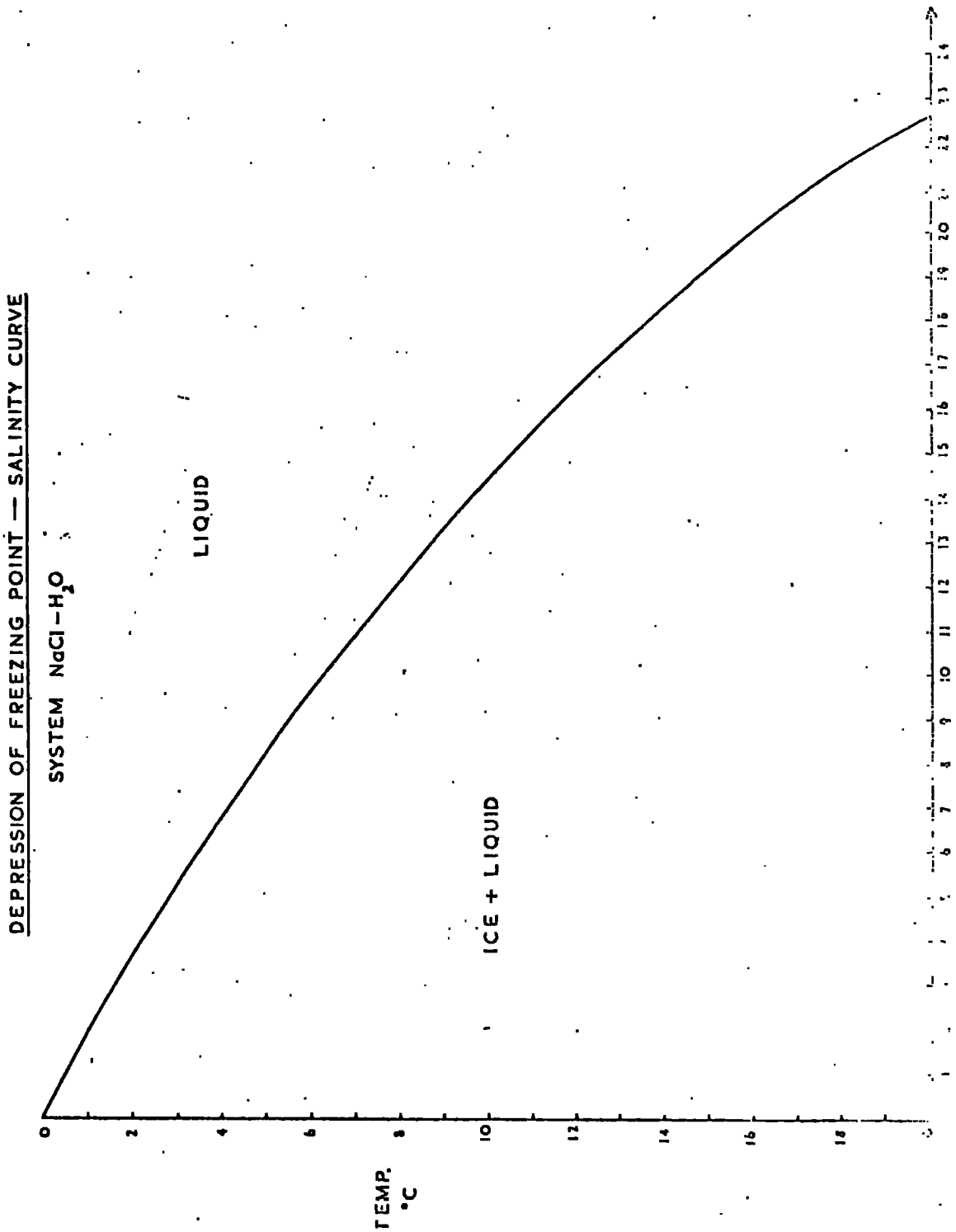
DEPRESSION OF FREEZING POINT — SALINITY CURVE
SYSTEM NaCl-H2O
LIQUID
ICE + LIQUID
TEMP. °C
WT. % NaCl
0
2
4
6
8
10
12
14
16
18
20

Most of the inclusions studied were subspherical or multifaceted in form and no larger than 150 μm in diameter. Homogenization measurements were repeated twice as a check against possible leakage during the first heating run. For very small inclusions (< 10 μm) the increased surface tension forces gave filling temperatures several degrees below those of larger cogenetic inclusions. They also exhibited fluid hysterisis where on cooling the vapour bubble reappeared 3°-5°C below the observed filling temperature.

The heating stage presented no serious problems but very little success was achieved with the freezing stage. As a result only 5 salinity measurements were obtained in the time available. In retrospect, excluding thermo-module failures, this can now be shown to be due to inclusion metastability. Recent studies by the author at the Institute of Geological Sciences 1972-73 using a different technique have demonstrated a pronounced supercooling phenomenon of the inclusions in calcite and quartz crystals from the West Cumberland orefield. (Ice nucleation requires 2 - 3 hours at - 170°C). This evidence seriously questions the validity of previous salinity data described as being greater than the maximum limit of the tuffnol cube equipment.

FIGURE 5

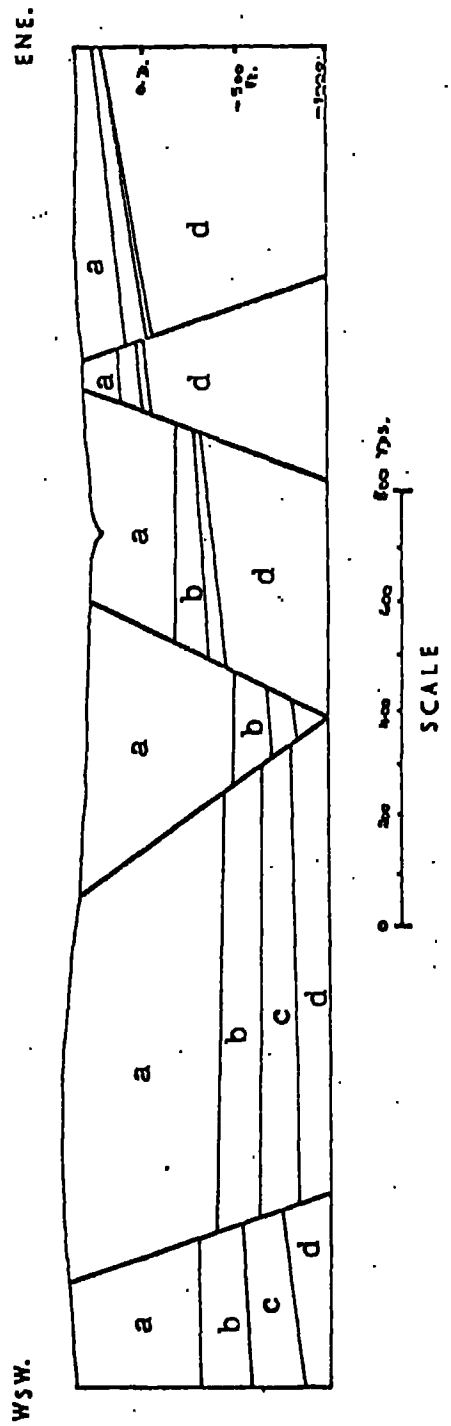

KEY

a. St.Bees Sandstone
b. Brockram
c. Carboniferous Limestone Series
d. Borrowdale Volcanic Series

SECTION THROUGH THE BECKERMET – HAILE AREA

showing Permo-Triassic transgression

8. STATISTICAL TECHNIQUES

8.1. Introduction

To help interpret the ore geochemistry various numerical techniques were used to reduce the complex multivariate data to a more manageable form. In addition to calculating the standard functions of central tendency and dispersion (arithmetic mean, standard deviation and variance), three advanced analytical methods were used: linear discriminant function analysis (L.D.F.A.), trend surface analysis (T.S.A.) and factor analysis (F.A.). Comprehensive accounts of these techniques can be found in several recent texts (Krumbein and Graybill 1965, Harbaugh and Merriam 1968) and only brief descriptions have been given to illustrate their application to the present data. Being parametric techniques the variables are assumed to be normally distributed and to ensure that this requirement was satisfied each variable was examined to determine the nature of its distribution. However, because of mixed populations it was necessary to supplement the primary visual classification of the ores by an objective classification based on total chemistry. For this purpose linear discriminant function analysis was selected despite the limiting "a priori" assumption of normality. It was considered that skewed distributions would have less effect in distinguishing diverse ore types than in isolating the components of variance in a single ore population. Due to sample size restrictions L.D.F.A., T.S.A. and F.A. were only applied to ores from the West Cumberland orefield.

8.2. Linear Discriminant Function Analysis (L.D.F.A.)

The technique operates by computing a linear combination of "m"

variables that most efficiently separates two groups of samples in "m" dimensional space such that the ratio of the between-groups variance to the within-groups variance is maximised.

$$R = \sum_{i=1}^{m} \lambda_i x_i$$

where x = variable :- Eq. - 1

λ = constant

An estimate of the separation is given by the Mahalonobis Generalised Distance (D^2) which is obtained by substituting the difference between variable means $\Delta \overline{X_i}$ into the discriminant function.

$$D^2 = \sum_{i=1}^{m} \lambda_i \Delta \overline{x}_i \qquad :- \text{Eq. - 2}$$

The larger the value the greater the discrimination. The significance of (D^2) can be tested as a normal "F" statistic.

$$F = \frac{(N_2 N_1)(N_2 + N_1 - m - 1)}{m(N_2 + N_1)(N_1 + N_2 - 2)} \cdot D^2 \qquad :- \text{Eq. - 3}$$

for m, $N_1 + N_2 - m - 1$ degrees of freedom.

For the haematite ores, L.D.F.A. was used to screen the raw sample populations for atypical ores due to wall rock contamination, mixed ore intergrowths and surface weathering. As certain elements were known to be lognormally distributed the data was first converted to the $\log_{10}$ form as a necessary precaution. On entering 33 botryoidal ores, 211 massive ores and 17 chemical variables into the discriminant function, the strongest discriminating variables were shown to be As 33%, Rb 20%, Ba 12%, Ti 8% Cu 6%, Pb 5%, Zn 5% and Sr 4%.

68 of the massive ores were rejected at the 0.01 significance level and 43 at the 0.05 level. Closer examination revealed that 24 were contaminated by small amounts of botroidal ore or silicified wallrock and were thus incorrectly chosen. The remaining samples were either misclassified because of extreme trace element values or were genuinely below the adopted significance level (i.e. a type II statistical error). For the original 33 botryoidal ores, 7 were rejected at the 0.01 and 0.05 levels of significance, of which 4 were misclassified because of very low Pb and Ba values. The corresponding D^2 and F (17, 226) values were 33 and 518 respectively (i.e. highly significant at the 0.001 level F (15, 120) = 3.36). The computer programme used was the I.B.M. Fortran IV Discriminant Function programme which included a useful printout of the probabilities associated with the largest discriminant function. This permitted the most suitable samples from each locality to be chosen for further study.

To summarise, L.D.F.A. provided a quantitative method for screening several hundred massive and botryoidal ores from the West Cumberland orefield. Samples accepted at the 0.01 significance level were considered to have population identity probabilities >99% and formed a pool of reliable samples for further statistical tests.

8.3. Frequency Distribution Analysis (F.D.A.)

96 of the screened West Cumberland massive ores (one from each locality) were then examined to determine the distribution characteristics of the geochemical variables. After rejecting samples below the detection limit, histograms were constructed using both normal and $\log_{10}$ data. As expected the normal data showed a predominance of positively skewed distributions which became approximately lognormal after applying a $\log_{10}$

transform. Notable exceptions were Fe, Rb, Sr and Ca which remained skewed. The plots also revealed a number of discrete subpopulations indicating subtle variations within a single population. By comparison, results for the botryoidal ores were poor because of an insufficient number of samples and the corresponding histograms have therefore been omitted. A full description and geological interpretation of the F. D. A. results is given in chapter 9.

8.4. Trend Surface Analysis (T. S. A.)

In an attempt to identify the major channelways of the mineralizing fluids in the West Cumberland orefield trend surface analysis was used to differentiate between local and regional variations in ore geochemistry. T. S. A. is an empirical technique for isolating the components of variation in numerical map data by computing a least squares regression surface. (i. e. an extension of 2- dimensional linear regression analysis into 3-dimensional space). The total variation is considered to comprise three smaller components of varying magnitude:

(i) A regional component which extends over most of the area and reflects a major geological process.

(ii) A local component which consists of deviations from the regional due to processes in restricted areas.

(iii) A noise component which includes data error and very localised geological factors.

The regression surface or "trend surface" is computed by fitting a polynomial regression equation to the observed data of the type:

$$Z = b_0 + b_1X + b_2Y + b_3X^2 + b_4XY + b_5Y^2 \text{---} b_nY^m$$

Where Z = variable; X and Y = grid co-ordinates b = coefficients of X and Y

;- Eq. - 4

Polynomials are used because they approximate to a wide variety of other smooth continuous functions. The precise form of the surface is that for which the sum of squares of the differences between the observed and calculated values is a minimum. Thus the trend surface contains the regional component whilst the residuals include the second and third components of variation. Where residuals are autocorrelated (i.e. clusters of + and - values) the second component is considered dominant but where adjacent values are unrelated the deviations are attributed to noise and extreme local variation.

By introducing higher order polynomial terms into Eq. - 4 a series of progressively more complex surfaces can be generated. These are generally named according to the highest polynomial term entered into the regression.

	Linear Component	Quadratic Component	Cubic Component
Linear Surface contains the terms	(X, Y)		
Quadratic " " " "	(X, Y)	+ (X^2, XY, Y^2)	
Cubic " " " "	(X, Y)	+ (X^2, XY, Y^2)	+(X^3, X^2Y, and XY^2, Y^3)

(Also referred to as the 1st, 2nd and 3rd order surfaces)

The total variation (V) is defined as:

$$V = \sum (Zobs. - Zmean)^2 \qquad : Eq. - 5$$

the unexplained residual variation (R) as:

$$R = \sum (Zobs. - Zcalc.)2 \qquad : Eq. - 6$$

and the variation explained by the surface (E) as:

$$E = V-R = \sum (Zobs. - Zmean)^2 - \sum (Zobs. - Zcalc.)^2 \qquad : Eq. - 7$$

The programme used was the Fortran IV programme of the Kansas Geological Survey (O'Leary et al. 1966) which permits the computation and plotting of trend surfaces containing up to the sixth order polynomial term. A failure of the programme however is the method by which the significance of the explained variation is tested (Chayes 1970).

$$\text{Coefficient of Correlation (L)} = \sqrt{\frac{E}{V}} \qquad :- \quad Eq^{n} -8$$

This equation only succeeds in testing the cumulative variation (E) for all terms and merely shows that the reduction in residual variation obtained by the linear surface is not eliminated by the inclusion of higher terms.

Chayes (1970) shows that for a surface to be considered significant the variation associated with the terms of order (K + 1) must be tested against the residual variation at order (K + 1). Thus for a cubic surface, only the terms (X^3, X^2Y, XY^2, Y^3) should be tested against the residual and not the combined linear/quadratic/cubic terms. By judiciously using an "F" test it can then be decided whether the average variation per term of order (K + 1) is greater than that associated with each degree of freedom of noise. "The Occam Razor Rule". On applying this test to West Cumberland ores it was shown that the elaborate high order surfaces produced by the Kansas programme (up to 40% E) were simply mathematical derivatives of no statistical significance. The failure of the ores to respond to T. S. A., with the exception of a small number of linear surfaces, can be attributed to two main causes:

(i) Presence of strong local and noise components in the data superimposed on a gently inclined regional surface.

(ii) Poor distribution of data points due to clustering and elongation of the test area.

The first is an invariable function of the data, for which there is no solution, while the second produces distortion of the trend surface. Doveton and Parsley (1970) have recently shown that allowances for this distortion can sometimes be made using geometrical models to simulate the problem. Their work clearly indicates the dangers of interpretion but was conducted on "high explanation" surfaces, quite different from those of the haematite ores. A summary of the T.S.A. work is included in chapter 11.

8.5. Factor Analysis (F.A.)

Factor analysis is a multivariate technique developed primarily by psychologists for determining the number of elements in a complex multivariate set which describe the whole set (i.e. a small number of linear combinations "factors" of "m" variables). Detailed descriptions of this method and its geological application are given by Krumbein and Graybill (1965) and Miller and Cain (1962). The programme used was the University of Durham "R - mode" factor analysis programme written by Reeves (1970) which examines the relationship between variables. It adopts the principal components technique for fitting orthogonal factor axes followed by their rotation, first orthoganally "Varimax solution" and then obliquely "Promax solution". These rotations progressively improve the best fit positions of the factor axes in "m" vector space with those of the original variables. Theoretically the number of factors extracted depends upon the number of non-zero eigen values in the correlation matrix. However because of sampling and analytical errors the zeros are never quite zero and in the present study factors accounting for less than 3%

of the total variation were excluded. Chapter 12 presents a full description and interpretation of the F. A. results for the West Cumberland massive ores.

9. ORE GEOCHEMISTRY

9.1. Introduction

This chapter refers mainly to the geochemical data for samples from the West Cumberland orefield because they are considered to be:

(i) More spatially representative of the mineralization.

(ii) Sufficiently numerous to allow significance tests to be carried out on the derived statistics.

Using only screened material the West Cumberland orefield is established as the type area for mineralization, and comparisons made with ores from other environments in the province. Special consideration is given to the geochemical similarity between trace element assemblages in the Eskdale-Ennerdale complex and those in the cross-cutting haematite veins. Sub-populations in element frequency distributions are attributed to variations in wall rock chemistry and wall rock - ore fluid interactions.

A less rigorous interpretation is possible for ores from the Lower Palaeozoic vein deposits because there are too few reliable samples to permit a thorough statistical analysis. Furthermore only the botryoidal ores can be used since the massive ores, especially those from veins in the Skiddaw Slate Series, contain pseudo-massive haematite, a product resulting from the silicification and recrystallization of botryoidal ore. The process of morphological convergence is also accompanied by a loss of trace elements particularly As, Cu, Ni, Pb and Zn. Fortunately pseudo-massive ores are not known to be associated with metasomatic replacement orebodies and thus do not invalidate the following conclusions.

9.2. Replacement Ores from the West Cumberland Orefield

The occurrence of discrete sub-populations in several element

frequency distribution graphs indicates that the parent populations are not entirely homogeneous. Recognition of these subgroups is important because they influence the values of correlation coefficients and provide additional information on the genesis of the ores. Simplified diagonal correlation matrices for the massive and botryoidal ores are given in figures 12 and 13.

(N. B. Because it was necessary to reject values below the 3 σ detection limits the total number of samples in each histogram varies slightly).

In interpreting the ore chemistry one must also consider the direct and indirect influence of the wallrocks. Massive ores representing the end product of replacement should contain a strong residual component of the wall rock chemistry whereas botryoidal ores should provide a closer approximation of the primary ore fluid composition. This ideal is rarely achieved however because of material entering into solution at the site of deposition and continually modifying the fluids. Botryoidal ores contain therefore a small but additional component of the wall rock chemistry.

(i) Iron and Silicon (Fig. 14)

Differences between the mean iron and silica contents for the two ores are readily explained by the presence of quartz intergrowths and quartz filled vugs in the massive ore and their absence in the botryoidal ore. The weakly developed bimodality for Fe in the massive ores and the suspected polymodal irregularities for Si before smoothing are thought to reflect subtle differences in the physicochemical nature of the original wallrocks or small changes in the mechanism of metasomatism. Average analyses for quarried limestones in the West Cumberland area(Daysh 1951) indicate that sufficient silica is available from within the system without

FIG. 12. SIMPLIFIED DIAGONAL CORRELATION MATRIX FOR THE MASSIVE ORES, WEST CUMBERLAND (Log_{10} Data)

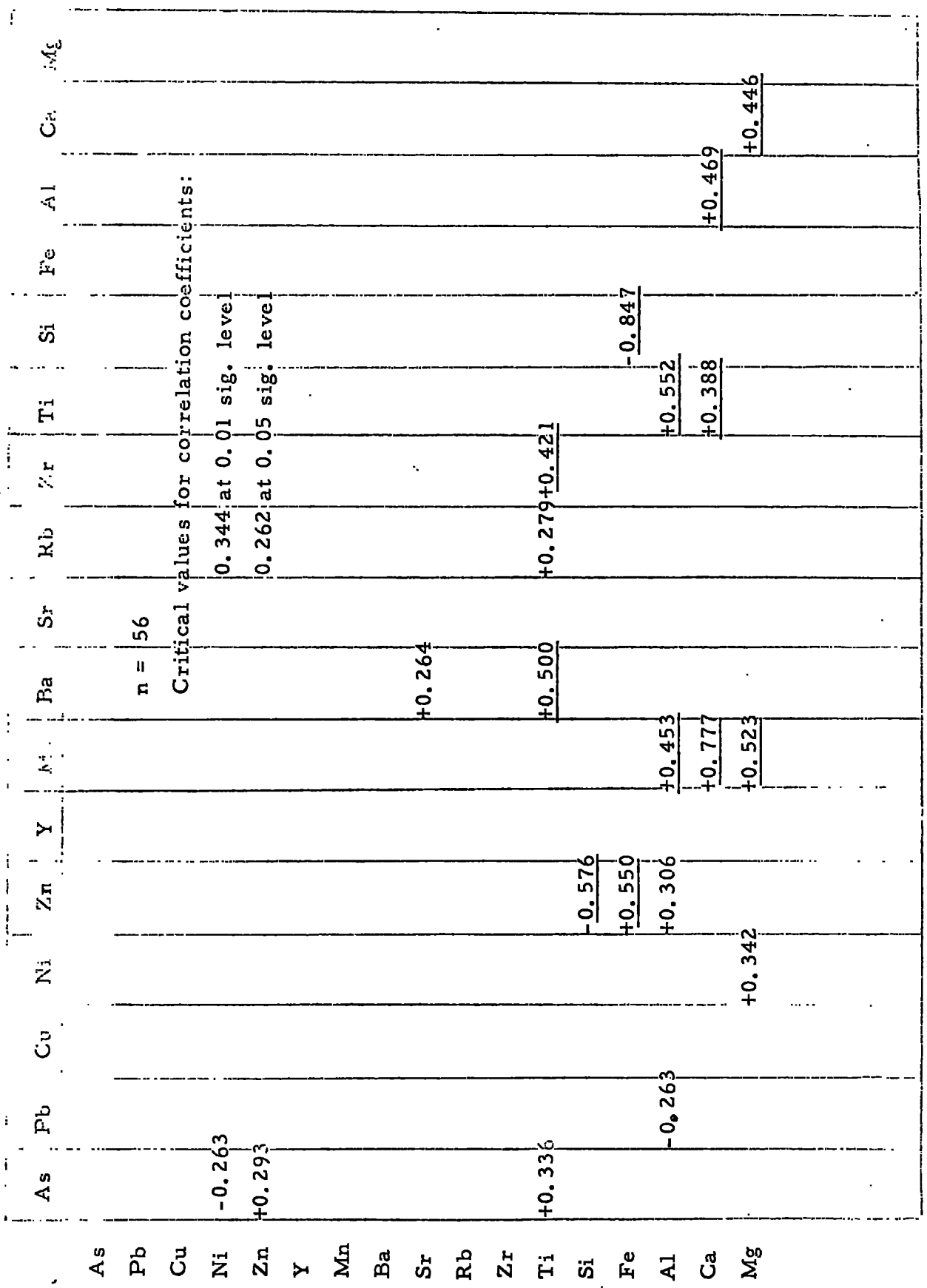

FIG. 13 SIMPLIFIED DIAGONAL CORRELATION MATRIX FOR THE BOTRYOIDAL ORES, WEST CUMBERLAND.

(Log_{10} Data)

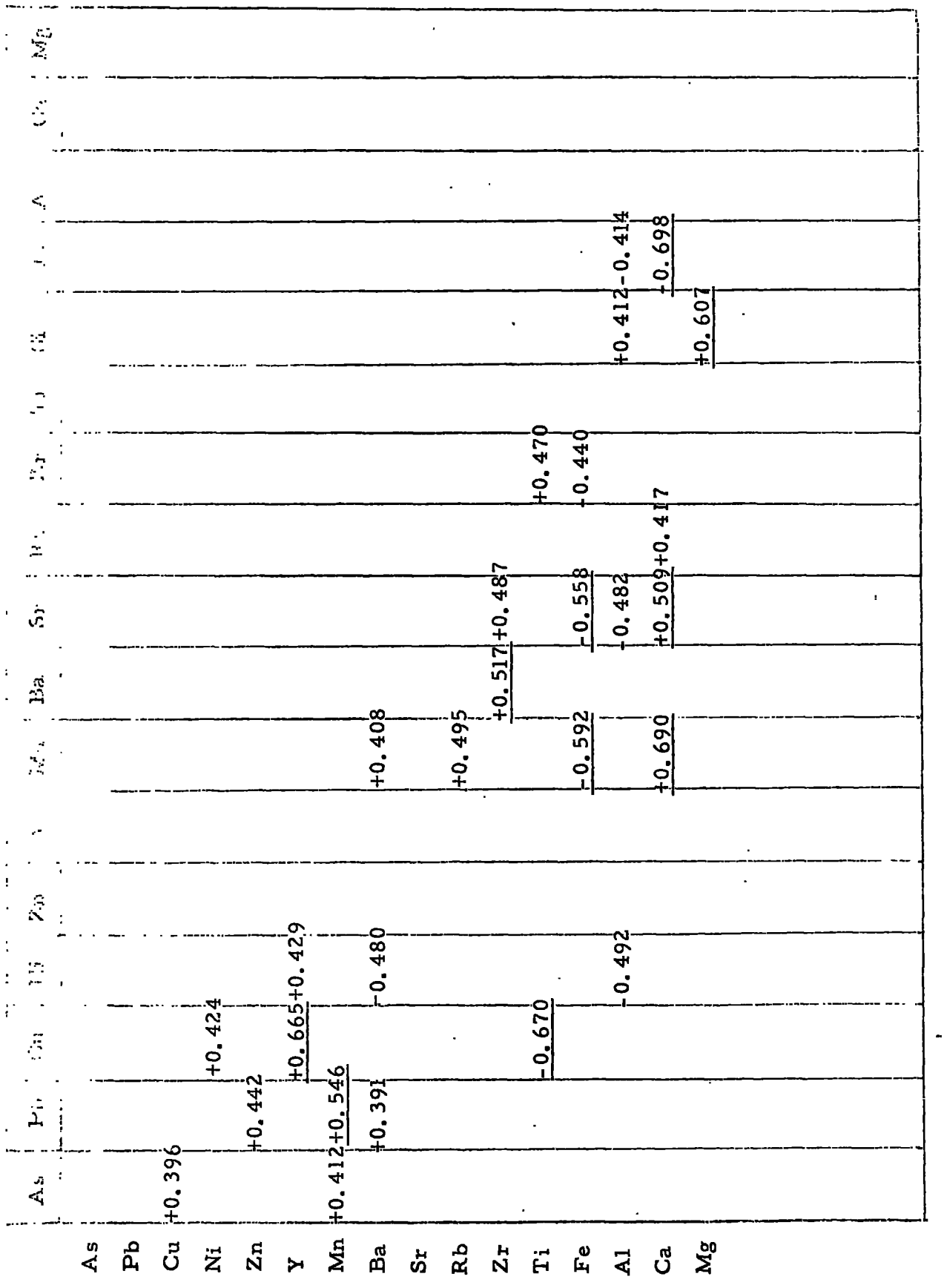

FIGURE 14

FREQUENCY DISTRIBUTION PLOT FOR SILICON

log (Si)

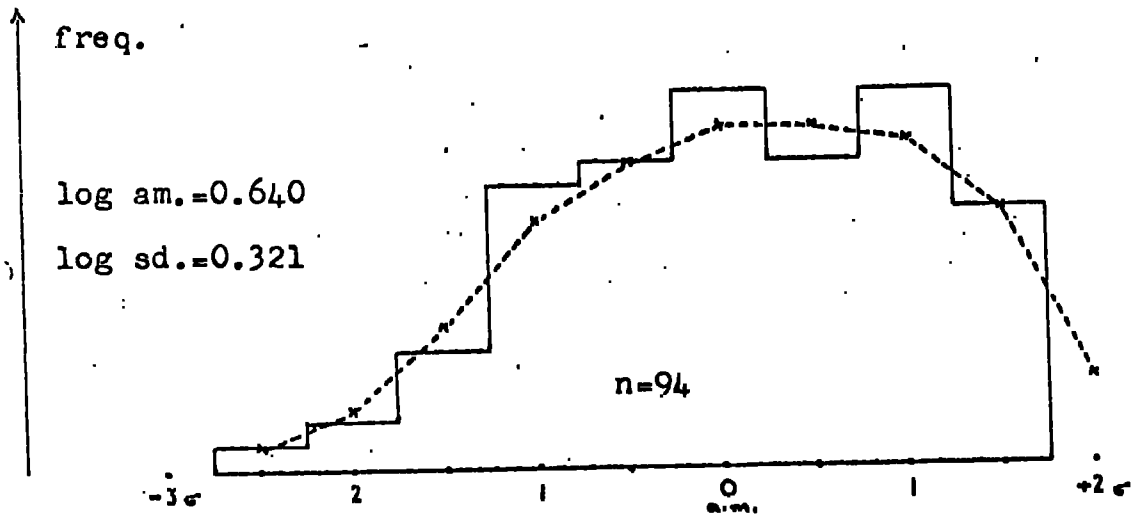

-------smoothed by weighting $\frac{1.2.1}{4}$

FREQUENCY DISTRIBUTION PLOT FOR IRON

log (Fe)

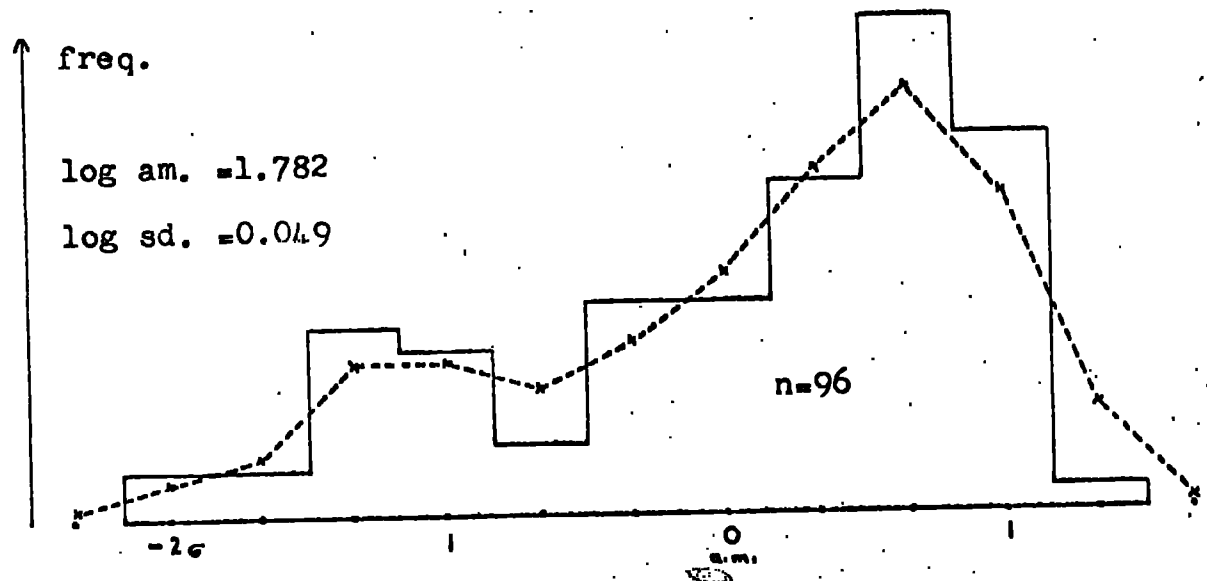

------ smoothed by weighting $\frac{1.2.1}{4}$

requiring a major contribution from the primary ore fluids. The strong negative covariance Fe : Si (-0.847) is considered to have no geochemical significance and is believed to be an artificial feature generated by the "built-in" interlock of the closed system (Chayes 1960).

(ii) Aluminium, Calcium and Magnesium (Figs. 15 and 16)

A. Massive ores

In agreement with their proposed mode of formation the massive ores display a greater range and concentration of Al, Ca and Mg than the associated botryoidal ores. They also show strong positive correlations for the pairs Ca ; Al (+0.469) and Ca : Mg (+0.466) which suggests that the assemblage Al, Ca and Mg is best interpreted as a residual component of the wallrocks and not as a component of the ore fluids. Furthermore the bimodal distribution for Ca indicates the replacement of two distinct carbonate host rocks whose chemistry is characterised by a difference in total calcium content. The lower subgroup is most probably an expression of those limestones affected by secondary dolomitization which is developed throughout areas of the orefield.

B. Botryoidal ores

Calcium and magnesium contents are related to the abundance of calcite veining and micro-layering in the ores. The Ca/Mg ratios can thus be referred to the composition of carbonates deposited in chemical equilibrium with the orefluids. The negative covariance Ca : Fe (- 0.688) is probably analogous to the Si : Fe relationship for the massive ores.

(iii) Nickel, Rubidium, Strontium, Yttrium, Zinc, Zirconium (Figs. 16, 17 and 18)

These elements all have values very close to their respective detection limits but by including values between the 2σ and 3σ limits it can be shown that the geometric means for Ni, Y, Zn and Zr are slightly

FIGURE 15

FREQUENCY DISTRIBUTION PLOT FOR ALUMINIUM

log (Alx10)

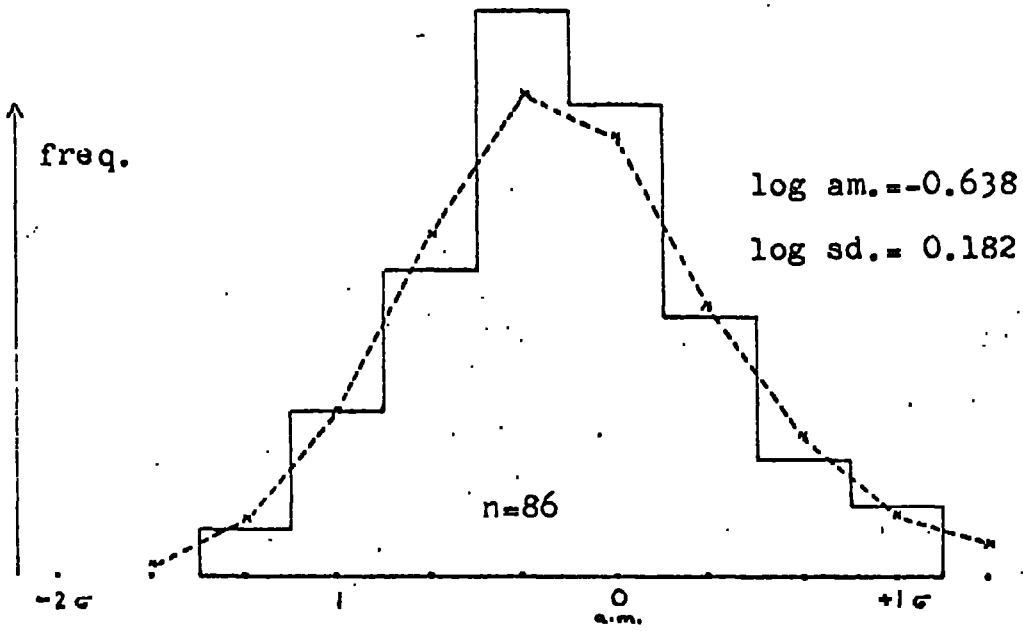

----- smoothed by weighting $\frac{1.2.1}{4}$

FREQUENCY DISTRIBUTION PLOT FOR CALCIUM

log (Cax10)

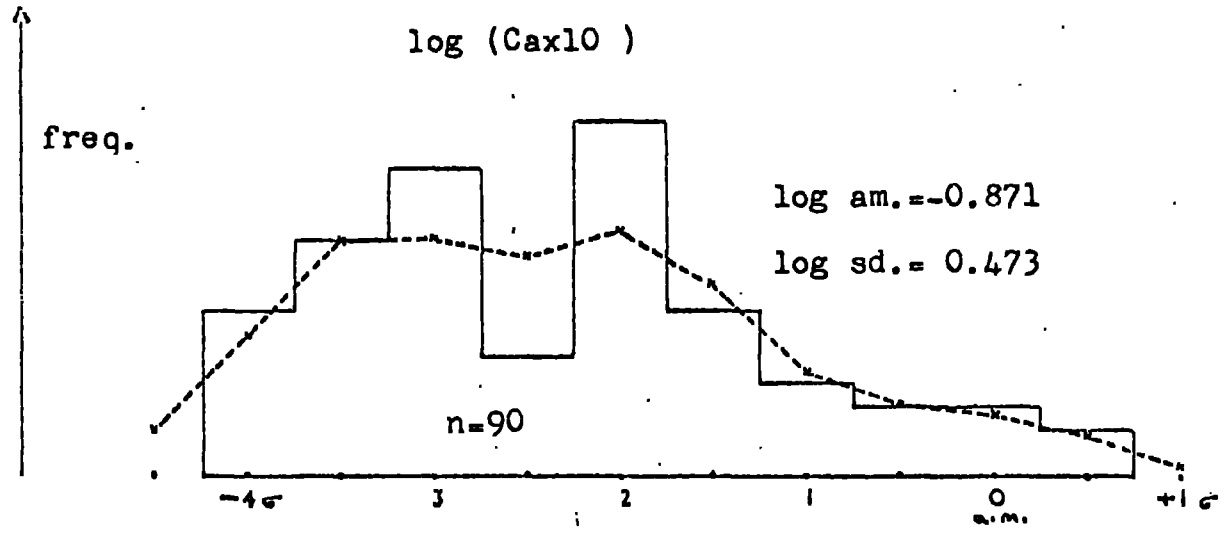

------ smoothed by weighting $\frac{1.2.1}{4}$

FIGURE 16

FREQUENCY DISTRIBUTION PLOT FOR MAGNESIUM

log (Mgx10)

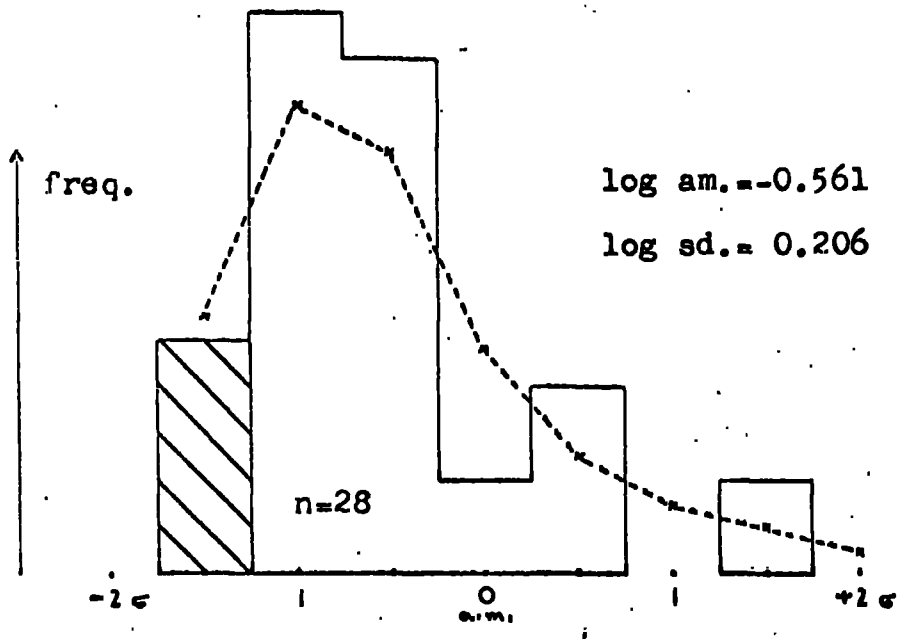

------smoothed by weighting $\frac{1.2.1}{4}$

FREQUENCY DISTRIBUTION PLOT FOR NICKEL

log (Ni)

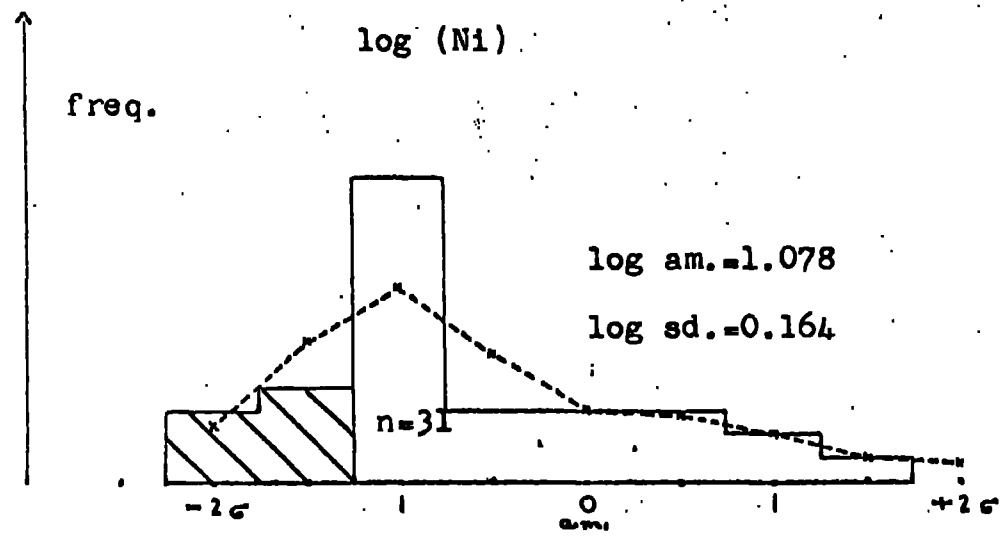

------smoothed by weighting $\frac{1.2.1}{4}$

values between 2σ& 3σ detection limits

FIGURE 17

FREQUENCY DISTRIBUTION PLOT FOR YTTRIUM

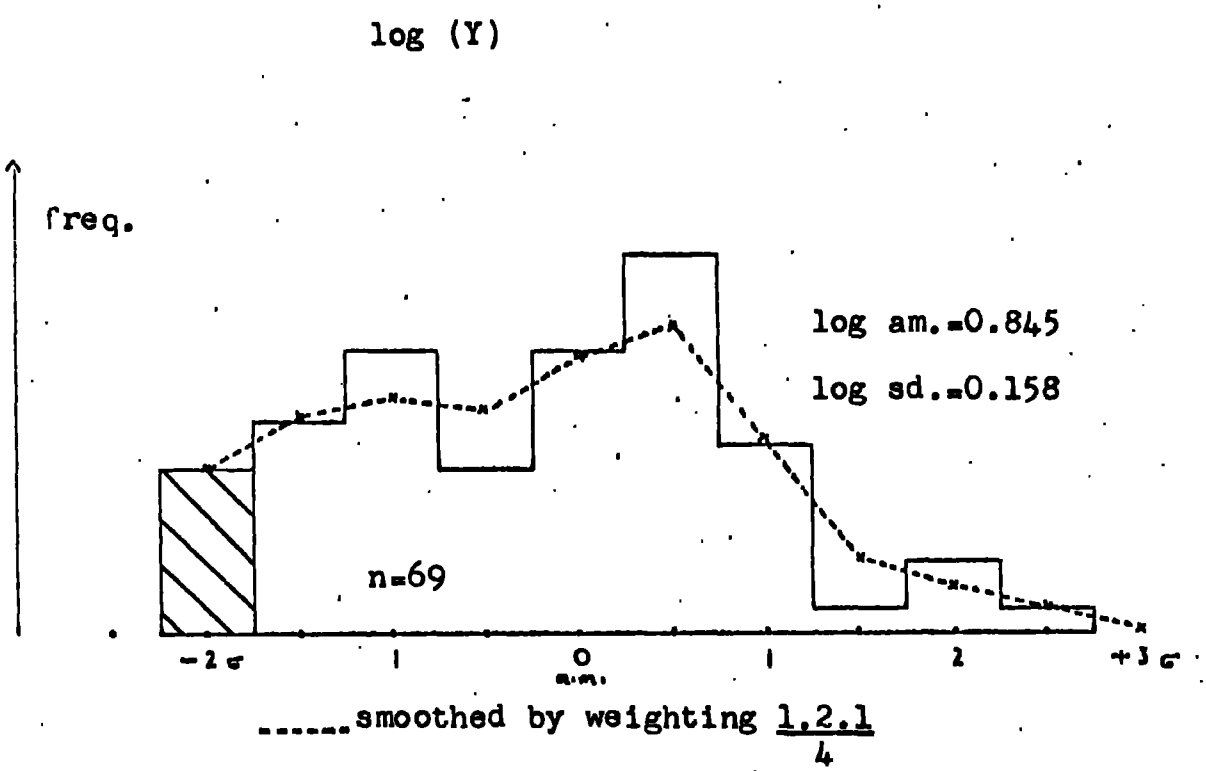

FREQUENCY DISTRIBUTION PLOT FOR ZINC

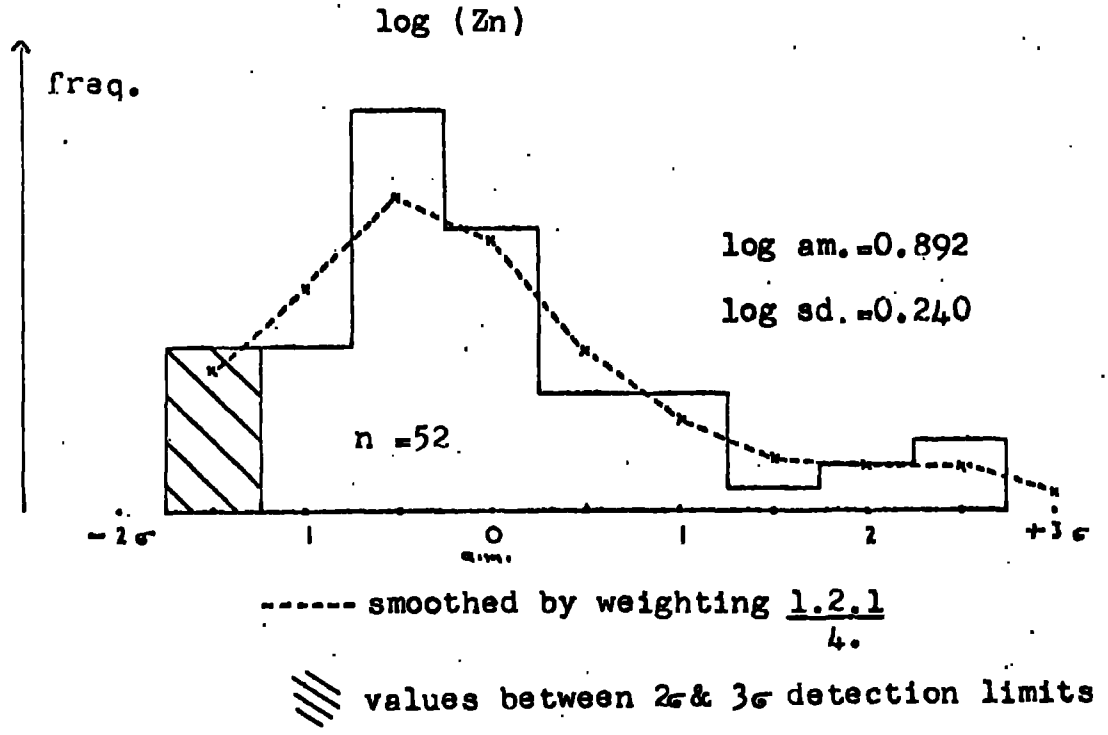

FIGURE 18

FREQUENCY DISTRIBUTION PLOT FOR ZIRCONIUM

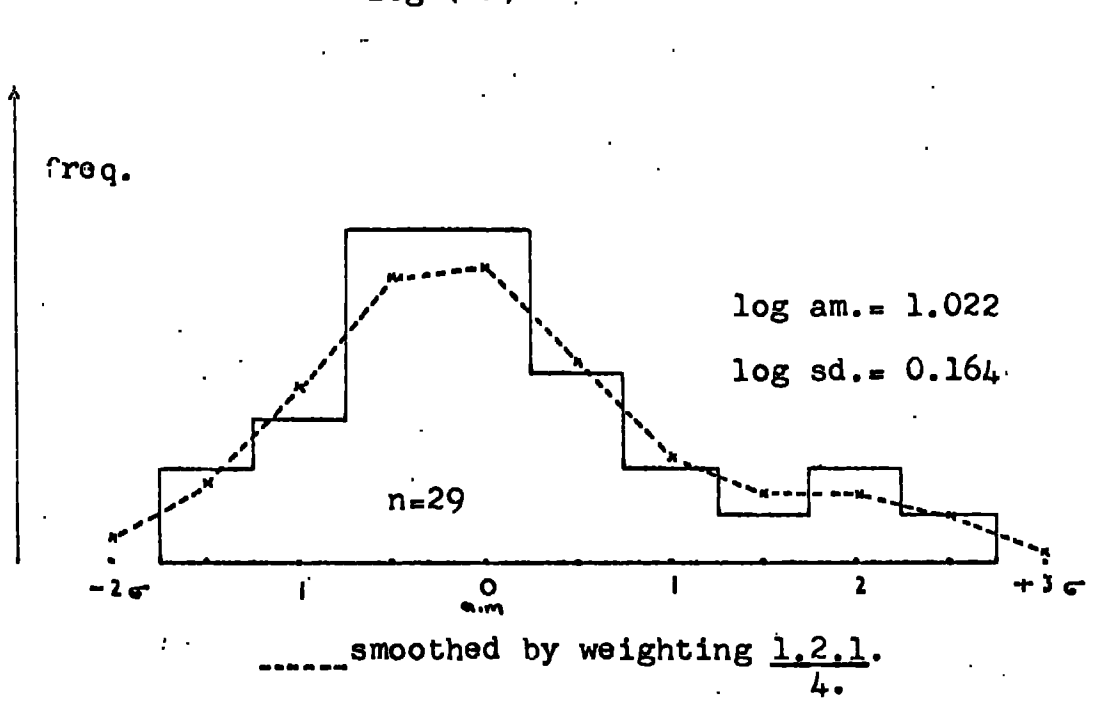

_____smoothed by weighting $\frac{1.2.1}{4}$.

FREQUENCY DISTRIBUTION PLOT FOR BARIUM

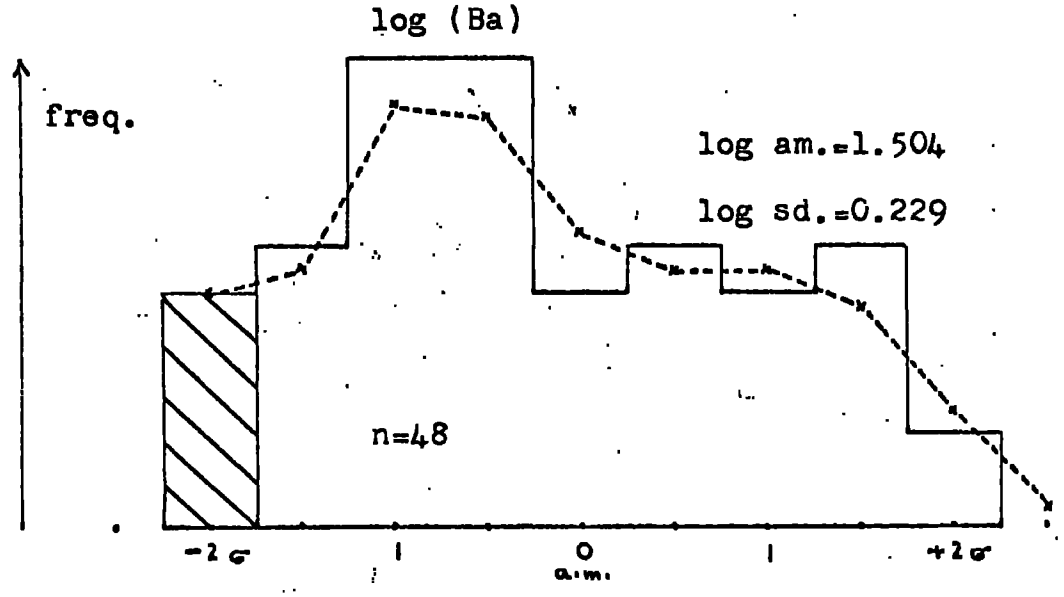

------smoothed by weighting $\frac{1.2.1}{4}$

values between 2σ & 3σ detection limits

above the 3 minimum. For Rb and Sr the means are well below and provide no meaningful estimate of the average ore. However there are a sufficient number of samples with higher Rb and Sr values to permit a limited interpretation of inter-element covariance.

A. Massive Ores

The monomodal distributions for Ni, Y, Zn and Zr are considered to be trace elements expressions of the original wallrocks and cannot be related to any other factor. By comparing high Rb and Sr values with their respective carbonate index values (i.e. Al, Ca and Mg) two important associations emerge:

(a) An association between high Sr values and Ca/Mg > 2; and low values with Ca/Mg < 1.

(b) An association between high Rb values and Ca/Mg < 2 >1 (plus high Al values); and low values with Ca/Mg > 2

Assuming a metasomatic replacement model it is possible to relate these associations to three main carbonate lithologies:

Undolomitized limestone - Ca/Mg ratios >2, high Sr and low Rb
Dolomitized limestone - Ca/Mg ratios <1, low Sr and low Rb
Argillaceous limestone - Ca/Mg ratios <2 >1, high Al and high Rb

The corresponding theoretical correlations with Al, Ca and Mg are not observed and are probably masked by the skewed distributions for Ca, Rb and Sr. In response to the negative covariance between Ca and Fe there is a corresponding antipathetic relationship between Sr and Fe (-0.558).

B. Botryoidal Ores

The positive correlation Ca : Sr (+ 0.509) is thought to represent the presence of small amounts of calcite deposited in chemical equilibrium with the ores and unaffected by post-depositional recrystallization

(iv) Barium, Titanium (Figs. 18 and 19)

A. Massive Ores

A fourfold enrichment of Ti in the massive ores compared to the syngenetic botryoidal ores, together with the covariance Ba: Ti (+0.500) suggests that both Ba and Ti provide a measure of the original clay content of the carbonate wallrock. Simple correlation coefficients do not however indicate the involvement of both elements in the process of intrastratal fluid mixing as revealed by factor analysis and spatial distribution studies. It is only by using these special techniques that one is able to explain the bimodal distributions for Ba and Ti. As shown later the upper Ba sub-population is related to the mixing of the ore fluids with intrastatal fluids.

B. Botryoidal Ores

No obvious explanation can be given for the correlation Ba : Zr (+0.517) but since it also occurs in ores from Eskdale granite it is assumed to be a minor component of the ore fluids. Low Ti values confirm the mechanism proposed for Ti variation in the massive ores.

(v) Manganese (Fig. 19)

A. Massive Ores

Manganese variation is closely related to the variation in total Ca and Ca/Mg of the ore (Mn : Ca (+ 0.777)). The lowest values are associated with ores having a Ca/Mg<1 which agrees with the observed remobilisation of Mn during dolomitization. Conversely the highest values are recorded for samples having a high Ca content and Ca/Mg > 1. Manganese also shows a correlation with Al (Mn : Al (+ 0.453)). Both relationships imply that Mn is a residual component of the carbonate wallrocks.

B. Botryoidal Ores

The possibility of the ore fluids having carried a primary Mn

FIGURE 19

FREQUENCY DISTRIBUTION PLOT FOR TITANIUM

log (Ti)

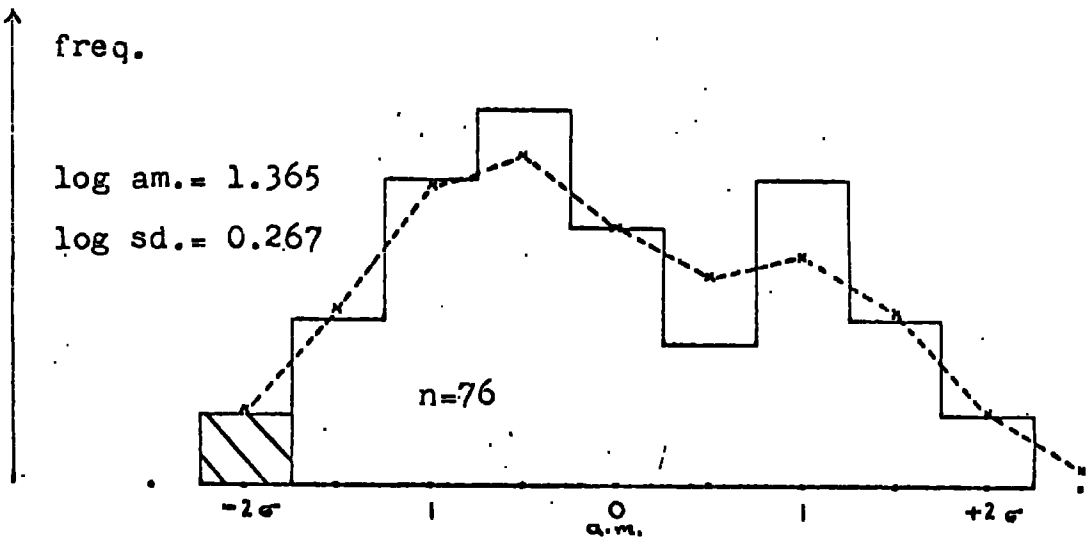

------smoothed by weighting $\frac{1.2.1}{4}$

FREQUENCY DISTRIBUTION PLOT FOR MANGANESE

log (Mn)

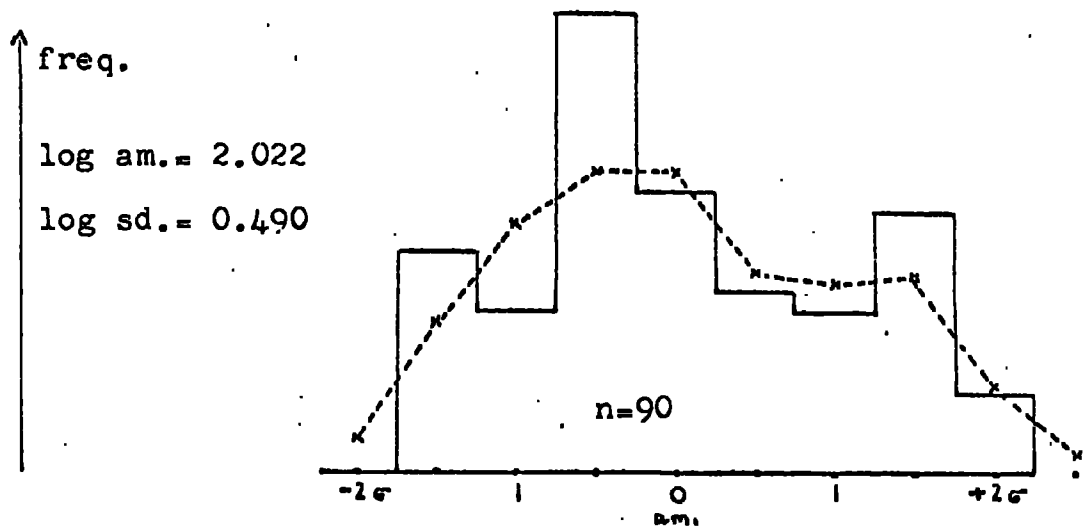

--------smoothed by weighting $\frac{1.2.1}{4}$

values between 2σ & 3σ detection limits

component cannot be disregarded since botryoidal haematite contains at least several hundred ppm Mn, irrespective of its geological environment. However the positive covariance between Ca and Mn (+ 0.690) suggests that Mn concentrations are determined by the amount of included carbonate gangue and that the negative correlation Fe : Mn (- 0.592) is a function of the antipathetic relationship between Ca and Fe (- 0.688). Unfortunately there is no way of calculating the contribution from each source.

(vi) Arsenic, Copper, Lead (Figs. 20 and 21)

Of all the trace elements arsenic is the most distinctive. It is several times more abundant than any other element and in the botryoidal ores its mean value far exceeds the maximum recorded concentration in sedementary iron ores with the exception of oolitic ores from the Kerch Basin, Russia. (James 1966)

A. Massive Ores

Analyses of unmineralized limestone in the West Cumberland area (Appendix II) indicate that arsenic concentrations are well below the detection limit which suggests that the wallrocks are not the original source (c.f. Arsenic crustal abundance 2 ppm. Mason 1958, p. 44).
It also means that As variation in the limestones does not account for the observed bimodal distribution in the ores. Arsenic is therefore best described as a diagnostic component of the primary ore fluids.
For reasons described later Cu is grouped geochemically with As.
Lead values are consistently low and four times lower than in the botryoidal ores.

FIGURE 20

FREQUENCY DISTRIBUTION PLOT FOR ARSENIC

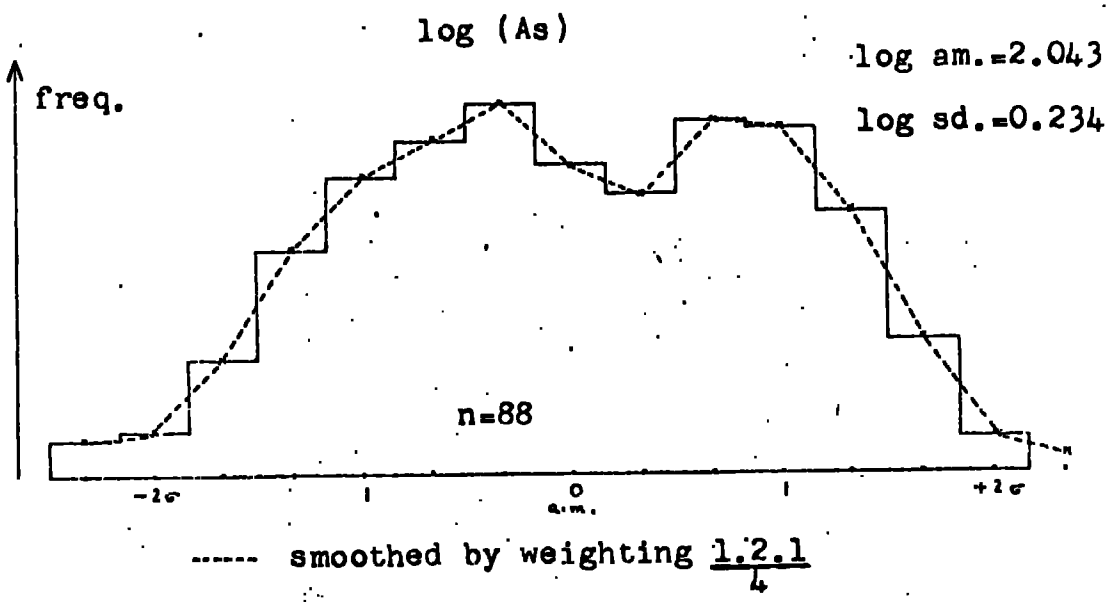

FREQUENCY DISTRIBUTION PLOT FOR COPPER

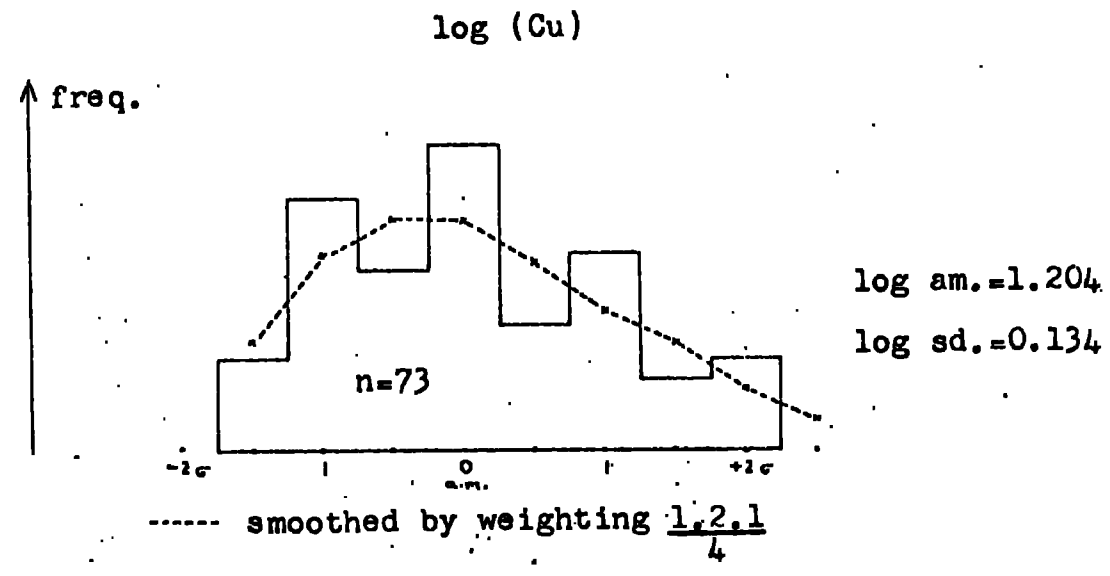

FIGURE 21

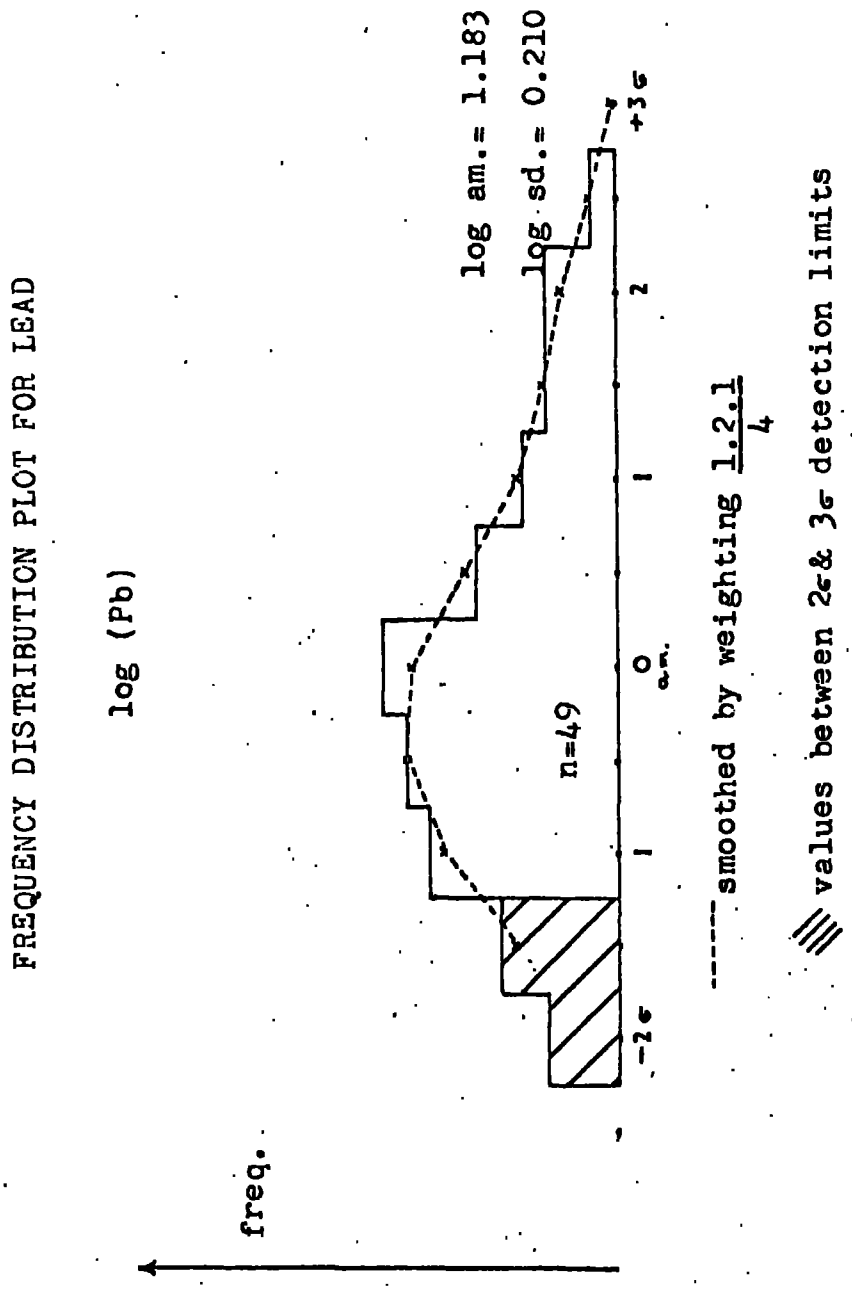
FREQUENCY DISTRIBUTION PLOT FOR LEAD
log (Pb)
log am.= 1.183
log sd.= 0.210
+3σ
2
1
0
a.m.
1
-2σ
n=49
freq.
smoothed by weighting 1.2.1/4
values between 2σ & 3σ detection limits

5. Botryoidal Ores

The high lead content of the botryoidal ores cannot be explained by selective adsorption onto hydrated ferric oxide species because there are no comparable concentrations of other available metals (e.g. Cu, Ni, Ti, Zn). The lead content must therefore be related to the initial lead concentration in the ore fluids. In which case the relative depletion in the massive ores must be due to some mechanism inhibiting the uptake of lead. A similar control may acccount for the pronounced enrichment of arsenic in the botryoidal ores.

9.3. Comparison with ores from the Skiddaw Slate Series (Table 4)

Botryoidal ores from the Kelton Fell complex contain higher concentrations of As (a.m. 830ppm), Mn (a.m. 1300 ppm), Ni (a.m. 35 ppm) and Zn (a.m. 12 ppm) than the adjacent replacement ores. To attribute this difference to a change in primary ore fluids is inconsistent with the almost uniform composition shown along the entire limestone belt. Alternatively one may invoke a process of localised chemical interaction between the ore fluids and the wallrocks. In this way slight enrichments of Mn, Ni and Zn in the slates would account for these differences. Unfortunately this concept does not apply to arsenic and it may be necessary to envisage a mechanism which is controlled by a partition function (i.e. the value of this function determining the partitioning of arsenic between the ore fluid and the precipitating haematite). In all other respects the ores are identical to those of the type area.

9.4. Comparison with ores from the Eskdale granite (Table 4)

Botryoidal ores from veins in the Eskdale valley contain the highest recorded trace element concentrations: As (a.m. 1800 ppm), Ni (a.m. 20 ppm)

SUMMARY GEOCHEMISTRY FOR THE HAEMATITE ORES

(arithmetic means)

	West Cumberland		Millom-Furness		Skiddaw slates	Borrowdale volcanics	Eskdale granite
	M (screened)	B	M (unscreened)	B	B (unscreened)	P-M (unscreened)	B (unscreened)
As ppm	118	497	182	1820	830	129	1800
Pb ppm	12	49	44	60	46	15	450
Cu ppm	15	9	15	14	15	10	12
Ni ppm	7	6	13	15	35	7	22
Zn ppm	6	7	16	20	12	7	105
Y ppm	6	7	6	5	8	20	20
Mn ppm	367	496	707	474	1300	345	3500
Ba ppm	58	46	23	15	31	31	18
Sr ppm	5	13	4	16	4	7	20
Rb ppm	2	4	2	2	5	10	7
Zr ppm	5	5	12	4	3	17	6
Ti ppm	33	16	79	13	6	100	5
Si ppm	5.77	1.23	3.23	0.80	0.48	6.20	1.01
Fe ppm	60.63	68.20	61.44	68.78	69.37	56.03	64.89
Al ppm	0.24	0.27	0.32	0.22	0.25	0.61	0.33
Ca ppm	0.39	0.48	1.17	0.36	0.04	0.18	1.57
Mg ppm	0.14	0.11	0.09	0.04	0.10	0.11	1.11

Key:- M = massive ore, B = botryoidal ore, P-M = pseudomassive ore

TABLE 4

Pb (a.m. 450 ppm), Y (a.m. 20 ppm) and Zn (a.m. 105 ppm). Manganese values are correspondingly high and vary sympathetically with the Ca content of the ore suggesting carbonate contamination either as manganoan calcite or pyrolusite-veined calcite. Otherwise the analyses are similar to those of the type area.

9.5. Comparison with ores from the B. V. S. (Table 4)

Although a single specimen of botryoidal ore from the Tongue Gill vein does not warrant serious discussion, the atypical pseudo-massive ores show certain geochemical features which deserve further consideration. Assuming no chemical change in the primary ore fluids the mean contents of Ni (a.m. 7 ppm), Pb (a.m. 15 ppm) and Zn (a.m. 12 ppm) in the pseudo-massive ores are well below those of material morphologically intermediate between massive and botryoidal ore. This impoverishment is most likely due to a loss of trace elements during recrystallization and minor silicification of the original botryoidal ore (a.m. Si 6.2%). In contrast the Ti concentrations are unusually high (a.m. Ti 106 ppm) which suggests a high degree of initial interaction between the ore fluids and the Ti-rich volcanic wallrocks (e.g. illmenite, titanaugite and leucoxene).

9.6. Comparison with ores from the Millom-Furness orefield (Table 4)

Samples collected during the reconnaissance survey indicate that apart from minor chemical differences the replacement ores are indistinguishable from those of the West Cumberland orefield. Since the data refers to unscreened material only the more obvious points are discussed.

A. Botryoidal Ores

These show the greatest contrast with ores from the type area especially the increases for As (a.m. 1820 ppm), Pb (a.m. 60 ppm).

Sr (a.m. 10 ppm) and Zn (a.m. 20 ppm), and the decreases for Ba (a.m. 15 ppm) Y (a.m. 5 ppm) and Si (a.m. 0.80%). Unless these differences are related to geochemical variations in the "granite" basement, one must assume chemical partitioning as the possible mechanism.

B. Massive Ores

Allowing for certain misclassification errors the distribution patterns for Al, As, Fe and Si are markedly bimodal and are thought to represent the replacement of two lithologically dissimilar carbonate units. Although this feature is characteristic of the type area, the stronger bimodal distributions agree with greater specificity of replacement observed in the Millom-Furness orefield:

Al	g.m.	at	0.23%	and	0.30%
As	"	"	25 ppm	"	45 ppm
Fe	"	"	62%	"	66%
Si	"	"	1.50%	"	2.75%

Not only is the mean arsenic content lower but the botryoidal/massive enrichment factor is higher. This again suggests the operation of a partition function whose value is determined by the overall environment of deposition. The close geochemical similarity with those of the type area provides additional evidence for a common origin.

9.7. Fluid Inclusion Results

From an original 157 samples, 31 quartz samples and 3 fluorite samples were finally selected for analysis. (N.B. Inclusions showing incipient "necking" or suspected leakage along microfractures were rejected.) Calcite and barite crystals were free from primary inclusions and contained only planar arrays of unusable minute secondary inclusions. The quartz

crystals were extracted from vugs in the massive ore and normally displayed one or more growth surfaces. Euhedral fluorite specimens were hand picked from irregular cavities in the massive ore and were observed to post-date the quartz deposition (Chapter 4). The inclusions were all two phase systems (vapour-liquid) and free from daughter minerals. Chilling below $0^{o}C$ failed to produce any evidence for liquid CO_2 (critical temperature $+31^{o}C$, but very sensitive to absorbed infra-red radiation). Several homogenization measurements were made on each specimen; the details of which are given in Table 5. The mean temperature for the West Cumberland quartz gangue (Fig. 22) agrees closely with the value of $105^{o}C$ for quartz crystals from the Robertgate orebody, Beckermet (Ineson 1967). Fluorite shows a slightly higher mean of $115^{o}C$. A failure to obtain similar information for the Lower Palaeozoic vein deposits because of unsuitable material was particularly disappointing. However current research by the author on the Millom-Furness ores indicates a mean temperature of $95^{o}C$ for calcite gangue. The apparent temperature difference between the northern and southern sections of the limestone belt may indicate deposition at a higher structural level relative to the basement "granites" in the latter area. A plot of the mean temperatures for each locality reveals no discernible trend and unless there is a small vertical gradient concealed by the uncontrolled stratigraphic sampling the temperature distribution is noticeably uniform.

Homogenization temperatures provide only the minimum temperature of formation and to derive the actual filling temperatures one needs to correct for pressure and salinity. Under ideal conditions a pressure correction can be obtained from the partial homogenization temperatures of liquid CO_2 inclusions, but usually one must estimate the pressure indirectly from overburden thicknesses at the time of deposition. For the

TABLE 5

FLUID INCLUSION RESULTS FOR THE WEST CUMBERLAND GANGUE MINERALS

Sample Number	Material	Number of Inclusions	Mean Homogenization Temp. oC	Salinity wt% NaCl equip
18	Quartz	3	104	-
23	"	7	102	-
26	"	30	107	-
32	"	17	113	-
36	"	12	121	-
40	"	4	108	-
42	"	10	115	-
69	"	6	94	-
86	"	2	102	-
88	"	4	116	-
89	"	8	105	-
91	"	4	102	-
101	"	2	108	10, 15 & 1(
107	"	3	109	-
112	"	4	115	18 & 21
114	Fluorite	5	117	-
125	Quartz	4	107	-
127	"	2	109	-
134	"	1	+ 104	-
150	"	5	99	-
153	Fluorite	7	106	-
154	Quartz	1	95	-
160	"	2	113	-

* N. B. Sample Number refers to sample locality number given in Appendix II

HISTOGRAM of HOMOGENIZATION TEMPERATURES for QUARTZ GANGUE from 25 localities, WEST CUMBERLAND

MEAN TEMP = 108°C (cf. MILLOM-FURNESS 95°C)

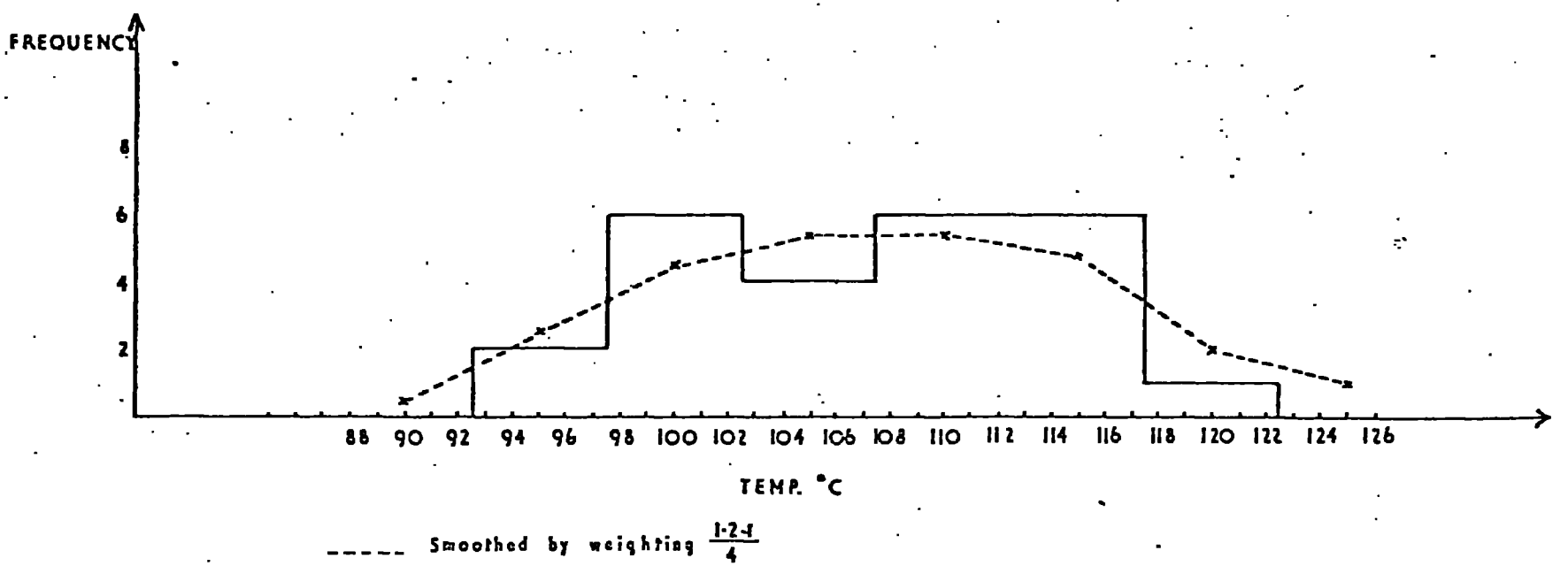

FIGURE 22

West Cumberland area the precise age of the mineralization and thickness of the superincumbent sedimentary cover are unknown and thus any such estimate is pure supposition. However because the orefluids are little more than heated groundwaters it is possible to equate them with thermally equilibrated groundwaters under a normal geothermal gradient. Obviously this demands certain assumptions but the theoretical model approximates closely to the proposed theory of ore genesis and would account for the uniform temperature distribution. As stated by Sass (1971) "the intrusive part of the crust within a given thermal province may be treated as a single system, and, after the actual heat of intrusion has been dissipated, the temperature - depth curve below any point can be calculated from a knowledge of the surface activity, A, at that point". Geologically the Lake District granites are analogous to the Sierra Nevada thermal province described by Lachenbruch (1970). Using the upper mean heat flow for Palaeozoic orogenic areas (77 mWm^{-2}) a geothermal gradient of 35^{o}-40^{o}C/Km is indicated (Fig. 23). Assuming only a negligible contribution from the Triassic cover this gives a depth of 2.5 - 3 Kms for the West Cumberland ore deposits; or in terms of pressure equivalents a lithostatic load of 0.68 - 0.81 Kbs. or a hydrostatic load of 0.25 - 0.30 Kbs. Figure 24, after Ingerson (1947) illustrates the pressure corrections for pure water at varying pressures. (N.B. For low temperatures and moderate pressures salinity differences have little effect on the correction values). Since the metasomatic deposits are connected to throughgoing fault structures it is doubtful whether deposition took place under purely lithostatic conditions (i.e. a pressure correction of 45^{o}C). If, however, the alternative circulating groundwater model is used the correction is reduced to + 15 - 20^{o}C.

FIGURE 23

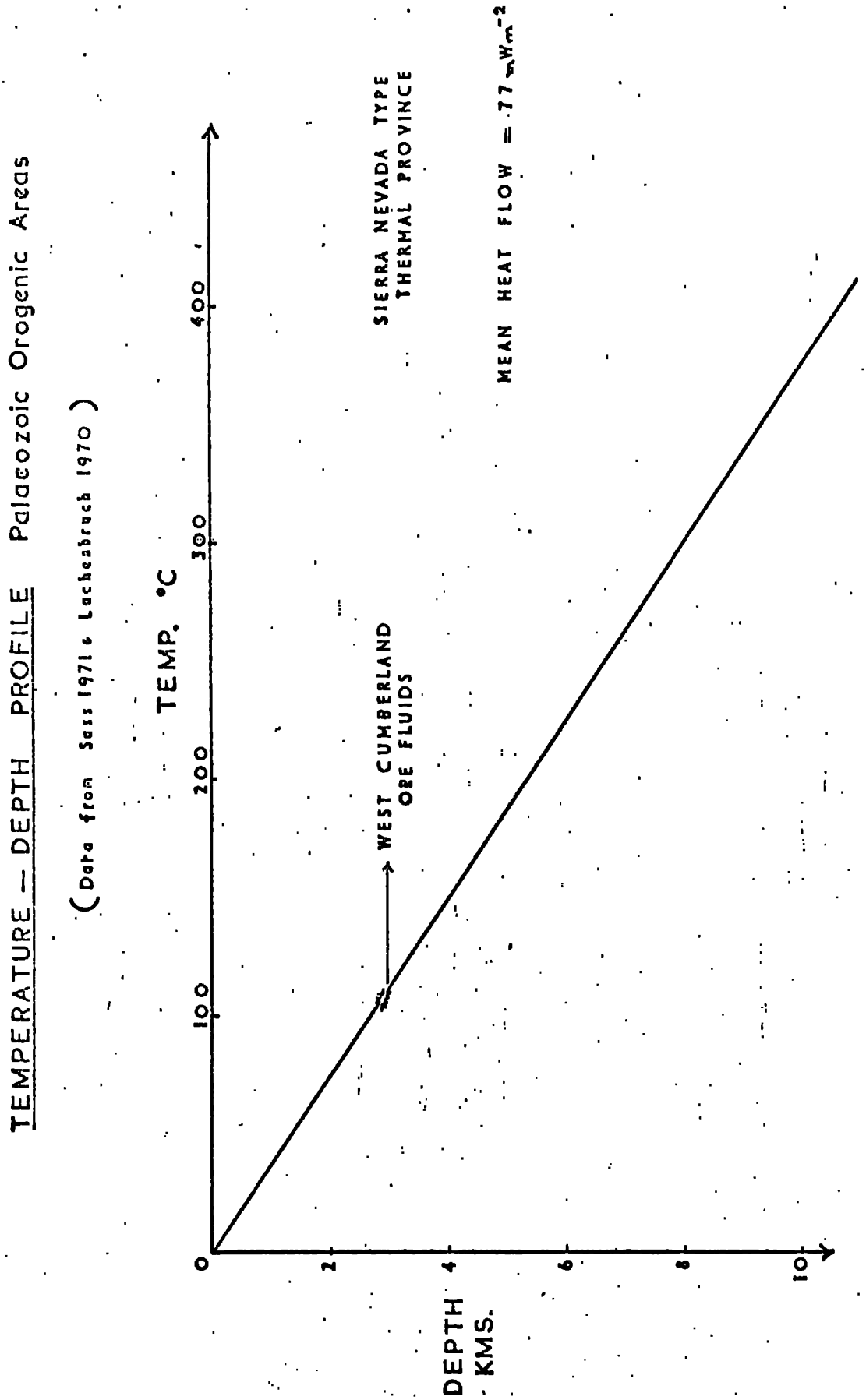
TEMPERATURE — DEPTH PROFILE Palaeozoic Orogenic Areas
(Data from Sass 1971 & Lachenbruch 1970)
TEMP. °C
0
100
200
300
400
DEPTH KMS.
2
4
6
8
10
WEST CUMBERLAND ORE FLUIDS
SIERRA NEVADA TYPE THERMAL PROVINCE
MEAN HEAT FLOW = .77 μWm⁻²

FIGURE 24

PRESSURE CORRECTION GRAPH FOR HOMOGENIZATION TEMPERATURES

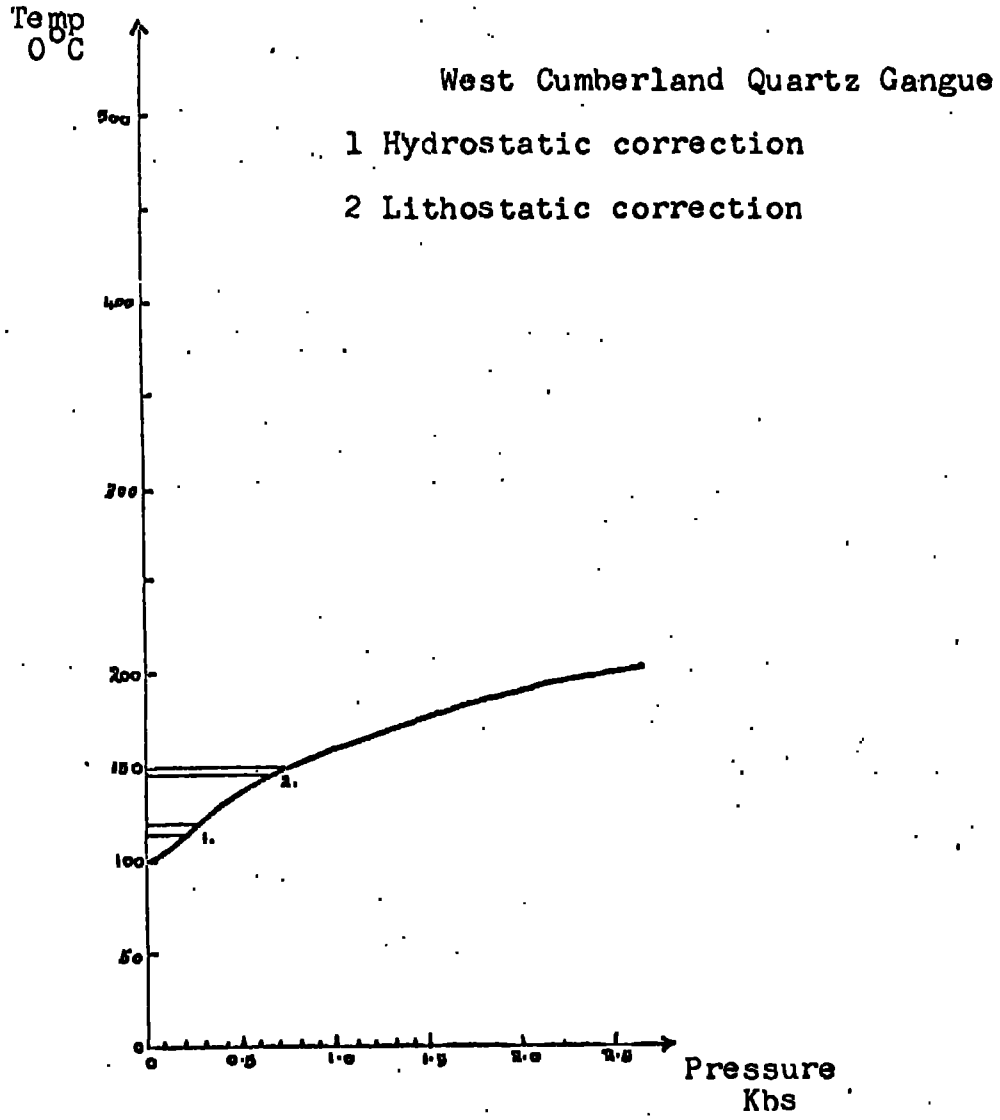

Observed homogenization temperature is given at the left hand side of the curve; the curve showing increasing filling temperatures corresponding to higher pressures (ie increasing temperatures of formation)

The problem of supercooling encountered during freezing runs provides indirect evidence that the orefluids were free from suspended particulate debris, a feature typical of very slow flow rates. This is completely in accordance with the kinetics of metasomatism where the rate controlling step is the diffusion of material towards and away from the reaction interface (Ames 1961a and 1961b). The salinity data is too limited to allow prognostication on the composition of the ore fluids but does indicate that the fluids were relatively saline brines (10 - 21 wt% NaCl equivalent) and not simple groundwaters of subsurface hydrological systems (Table 5).

To summarise, the fluid inclusions results for gangue minerals from the West Cumberland orefield reveals two important features of the mineralizing fluids:

(i) The fluids appear to have maintained a low uniform temperature over wide areas during the main phase of mineral deposition. This condition is best described as an equilibration with the regional geothermal gradient rather than a discharge of warm juvenile fluids into a cooler hydrological environment along local channelways. The latter system would possess a strong thermal boyancy with flow rates in excess of those inferred from the degree of supercooling. In contrast a heated groundwater model would have a much lower bouyancy and convective overturn without associated thermal streaming along fault structures.

(ii) Compositionally the fluids represent moderately saline brines having a mean temperature of 125-130^{o}C (i.e. a mean homogenization temperature of 108^{o}C corrected for a hydrostatic pressure of 0.25 - 0.30 Kbs.). The origin of the saline fluids is discussed more fully in chapters 11 and 13.

7.8. Conclusions

The complete lack of regional variation is undoubtedly the most important single characteristic of the ore geochemistry which combined with the mineralogical data indicates that the ore fluids were derived either from an extensive homogeneous source or from a local source by extreme lateral migration, without undergoing chemical differentiation. In view of the geophysical evidence for a "granite" basement beneath the area and the well defined nature of the mineralized zone the first model appears most likely. As shown by various inter-element associations the chemical constituents of the ores fall into two main groups; the primary ore fluid components and the wall rock components. The first group represented by As, Cu, Fe, Pb and possibly Si are interpreted as diagnostic indices of the ore fluids and were introduced into the area of deposition. The second group represented by Al, Ca, Mg, Mn, Ba, Ni, Rb, Sr, Ti, Y, Zn and Zr are thought to be the residual components of the original wallrocks or components released into ore fluids during wall rock interactions (e.g. Ti enrichment in veins in the Borrowdale volcanics). Certain residual components can be related to the replacement of major lithological rock types and at a lower level by subpopulations in element frequency distributions. The observed difference in concentration for trace elements in the massive and botryoidal ores does not appear to be related to selective adsorption and is probably a function of chemical partitioning between the ores and ore fluids.

Fluid inclusion results for gangue minerals in the replacement ores indicate a uniform temperature distribution for the limestone belt and thus support a common origin for the Cumbrian haematite ores. The inferred flow and mean temperature of the ore fluids are consistent with a model of circulating saline groundwaters in equilibrium with a regional geothermal gradient.

10. RELATIONSHIP BETWEEN BASEMENT GEOCHEMISTRY AND MINERALIZATION

10.1. Geochemistry of the Intrusives

Relative to other Caledonian granites in the north of England, the Pink variety of the Eskdale granite is unusually low in CaO and MgO (c.f. Skiddaw granite 1.78% CaO, 1.01% MgO; Shap granite 1.78% CaO, 1.46% MgO Weardale granite 0.86% Cao 0.70% MgO). These depletions are probably related to the intensity of late stage chloritization and sericitization. By comparison the losses for total Fe, K_2O and Na_2O are negligible and agree with the theoretical interpretation of the above processes (Table 6). As suggested in chapter 2 the expulsion of CaO from the system may account for the conspicuous epidote metasomatism of the Borrowdale volcanics surrounding the Eskdale granite and its concealed extensions.

For the haematized Pink granite analyses show a 50% decrease in total Fe, significant reductions in Al_2O_3, MnO and TiO_2, and further losses of CaO and MgO. Comparable reductions are also observed for As, Pb and Zn but not for elements firmly held in the chlorite-sericite lattices (i.e. K and Rb). The zone of most intense haematization and concommitant leaching occurs along the Esk valley and coincides with both the centre of the Bouguer anomaly and the projected extension of the Hardknott shatter belt.

As shown in table 6 the Ennerdale granophyre is chemically distinct from the adjacent granite and displays neither large scale alteration nor pervasive haematization. Veins are confined to well defined fault planes and there are no haematite-wallrock intergrowths as in the granite. Complete analyses of the granite and granophyre samples are given in Appendix II.

10.2. Geochemical affinities between granite and haematite ore

TABLE 6

SUMMARY GEOCHEMISTRY FOR THE ESKDALE AND ENNERDALE INTRUSIVES

	Eskdale granite			Ennerdale granophyre
	(a) Pink Var.	(b) Haematised Pink Var.	(c) Grey Var.	(a) Main central phase
SiO_2	76.69%	75.30%	66.44%	74.62
Al_2O_3	15.06	14.53	16.15	14.83
Total Fe	1.79	0.88	5.22	1.32
MgO	0.21	0.15	1.54	0.53
CaO	0.25	0.08	1.91	0.68
Na_2O	3.52	3.33	3.19	5.73
K_2O	5.06	5.02	4.55	0.08
TiO_2	0.17	0.11	0.70	0.35
MnO	0.02	0.00	0.11	0.02
Ba	86 ppm	70 ppm	855 ppm	N.D.
Zr	120	77	268	262 ppm
Y	26	23	40	36
Sr	28	27	242	97
Rb	400	420	173	10
Zn	35	11	75	6
Cu	N.D.	N.D.	30	N.D.
Ni	6	4	10	N.D.
As	14	N.D.	7	N.D.
Pb	18	9	22	6

N.D. - values below analytical detection limit.

Mean analyses for the Eskdale botryoidal ores and Pink granite indicate a sympathetic relationship between the relative abundances of As, Pb and Zn in the ores and the intensity of corresponding depletions in the granite during haematization:

	Pink Granite	Haematized Pink granite	Relative Depletion	Botryoidal Ore	Relative abundance in the ore
As	14 ppm	3 ppm	78%	1810 ppm	18
Pb	18 ppm	9 ppm	50%	450 ppm	4
Zn	33 ppm	11 ppm	30%	104 ppm	1
Fe	1.8%	0.97%	50%	-	-
Rb	420 ppm	400 ppm	5%	7ppm	-

This evidence together with the known distribution of veins suggests that the haematite oreshoots in the Eskdale granite were formed by the remobilisation of iron from adjacent areas of the granite. The process is envisaged as a two stage system:

Stage 1. The release of iron from ferromagnesian minerals (+? particulate haematite in the feldspars) during late-stage alteration, followed by localised redeposition of the iron as haematite to produce the Pink granite.

Stage 2. Remobilisation of the free haematite by circulating brines and partial redeposition within the granite along faults, fractures and joint planes. The feldspars may also have undergone a further phase of alteration at this stage.

The mechanism envisaged for stage 1 corresponds closely with that described by Boone (1969) for haematiferous albites in a granite porphyry in the Gaspé peninsula of eastern Canada. Large areas of the porphyry are characterised by the sub-assemblage red albite + chloritised biotite which grade into restricted areas of grey porphyry with the critical sub-assemblage oligoclase - andesine + less altered biotite. The chemistry

and texture of the feldspar phenocrysts shows that the haematiferous albites are relict phenocrysts of more calcic and potassic plagioclases. They are related to the less altered feldspars by a paragenetic model involving reaction between ternary feldspar, a vapour phase and Fe ± Mg released during the decomposition and oxidation of primary mafic phases. Lowering of H+ activity at the sites of alteration is used to explain the localised precipitation of haematite. Three independent equations summarise the observed alteration:

$$2\,K\,Al\,Si_3O_8 + 3\,Ca\,Al_2\,Si_2\,O_8 + 4\,H^+ + 2\,Na^+ \longrightarrow$$

Potash feldspar Calcic plagioclase

$$2\,K\,Al_3\,Si_3\,O_{10}\,(OH)_2 + 2Na\,Al\,Si_3\,O_8 + 3\,Ca^{2+}$$

Sericite Albite

$$2\,CaAl_2\,Si_2\,O_8 + 5\,Mg^{2+} + 2\,H_2O + 4H^+ \longrightarrow$$

Calcic plagioclase

$$Mg_5\,Al_2\,Si_3\,O_{10}\,(OH)_8 + 2\,Ca^{2+} + 2\,Al^{3+} + Si^{4+}$$

Chlorite

$$2\,Fe^{2+} + 3\,H_2O \longrightarrow Fe_2O_3 + H_2 + 4\,H^+$$

Haematite

Boone's conclusions apply to the Eskdale alteration with very little modification and provide a satisfactory mechanism for the distribution of free haematite in the Pink granite and the calcium metasomatism of the country rocks. Since other areas of the haematite province are known to be underlain by granite and show no significant differences in mineralogy or geochemistry it follows that a granite source model may also apply at a regional level. The style of veining in the Ennerdale granophyre and its total enclosure by the Eskdale gravity "low" indicates a possible re-intrusion at depth of material equivalent to the granite. It is assumed that in the West Cumberland orefield the Ennerdale Shelf has undergone a similar process of alteration, especially along its western margins.

11. SPATIAL VARIATION IN ORE GEOCHEMISTRY, WEST CUMBERLAND

11.1. Introduction

By using screened data exclusively the West Cumberland massive ores show several spatial patterns not readily discernible in the original data. This is most noticeable for those elements having a large difference between their respective means in the two main ore types; where the risk of cross contamination is greatest. Some degree of local autocorrelation is shown by all elements but only As, Ba, Cu and Mg exhibit trends which are coherent and geologically meaningful. As expected, the patterns for residual wallrock components are highly confused. Magnesium provides an interesting exception to this rule because of its association with secondary dolomitization and has a distinctive spatial distribution. By comparison the trends for primary ore fluid components are relatively well defined (i.e. As and Cu.).

11.2. Arsenic and Copper

Being diagnostic geochemical indices of the ore fluids the patterns shown by As and Cu are of major significance in identifying the location of basement channelways. As shown in figures 25 and 26 both elements display a narrow zone of high values directly above the projected surface expressions of the Coal Fault and Egremont Lines. To the east of this zone the values gradually decrease towards the Carboniferous-Ordovician contact. These trends indicate the importance of the tectonised margins of the basement shelf in providing channelways for the ascending mineralizing solutions. Although chemical differentiation offers a satisfactory explanation for the observed E-W gradient, the same effect could be produced by a progressive

FIGURE 25

SPATIAL DISTRIBUTION PATTERN FOR ARSENIC,
WEST CUMBERLAND MASSIVE ORES (1)

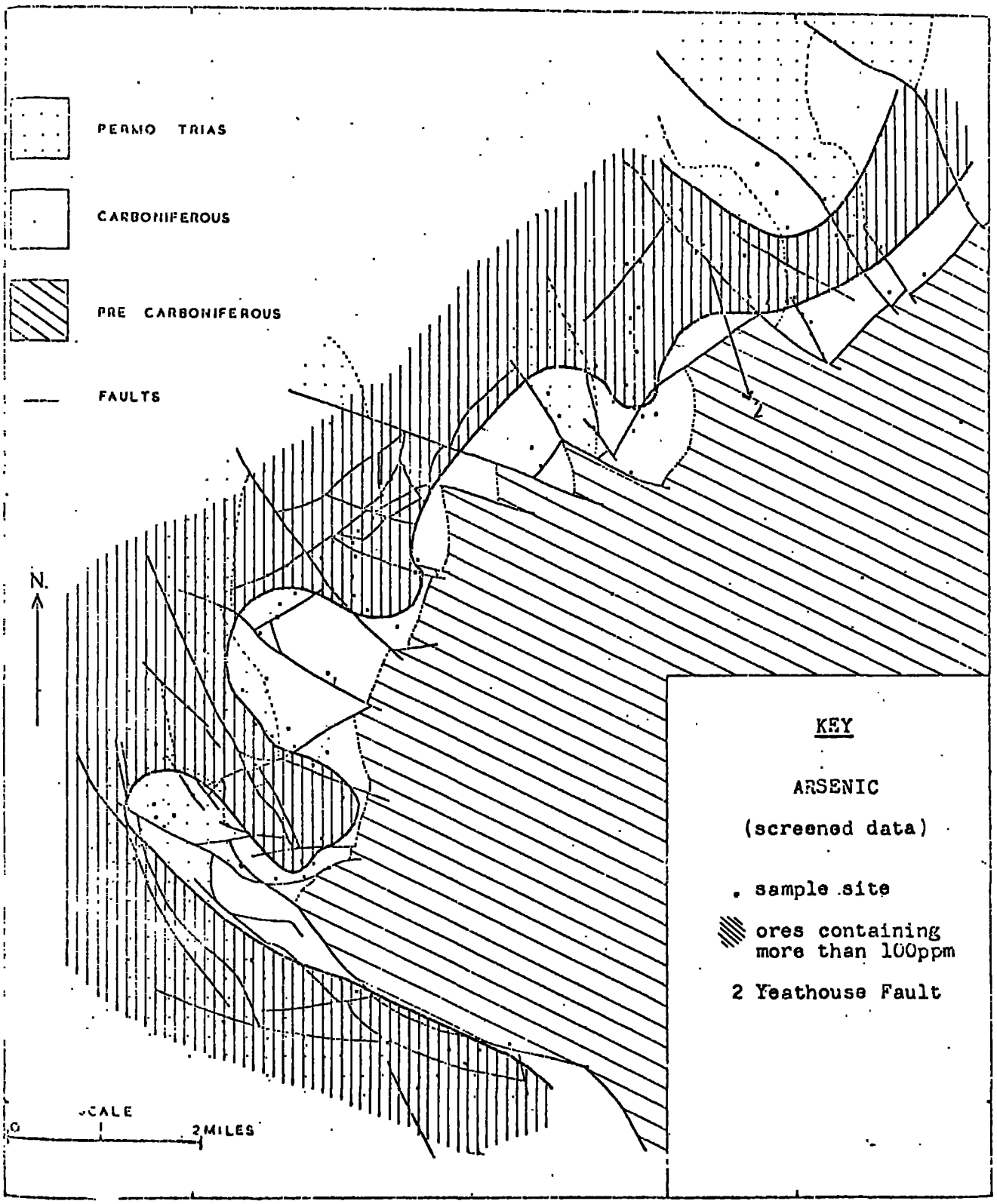

FIGURE 26

SPATIAL DISTRIBUTION PATTERN FOR COPPER,
WEST CUMBERLAND MASSIVE ORES

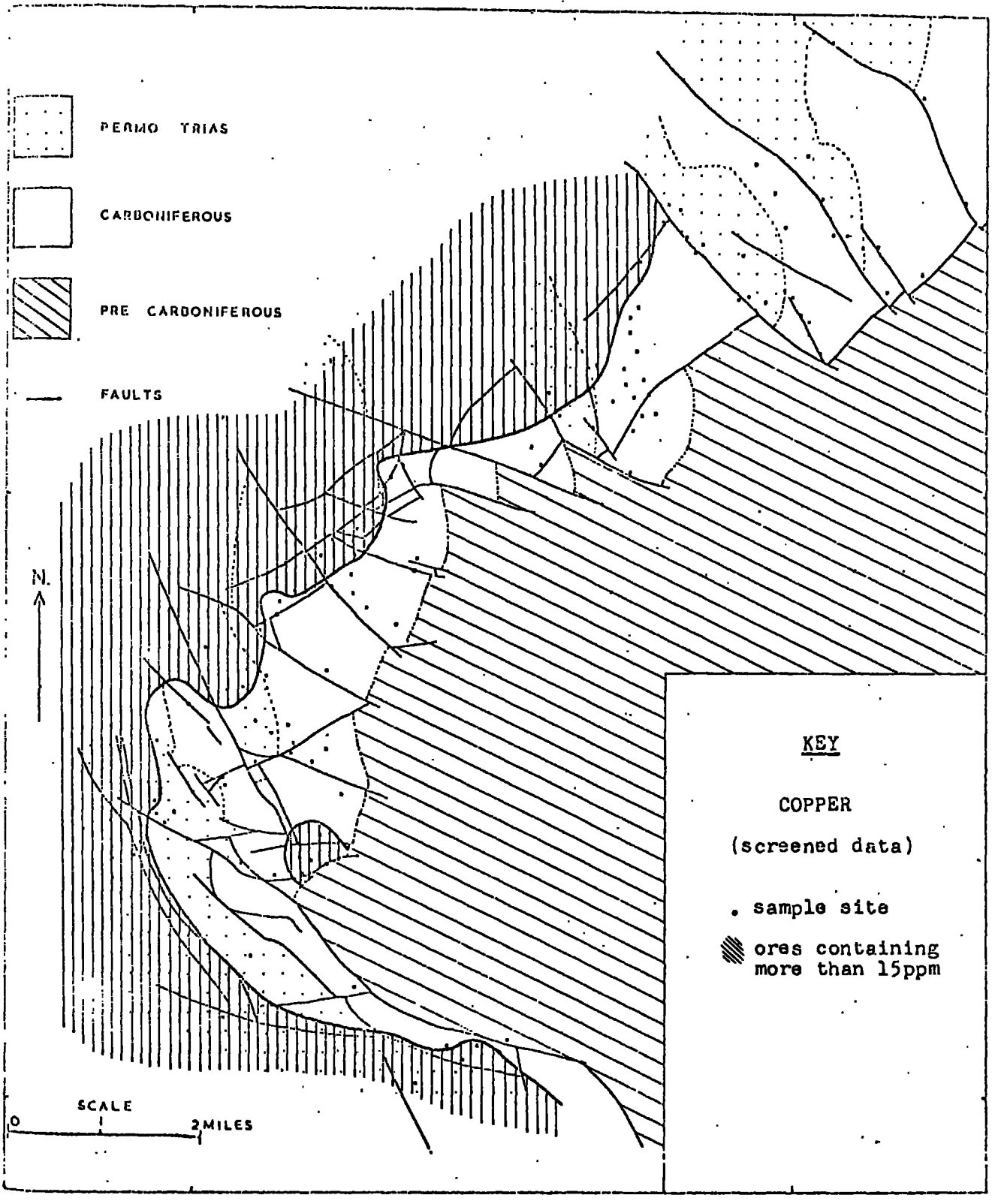

decrease in the degree of alteration in the basement "granite" away from the margins (i.e. relative changes in the degree of alteration producing lateral variations in the amount of As and Cu released from the "granite"). The absence of mineralization in the Hensingham inlier and the apparent paucity of orebodies north of the Coal Faults suggests that the zone of high values does not extend very far beyond the present limit of known mineralization. This implies an assymetric zoning about the margins of the Ennerdale Shelf and substantiates the hypothesis for the origin of ore fluids from within the "granite" basement. It also follows that if the ore fluids are modified connate waters they have acted only as a solvent for iron since there is no widespread haematization along identical fault structures west of the shelf.

The dextral offset to the arsenic zone, northeast of Frizington, probably reflects a corresponding offset to the Coal Fault Line by the post-Triassic Yeathouse Fault (estimated vertical throw + 1000 ft.). Although the eastern boundary of the arsenic zone shows preferential dispersion along prominent NW-SE faults the overall pattern indicates an insignificant amount of lateral migration. Figure 27 shows the corresponding variation in arsenic for the original data and illustrates the potential value of linear discriminant function analysis.

11.3. Magnesium

Assuming the interpretation of high Mg values is correct (Chapter 9) then the spatial variation for Mg as shown in figure 28 defines areas of pre-haematite dolomitization in the wallrocks along mineralized faults. The observed distribution also indicates that dolomitization cannot be ascribed to the downward percolation of Mg-rich solutions from the overlying Permo-

FIGURE 27

SPATIAL DISTRIBUTION PATTERN FOR ARSENIC,
WEST CUMBERLAND MASSIVE ORES (2)

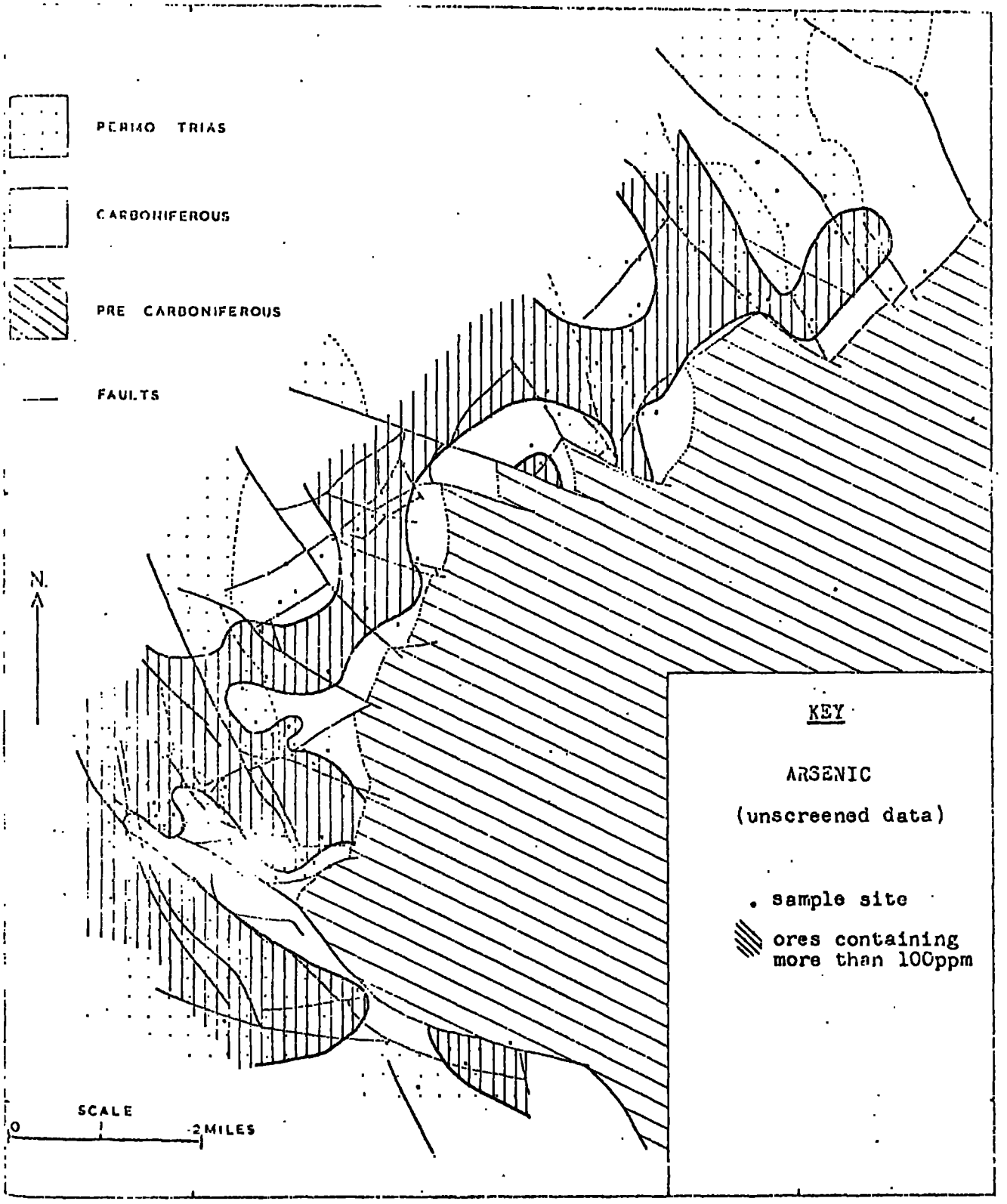

FIGURE 28

SPATIAL DISTRIBUTION PATTERN FOR MAGNESIUM,
WEST CUMBERLAND MASSIVE ORES

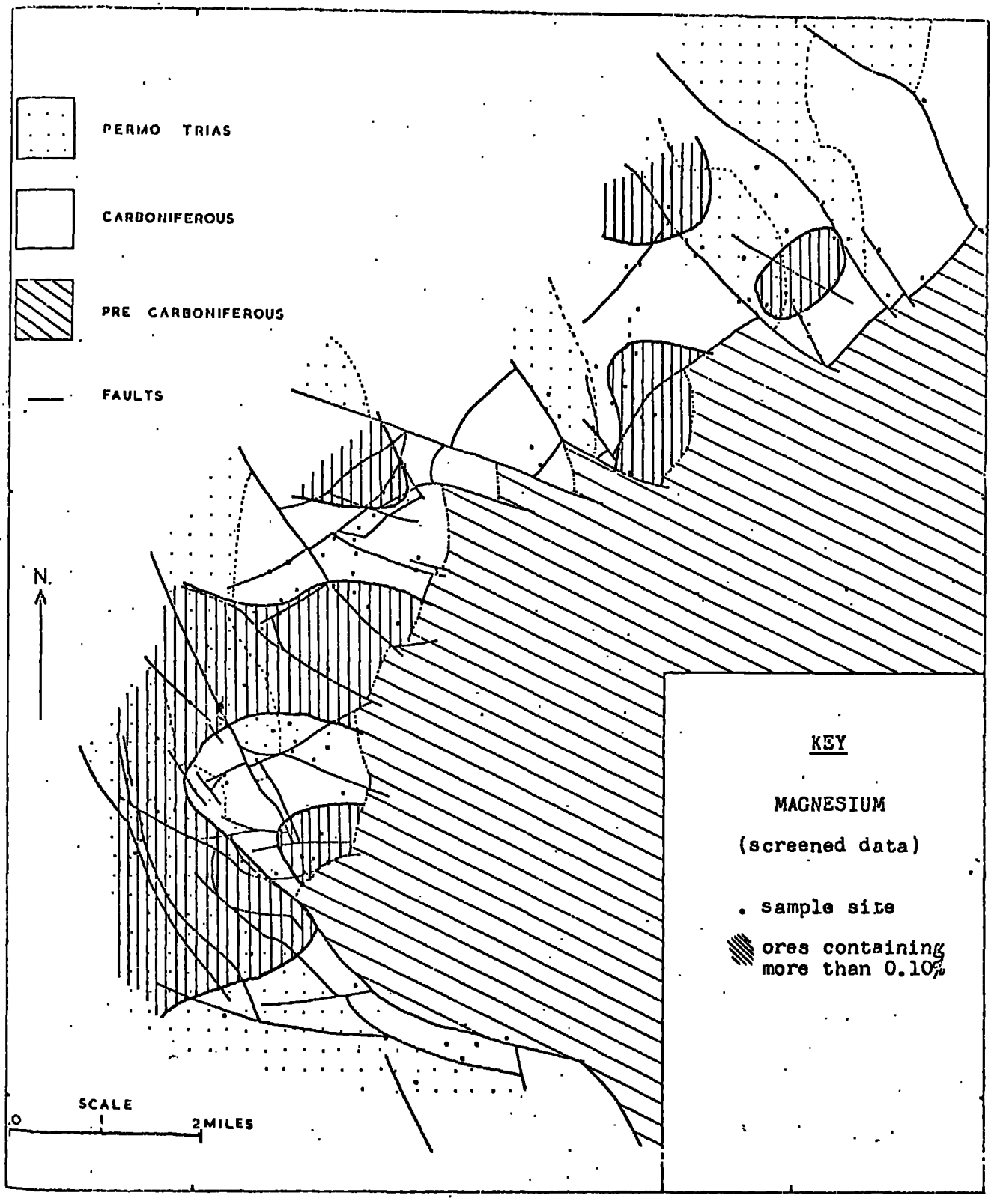

Triassics since there are areas of unaltered limestone directly beneath the Brockrams. Moreover the lack of correlation between magnesium enrichment and iron metasomatism discredits the theory of dolomitization as a process of ground preparation prior to mineralization.

11.4. Barium

The pattern for barium (Fig. 29) shows a general association between areas of Permo-Triassic sediments and massive ores containing more than 30 ppm Ba. This value is by no means arbitary and coincides with the inferred lower limit for the upper Ba subpopulation (Fig. 18). Although the overlap is strong it does suggest that each subpopulation refers to a separate geochemical process. As shown, anomalous ores are related to:

(i) Orebodies having or having possessed a Brockram roof or hanging wall.

or (ii) Orebodies developed along faults downthrowing major troughs of Permo-Triassic sediments.

11.5. Permo-Triassic Barite

The abundance of barite in the lower Permo-Triassic sequence of West Cumberland (Trotter 1945) is not without parallel and characterises the marginal zones of most other European Triassic basins. In the East Midlands it is almost ubiquitous and appears as a chemical cement in the sandstones (Sylvester-Bradley 1968). For the Ardéchois Triassic basin, French geologists believe that the deposition of barite is due to the migration of $BaCl_2$ brines outwards from the centre of the compacting basin into sulphate-rich peripheral zones (Bernard and Samama 1968).

11.6. Barite-Haematite Association

Trotter whilst reporting the occurrence of barite in the Beckermet

FIGURE 29

SPATIAL DISTRIBUTION PATTERN FOR BARIUM,
WEST CUMBERLAND MASSIVE ORES

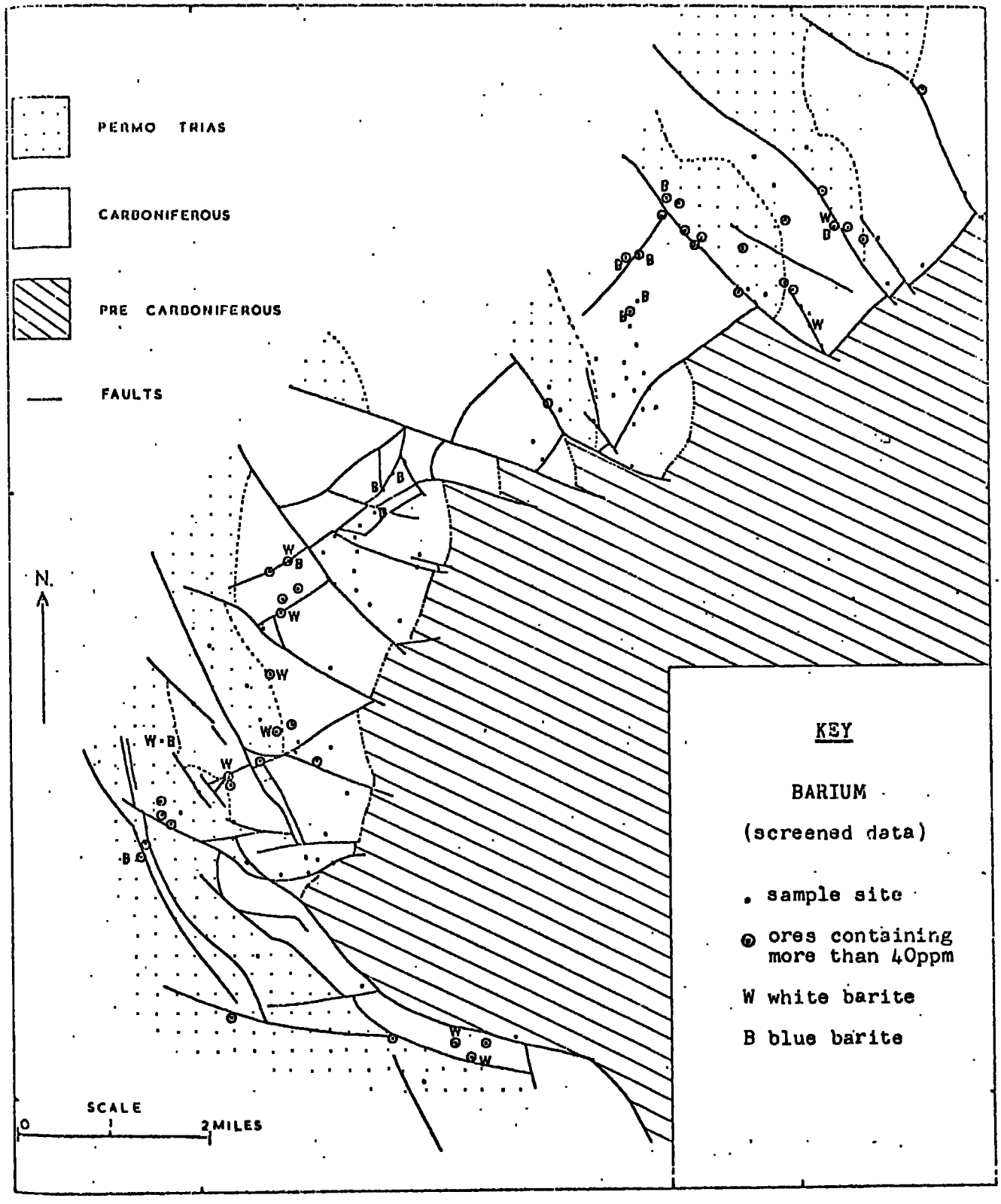

area also notes the marked association with ory sandstones. Of greater importance however is the development of barite as a major gangue mineral in many of the orebodies south of Egremont. Its occurrence as bladed masses within the massive ore suggests that the ore fluids were capable of depositing haematite and barite simultaneously. To account for the association of barite and haematite both in the lower Permo-Triassics and the Carboniferous limestones directly beneath the cover three basic models can be considered:

(i) $BaSO_4$ was carried in solution by the ore fluids and precipitated on mixing with less saline formational fluids in the Permo-Triassics.

(ii) $BaSO_4$ was precipitated by the mixing of sulphatic ore fluids with $BaCl_2$ brines in the Permo-Triassics.

(iii) $BaSO_4$ was precipitated by the mixing of Ba-rich ore fluids with sulphatic fluids in the Permo-Triassics.

Experimental work by Templeton (1960) and Gundlach et al. (1972) confirms the feasibility of the first model and has shown that the solubility of $BaSO_4$ increases with temperature and the ionic strength of the solvent. At 150°C and in 12 wt % NaCl solution, the molal concentration of $BaSO_4$ is 20X that of pure water at the same temperature. In view of the observed salinity of the ore fluids the precipitation of barite by dilution with less saline fluids circulating in the Permo-Triassics is quite conceivable.

The second model is analogous to the Ardéchois basin hypothesis and assumes the orefluids contained an appreciable sulphate component. Davidson (1966) in his last paper to the Institute of Mining and Metallurgy reports that barite is found under virtually every evaporitic formation in Europe and suggests the role of diagenetic waters from the overlying strata.

He also remarks on the development of barite as a cement in continental "red-beds", often in close proximity to gypsum and anhydrite deposits. The occurrence of gypsum-anhydrite beds in the Lower Permian of West Cumberland and the undisputed "red-bed" character of the St. Bees Sandstones offer a perfect environment for interstatal $BaCl_2$ fluids of the type envisaged by Davidson. Difficulties arise however in providing sulphatic ore fluids. For subsurface connate waters the average Cl/SO_4 ratio varies from 200:1 to 1000:1 (White et al. 1963) whilst for fluid inclusions the ratio is rarely below 20:1 (Roedder 1972). Thus unless the ore fluids were locally enriched in sulphate the process of deep circulation generates only chloride-rich fluids. The only possible sulphate source is the nodular anhydrite described by Llewellyn et al. (1968) in the Seventh Limestone. At present the total extent of the anhydrite is unknown but the apparent restricted nature of the occurrence precludes the massive involvement of sabkha sulphates to account for the observed abundance of barite. Probably the problem will only be resolved by an analysis of the inclusion fluids. (N. B. The presence of Visean evaporites beneath the Irish Sea, similar to those in the Republic of Ireland, cannot be discounted (West et al. 1968).

The third model is essentially the converse of the second and demands the existence of Ba-rich ore fluids and sulphatic Permo-Triassic fluids. It contains several features which make it more compatible with the origin of the haematite ores than the previous models. The development of thick evaporite (gypsum-anhydrite) sequences in the Permian succession adjacent to the orefield presents no problem in generating sulphate-rich formational fluids. To provide the complementary Ba-rich fluids one of two mechanisms may apply:

(i) Release of Ba from the basement granites as suggested by Rankama and Sahama (1955)

or (ii) Contamination of the orefluids by $BaCl_2$ brines.

Analyses of unmineralized and mineralized Eskdale granite show no significant depletion in Ba which makes the first mechanism doubtful. However the existence of Ba-rich Na-Ca chloride brines throughout the Durham-Northumberland coalfield makes the alternative hypothesis more tenable. Barium chloride brines although unusual are not uncommon and have been described in coal workings in the East Midlands (Ickes 1924), the Carboniferous of West Pennsylvanian(Puchalt 1967) and the Cretaceous of Texas (Brooks 1969). The author proposes that similar brines migrated beyond the Cumberland coalfield and became mixed with deep circulating connate waters before ascending along "through-going" structures in the basement "granites". Although there is no direct evidence for barium brines in the above coalfield it is interesting to note that the Millom-Furness orefield is both free from barite and isolated from known Upper Carboniferous coal basins.

Of all three models the second form of the third model appears most likely. As well as fitting the observed data it does not demand assumptions which have not been proved elsewhere. The development of barites beneath the Permo-Triassic cover is attributed to the downward penetration of sulphate-rich fluids into the Carboniferous succession along faults and fissures.

11.7. Evaluation of Trend Surface Patterns

Various reasons for the failure of the West Cumberland massive ores to respond to trend surface analysis have already been discussed in chapter 8. A measure of their failure is indicated by the Fischer-Snedecor "F" ratio

for each surface as given in Table 7. Only Fe, Ti and Zn appear to show any appreciable level of statistical significance. The first order surfaces for these elements are horizontal over the zone of sampling but plunge steeply along the margins of the orefield due to polynomial instability. The absence of flexuring and failure of the Quadratic surfaces probably reflects the lack of real variation in the data. Higher order fits for Zn are totally inexplicable and do not relate to any process previously ascribed to zinc. Hand contoured maps for the same data show no apparent geochemical relief and it must be assumed therefore that the Quadratic and Cubic surfaces are mathematical derivatives of the Linear surface.

11.8. Conclusions

The observed spatial variations for As, Ba, Cu and Mg are consistent with the interpretations given to factor loadings, correlations and other numerical associations. Both As and Cu describe the location of major channelways and are in keeping with the theory of ascending ore fluids derived from a "granite" basement. In contrast Mg illustrates the distribution of pre-haematite secondary dolomitization. Barium provides the third most important characteristic of the mineralization and indicates the mixing of the ore fluids with sulphate rich formational waters in the Permo-Triassics. Lastly, the absence of regional variation in the ore geochemistry confirms the hypothesis of an homogeneous source for the iron.

TABLE 7

ANALYSIS OF VARIANCE FOR TREND SURFACES

Source	Sum of Squares	Degrees of Freedom	Mean Square	"F" ratio	Confidence Level
		Si (n = 92)			
Due to Linear	2.94×10^{1}	2	1.47×10^{1}	1.13	< 75% > 50%
Devs. from Linear	1.15×10^{3}	89	1.29×10^{1}		
		Fe (n = 89)			
Due to Lin.	1.11×10^{2}	2	5.55×10^{1}	2.06	< 90% > 75%
Devs. from Lin.	2.31×10^{3}	86	2.68×10^{1}		
Due to Quad.	1.84×10^{1}	3	6.13	0.22	< 25% > 10%
Dev. frm "	2.22×10^{3}	83	2.76×10^{1}		
		As (n = 92)			
Due to Lin.	1.76×10^{3}	2	8.79×10^{2}	0.19	< 25% > 10%
Dev. frm "	4.05×10^{5}	89	4.55×10^{3}		
		Cu (n = 91)			
Due to Lin.	5.87×10^{1}	2	2.94×10^{1}	0.56	< 50% > 25%
Dev. frm "	4.60×10^{3}	88	5.23×10^{1}		
		Pb (n = 94)			
Due to Lin.	3.54×10^{1}	2	1.78×10^{1}	0.20	< 25% > 10%
Dev. frm "	8.07×10^{3}	91	8.87×10^{1}		
		Zn (n = 94)			
Due to Lin.	1.46×10^{2}	2	7.30×10^{1}	2.41	< 95% > 90%
Dev. frm "	2.77×10^{3}	91	3.04×10^{1}		
Due to Quad.	2.37×10^{2}	3	7.90×10^{1}	2.75	< 99% > 95%
Dev. frm "	2.53×10^{3}	88	2.87×10^{1}		
Due to Cub.	4.32×10^{2}	4	1.08×10^{2}	4.33	< 99% > 95%
Dev. frm "	2.09×10^{3}	84	2.49×10^{1}		
Due to Quart.	1.17×10^{2}	5	2.34×10^{1}	0.93	< 75% > 50%
Dev. frm "	1.98×10^{3}	79	2.51×10^{1}		
		Ti (n = 91)			
Due to Lin.	3.58×10^{3}	2	1.79×10^{3}	2.56	< 95% > 90%
Dev. frm "	6.15×10^{4}	88	6.98×10^{2}		
Due to Quad.	4.71×10^{2}	3	1.57×10^{2}	0.22	< 25% > 10%
Dev. frm "	6.10×10^{4}	85	7.17×10^{2}		

All other elements gave Linear explanations below the 75% confidence level.

12. FACTOR ANALYSIS

As described in chapter 8, factor analysis is a method for identifying mutually uncorrelated linear combinations of "m" variables such that the variability of the total system is described more efficiently. In any geochemical system certain elements behave as a coherent group in response to physicochemical changes. Factor analysis allows one to define these groups and thus makes it possible to interpret the process which is controlling thedistribution of elements within a given group. Similar results can be obtained using multiple linear regression analysis but the data is less readily interpretable and the technique contains no facility for maximising the correlations in "m" vector space. Being an analysis of variance, factor analysis provides a greater insight into the interelement relationships of the type:

$$X_1 \propto X_2^{\frac{1}{2}} \propto X_3$$

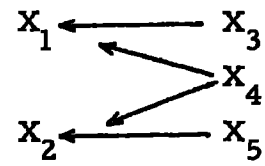

These tend to weaken the numerical value of simple correlation coefficients and so conceal significant geochemical associations. The following discussion refers only to the rotated "varimax" solution as the promax solution (for K min. = 2, 4 and 6) offered little refinement of the factor loadings. Because of the small sample/variable ratio for the botryoidal ores (i.e. 24/17) interpretation is restricted to the massive ores from the West Cumberland orefield (N. B. A ratio of at least 3/1 is recommended). In general the distribution of the factor loading is unknown and therefore the significance level of factor loadings, which are the correlation coefficients between the original variables and the factor, were estimated using the approximation:

$$r \text{ sig.} = \frac{\pm 2.5}{\sqrt{n}}$$ where n = nos. of samples (after Vistelius and Fuller 1969)

where $n \triangleq 100$ this value approximates to the 0.05 sig. level, but for smaller numbers the confidence limits are lower. For the massive ores ($n = 56$) the corresponding r value is 0.300. Rotated factor matrices are often presented in many forms:

(i) Factor matrix (Vistelius and Fuller 1969)

(ii) Factor loading graphs (Spencer 1966)

(iii) Scattergrams of factor scores (Le Maitre'68)

The second format contains most of the information of the original matrix and is more readily interpreted. In a factor loading graph each factor is allocated a vertical rectangular box whose height is divided into a scale between $\pm$ 1. The variables are positioned in the box according to their factor loadings.

As shown in figure 30, 10 factors account for 88% of the variance in the original data. Eigenvectors accounting for less than 4% of the variance were not rotated and thus contain the residual variance unexplained by the communalities (i.e. $h^2 < 1$). Factor loading graphs for the haematite ores are given in figure 31.

Factor 1: Carbonate Factor

This factor explains most of variation in Ca, Mg and Mn, and is considered to be an expression of the residual carbonate chemistry of the original wallrocks. It confirms the interpretation given to the correlations Ca: Mn and Ca: Mg and the role of carbonates in controlling the distribution of Mn.

FIG. 30. SIMPLIFIED VARIMAX FACTOR MATRIX FOR THE MASSIVE ORES, WEST CUMBERLAND

1	1	2	3	4	5	6	7	8	9	10	Communality h^2
As		+0.388		+0.349	+0.428	+0.385					0.81
Pb							+0.939				0.94
Cu		+0.304						+0.740		+0.345	0.86
Ni		-0.306						+0.748			0.85
Zn		+0.787									0.75
Y									0.944		0.93
Mn	-0.849		-0.356								0.89
Ba										+0.915	0.89
Sr						+0.923					0.93
Rb				-0.955							0.94
Zr					+0.911						0.89
Ti			-0.543		+0.440					+0.558	0.86
Si		-0.890									0.87
Fe		+0.898									0.88
Al	-0.268		-0.867								0.90
Ca	-0.811		-0.348								0.84
Mg	-0.832		+0.322								0.91

Values below 0.300 considered insignificant

FIGURE 31

FACTOR LOADING GRAPHS FOR THE WEST CUMBERLAND MASSIVE ORES
(Varimax solution using screened data)

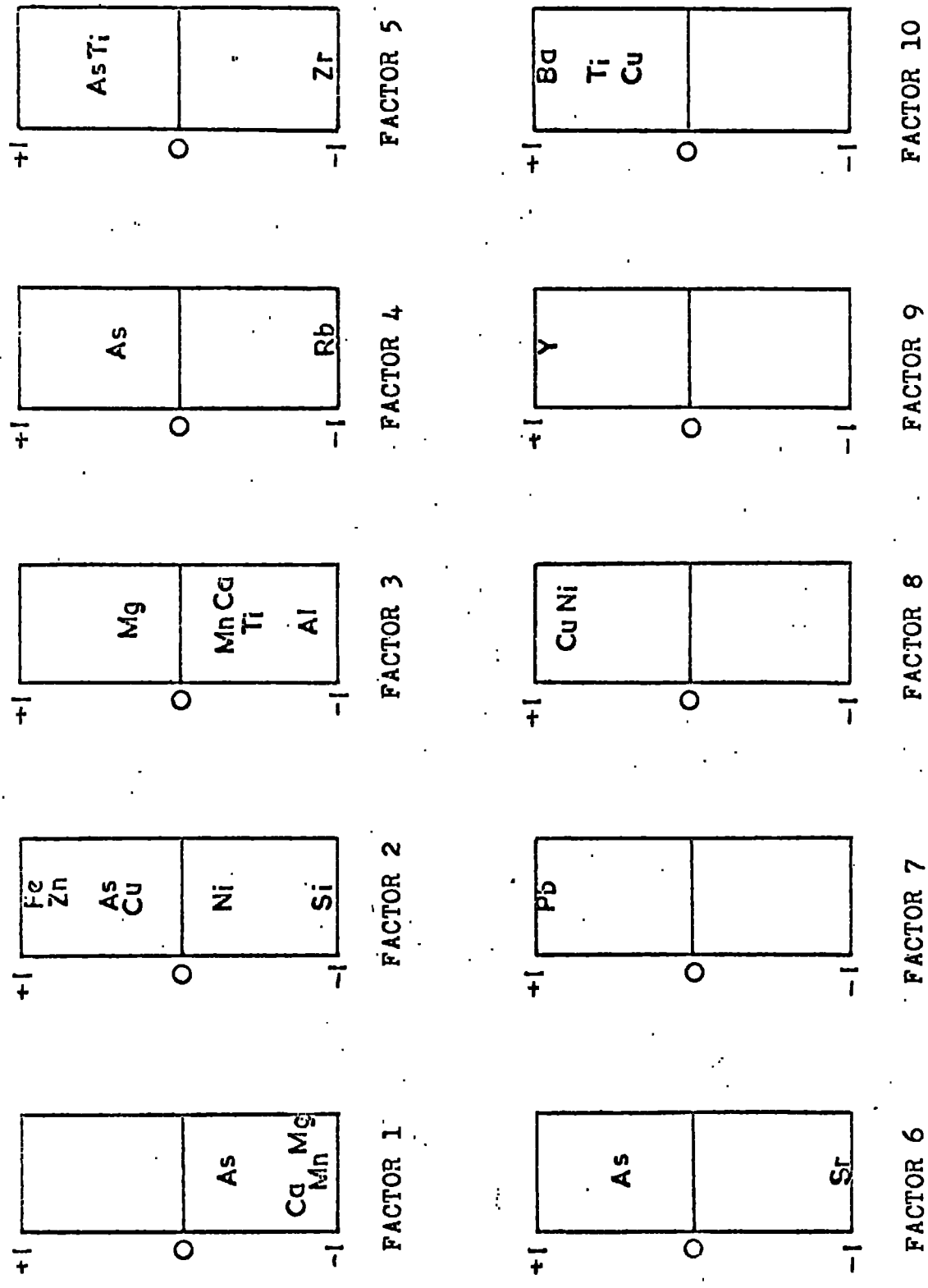

Factor 2: Primary Ore Fluid Factor

The negative loadings on this factor are a direct result of the mathematical interlock for systems containing variables of a constant sum and are therefore of doubtful significance (Chayes 1960). Since the primary ore fluids are characterised by an enrichment in Fe the sympathetic positive loadings for As, Cu and Zn are thought to indicate the trace element composition of the ore fluids. For this factor to have been interpreted as a function of selective adsorption by iron oxides similar loadings would have been expected for Ni, Pb and Ti.

Factor 3: Wallrock Dolomitization Factor

Throughout the West Cumberland orefield the main phase of haematization was preceded by a phase of secondary dolomitization. The process does not appear to have been directly connected with the mineralization because orebodies are equally developed in areas of dolomitized and undolomitized limestone. Accordingly the antipathetic relationship between negative Al, Ca, Mn and Ti loadings and the positive Mg loading is considered to be function of dolomitization. The process is preferentially expressed through the clay content of the limestone because this is least affected by the redistribution of Ca and Mg. Dolomitization may also account for the bimodal Ca distribution.

Factor 4, 5 and 6: Selective Replacement Factors

Factors 4, 5 and 6 have been grouped together because they each contain a positive loading for As together with one or more elements identified as residual wall rock components. This is thought to suggest the selective replacement of three lithologically dissimilar carbonate units. Evidence provided by the interelement relationships between Al, Ca, Mg,

Rb and Sr supports this view (chapter 9).

(i) Factor 4 is considered to be the metasomatism of argillaceous limestones for which the negative Rb loading indicates a relatively unfavourable degree of replacement. This agrees with the occurrence of undisturbed shale bands sometimes found within the massive ores.

(ii) Factor 5 is considered to be the metasomatism of arenaceous limestones where the positive Ti-Zr loadings indicate a more favourable degree of replacement. Both Ti and Zr are interpreted as the heavy mineral fraction of the limestone.

(iii) Factor 6 is considered to be the favourable metasomatism of normal limestones where the positive Sr loading indicates undolomitized non-argillaceous carbonate units.

The loadings for As on each of the above factors confirms the earlier suggestion that As variation is controlled by the nature of the original wallrocks and offers a possible explanation for its polymodal distribution.

Factor 7: Analytical Error Factor

The single loading for Pb on this factor is difficult to relate to any geochemical process and is probably due to the poor analytical precision for low Pb values.

Factor 8: Chalcopyrite Factor

Within the orefield there are several areas of chalcopyrite mineralization which appear to predate the haematite deposition. It is tentatively suggested therefore that the positive loadings for Cu and Ni represent contamination of the iron-bearing ore fluids by pre-existing copper (+ minor nickel) mineralization along common channelways.

Factor 9: Yttrium Factor

Unlike Pb, Y shows no significant analytical error and cannot be ascribed to low precision. The only possible link is with the Eskdale

botryoidal ores which are slightly higher in Y and show a positive correlation Cu: Y. On this limited evidence the yttrium factor is described as a trace element characteristic of the ore fluids.

Factor 10: Permo-Triassic Proximity Factor

The occurrence of barite gangue in orebodies directly beneath the Brockrams or along faulted troughs of Permo-Triassic sediments suggests that this factor expresses a change in the depositional environment on approaching the overlying Permo-Triassic cover. As described in Chapter II this feature is attributed to a mixing of the ore fluids with formational waters of different composition causing the precipitation of barite. For reasons unknown Cu and Ti are in some way involved in this process.

Factor analysis of the massive ores confirms the interpretation given to the simple correlation coefficients but extends the analysis by separating the components of variance for individual elements. As a result further inter element associations are revealed which would have otherwise been classified as unsignificant. The inferred role of more than one factor in controlling the variance of As, Ca, Cu, Ti, etc. agrees closely with the existence of discrete subpopulations in the frequency distribution patterns for these elements.

13. PROPOSED MODEL FOR HAEMATITE ORE GENESIS

13.1. Introduction

For an alternative theory of haematite ore genesis to be accepted it must offer a better explanation of the observed mineralization than previous theories. It must also attempt to reconcile the conflicting evidence proffered by rival schools of thought "ascensionists vs descensionists". In the author's opinion the theory described below satisfies these requirements and provides a dynamic model of ore genesis in which the process of haematization is integrated with the geological evolution of the area. Though based on new data, it incorporates the observations of earlier workers whose detailed accounts of workings now abandoned proved invaluable. The essential concept of the theory is the release of iron from a concealed granite basement, co-extensive with the Eskdale intrusive, by circulating sub-surface brines. The process in considered to have taken place in two distinct stages:

Stage 1: Late stage alteration of the granite producing a chemical breakdown of the primary constituents and localised precipitation of the iron as free haematite.

Stage 2: Remobilisation of the haematite by circulating sub-surface brines and redeposition at higher levels as epigenetic haematite deposits during the ? late Carboniferous and late Triassic.

13.2. Origin and Chemistry of the Ore Fluids

The period of initial alteration appears to have been confined to certain areas of the basement: the northern part of the Eskdale granite,

the concealed ridge beneath the Scafell and Langdale areas, and the deeper extensions of the basement beneath the Ennerdale Shelf. This is partly substantiated by the distribution of sympathetic epidotization in the Ordovician volcanics overlying the basement granites. All three areas occupy the central zone of the Eskdale gravity "low" and constitute a structural "high" relative to the surrounding sedimentary basins. The absence of similar alteration in the Shap and Skiddaw granites is complemented by a comparable absence of haematite mineralization.

Remobilisation during stage two is thought to have been less widespread and restricted to channelways controlling the convective circulation of sub-surface brines moving outwards from the Carboniferous and Triassic basins. Accordingly the metasomatic replacement deposits directly above the western margins of the Ennerdale Shelf probably owe their development to the excellent channelways provided by the system of deep faults along the edge of the basement granite. (Fig. 32). Elsewhere the penetration of brines into the centre of the structural "high" accounts for the spatial correlation between haematite veins in the Lower Palaeozoics and the position of the Eskdale gravity "low".

The present study provides no direct evidence for the chemical state of the iron in the ore fluids and one can make only general inferences based on the ore geochemistry and fluid inclusion data. Both Garrells (1960) and Hem (1960) have shown that the solubility product of $Fe(OH)_3$, the most stable species of iron in the Eh-pH range of natural waters, is extremely low except for pH 4. White(1963) however notes that the solubility is several orders of magnitude higher in chloride rich brines and reports a value of 110 ppm Fe for a Louisiana orefield brine having a pH of 6.3 (c.f. 0.1-0.001 ppm Fe at pH 5-6). Saline brines therefore possess the capacity for carrying

DIAGRAMMATIC SECTION THROUGH THE NORTHERN PART OF THE WEST CUMBERLAND ORE FIELD

(showing the position of the basement granite relative to the overlying haematite mineralization)

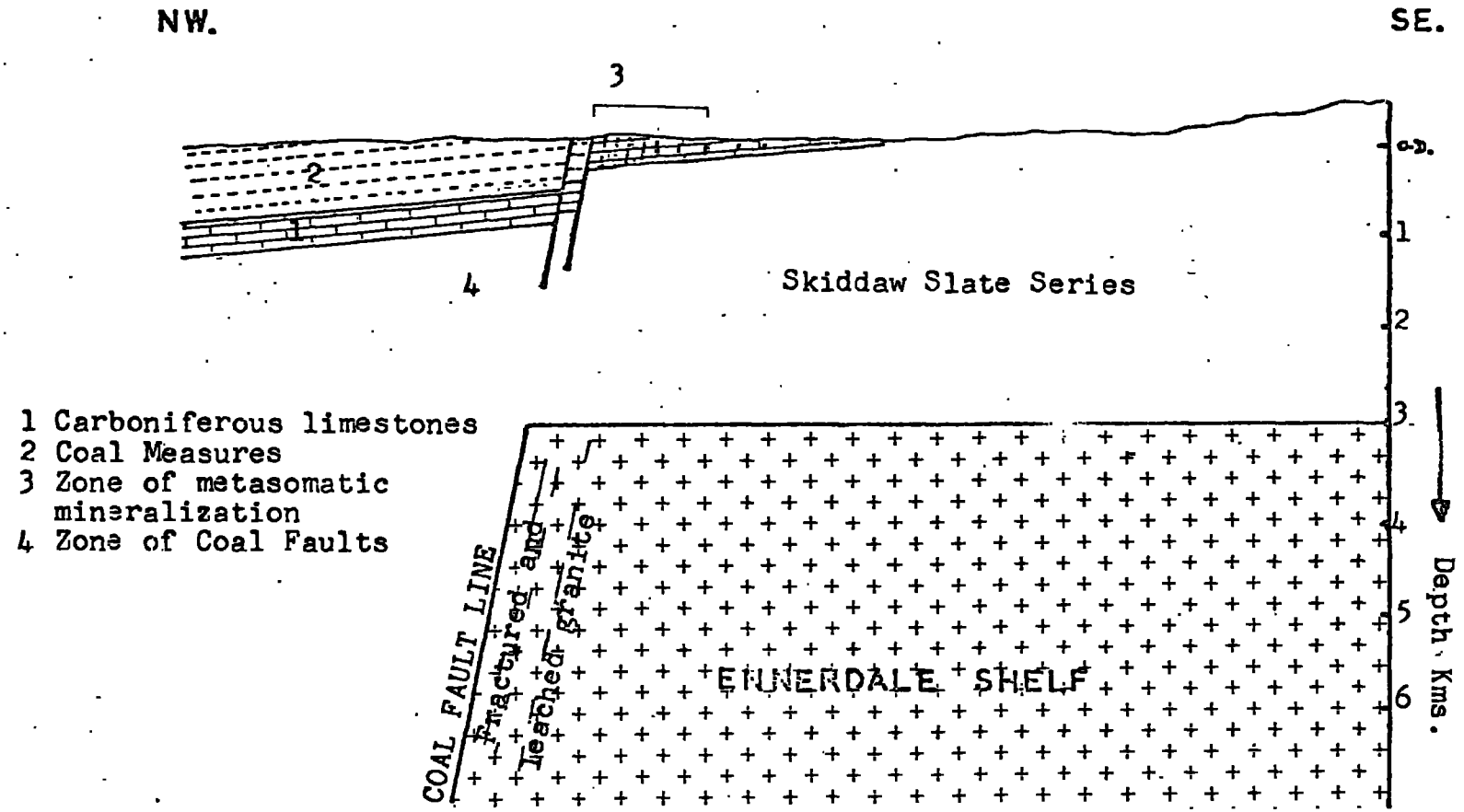

FIGURE 32

substantial quantities of iron in solution and acting as potential ore fluids. Recent experimental work by Collepardi et al.(1972) has revised much of the earlier work by Smith and Kidd (1949) on the stability of goethite and haematite in neutral solutions. Their results indicate that during the aging of iron oxide gels the transformation of goethite to haematite is accelerated by an increase in temperature, and in the presence of (Cl-)ions the crystallization of goethite is totally inhibited. This is in excellent agreement with the absence of goethite in the Cumbrian province and the high salinity of the fluid inclusions. Under such conditions siderite would not be expected since even at 25°C and p $CO_2 = 10^{-3.5}$ atmospheres the stability field for iron carbonate is remarkably small. Moreover the effect of "salting-out" and retrograde solubility at higher temperatures would lead to a further decrease in the activity of CO_2 in solution (Garrels 1960). Verification of the experimental relationship between (Cl^-) and haematite stability is given by the ferruginous precipitates associated with thermal springs in the Kurile Islands (Chukrov 1973). For chloride-rich thermal waters containing 1-13 ppm Fe the iron is precipitated directly as ferrihydrite; a colloidal mineral of the hydrous iron oxide group having the composition $Fe_2O_3 \cdot 4.5\ H_2O$. With time it alters spontaneously to haematite and has been identified in the Atlantis II Red Sea Deep, the Cheleken area of eastern Siberia and the East Pacific Rise.

The evidence presented by White, Collepardi and Chukhrov suggests that hot saline brines provide a suitable solvent for dissolving the free haematite from the basement granites and redepositing it higher levels under positive Eh /neutral pH conditions. The large overlap between the stability field for (SO_4^{2-}) and the Eh field for haematite is thermodynamically consistent with the simultaneous precipitation of barites as observed in Egremont area.

The (Cl^-) / haematite relationship also confirms the hypothesis for chloride-rich ore fluids and sulphatic waters in the Permo-Triassics. Conversely a model involving suphate-rich ore fluids would drastically reduce the activity of iron in solution and enlarge the stability field for goethite at the expense of haematite.

13.3. Age of the Mineralization

If Boone's interpretation of reddened feldspars is correct then the first stage of remobilisation must have occurred soon after the intrusion of the granite magma. The second stage is more difficult to define but is generally accepted as post-Triassic because of the distribution of orebodies along post-Triassic faults. Against this evidence however are the observations of Kendall who records the occurrences of haematite fragments in the Brockrams and the pre-Triassic dislocation of orebodies in the Frizington area. These indicate an apparent late Carboniferous or even early Permian age for the mineralization. The simplicity of the present model is its flexibility to accommodate several periods of mineralization; the formation of ore fluids being limited only by the migration of sub-surface brines into the basement granites. This is most likely to take place after a period of tectonic movement when new fractures are formed and old ones reactivated. Apart from minor instability the Lake District appears to have remained stable until the end of the Carboniferous and late Trias when there was considerable readjustment along the margins of the basement granites. During these periods deep fault structures were established along the Egremont and Coal Fault Lines providing suitable channelways for granite-brine interactions. It is thought that the West Cumberland mineralization occurred immediately after these periods, particularly the post-Triassic event. A minor phase of haematite remobilisation corresponding to late Carboniferous movement on the Coal Fault Line is

theoretically possible and would explain Kendall's observations without invalidating the main post-Triassic phase of mineralization. By analogy, deep level penetration of brines into the centre of the structural "high" would produce the numerous haematite veins now seen in the Lower Palaeozoics directly above the altered Eskdale granite and its concealed extensions. Although an upper limit for the post-Triassic age has not been determined the palaeomagnetic work of DuBois (1962) suggests that it is unlikely to be Tertiary. For the Florence orebody the mean direction of remnant magnetisation indicates a late Permian to early Triassic palaeomagnetic pole direction.

Using the West Cumberland orefield as a test case it can be shown that the volume of granite beneath the mineralized zone is capable of supplying several times the 90 million tons of haematite already mined. Assuming a basement of Eskdale granite (pink variety av. 1.72% total Fe) and a 25% precipitation of remobilised iron a source volume of 2.66×10^{10} cu yds is required to generate 100 million tons of ore. Expressed in terms of the geometry of the orefield this is equivalent to a wedge "12 miles X 0.75 miles X 0.54 miles". Since the gravity interpretation of the Ennerdale Shelf indicates a continuation at depth to 3.2 miles only the uppermost part of the granite need be leached.

13.4 Potential Areas for Future Exploration

As indicated in figure 6 the occurrence of metasomatic ore bodies beneath the 100 ft. isopachyte for the St. Bees Shale renders the shale/conglomerate transition hypothesis (Trotter 1945) an unsuitable basis for mineral exploration. According to the new theory however areas of limestone underlain by granite and penetrated by pre- or post-Triassic faults are primary target areas (Fig. 3). The most important of these is

the Linethwaite intersection area located at the northwestern corner of the Ennerdale Shelf. Because of the thick Permo-Triassic cover and absence of mineralization in the Hensingham inlier this area has received little systematic attention and deserves further investigation. By definition limestones west of the Egremont and Coal Fault Lines are considered poor prospects unless it can be proved that the degree of lateral migration is much greater. The southern extension of the productive Florence-Beckermet zone along the projected Egremont Line continues to rank as an important reserve area, subject to more accurate information on the Carboniferous isopachytes south of Calder Bridge. North of Frizington the area is relatively unfaulted but where developed the faults are invariably mineralized. In view of the favourable position of the Coal Fault Line and the occurrence of ore bodies at Rowrah and Lamplugh this area has further potential. The northern limit of exploration will depend mainly on additional geophysical work defining the northern margin of the Ennerdale Shelf beyond the present study area.

13.5. Conclusions

The proposed theory of haematite ore genesis envisages the migration of Carboniferous connate brines into the granite basement beneath the central Lake District after periods of tectonic readjustment. Subsequent interaction with areas of altered granite containing free haematite is thought to have caused a remobilisation of the iron and its redeposition at higher levels. The driving force behind the mechanism is considered to be the natural thermal bouyancy of a hydrological system in a region of slightly higher geothermal gradient. Localised mixing of the barium-rich ore fluids with sulphatic formation waters from the overlying Permo-Trias provides a satisfactory model for the distribution of baritic ore bodies. In the

West Cumberland area the metasomatic deposits are located directly above the faulted margins of a concealed granite shelf whilst in the eastern sector of the province the veins are clustered above the structural "high" provided by the Eskdale granite and its concealed extensions.

To summarise, the theory succeeds in explaining:

(i) The linear distribution of metasomatic ore bodies in the Carboniferous limestones and their genetic relationship to scattered vein deposits in the Lower Palaeozoics.

(ii) The haematization of the Eskdale granite.

(iii) The absence of mineralization in the Hensingham inlier and Wilton outlier.

(iv) The association between haematite and barites.

(v) The age and uniform nature of the mineralization.

14. CONCLUSIONS

1. The geochemical investigation of epigenetic haematite deposits in the western, central and southern areas of the Lake District reveals a marked uniformity in the style and nature of the mineralization. The ores are characterised by a very simple mineral assemblage (haematite, quartz, calcite + minor barite, fluorite, dolomite and siderite) in which the gangue minerals are subordinate.

   Locally barite is abundant and exceeds the total amount of quartz and calcite.

2. A comparison between the Bouguer gravity field for the Lake District and the occurrence of haematite veins in the Lower Palaezoics indicates a spatial correlation related to the presence of granite in the basement. This is particularly well developed for the Eskdale granite and its concealed extensions beneath the Scafell and Langdale areas. Closer examination shows that the mineralization is associated with a specific variety of the intrusion containing an abundance of free haematite released during late stage alteration of the partially consolidated magma.

3. A detailed interpretation of the gravity anomaly over the West Cumberland orefield indicates that the zone of maximum metasomatism in the Carboniferous limestones occurs directly above the western margins of a concealed granite shelf extending outwards from the Ennerdale granophyre beneath a relatively thin cover of Lower Palaeozoics. The edges of the shelf are steep and well defined, and appear to have controlled the development of faulting and associated

mineralization. The absence of haematization in the Hensingham inlier and Wilton outlier confirms the suggestion that the distribution of mineralization has been determined by the structure and composition of the basement. It also implies a minimum degree of lateral migration by the ore fluids.

4. Factor analysis and complementary techniques demonstrate that the chemical constituents of the West Cumberland massive ores can be divided into two main groups: a primary ore fluid group (Fe, As, Cu, Pb) and a residual wallrock group (Ca, Mg, Al, Si, Rb, Sr, Ti). The former group represent elements introduced into the area of deposition whilst the latter group represent the chemical residue of the wallrocks. Silicon is classified as a residual component because there is sufficient silica in the limestones to account for the observed variation in quartz without requiring a substantial contribution from the ore fluids. The characteristic polymodal distributions for certain elements are attributed to the replacement of different carbonate lithologies and can be used to define the original composition of the wallrocks.

5. Except for As, Cu, Mg, and Ba the West Cumberland massive ores show no significant spatial variation in ore geochemistry. The patterns which do exist are only discernible in the screened data and are either obscured or discontinuous in the raw data. For As and Cu there is a slight assymetric zoning about the projected margins of the Ennerdale Shelf; the decrease in values being steeper to the west. This agrees with the sharp cut-off in mineralization west of the Coal Faults and is consistent with a model of ore genesis in which

the basement granites are the source of the iron. The pattern for magnesium is entirely different and is related neither to the distribution of haematite orebodies nor the disposition of the Permo-Triassics, thus discrediting any theory regarding dolomitization as a necessary precursor of iron metasomatism. In view of its negative covariance with other diagnostic wallrock components it is interpreted as an index of pre-haematite secondary dolomitization. Barium, unlike magnesium, is intimately associated with the haematite and has a distribution which is best described by the mixing of barium-rich ore fluids with sulphatic formation waters from the Permo-Triassic cover.

6. Fluid inclusion studies on gangue minerals coeval with the haematite indicate a uniform temperature of deposition throughout the West Cumberland area (av. min. temp. 108°C). By using a convective groundwater model the pressure correction is only +15 - 20°C for an hydrostatic system. Limited salinity measurements suggest that the ore fluids were moderately saline brines containing 10-21 wt% NaCl equivalent.

7. Based on the above evidence a new model of ore genesis is proposed which envisages the leaching of iron from selective areas of the granite basement beneath the Lake District by heated subsurface brines, and its redeposition at higher levels as epigenetic haematite. The upward movement of the ore fluids being controlled by the distribution of through-going fault structures linking major dislocations in the basement with open channelways in the Palaeozoic cover. Thus the West Cumberland orefield owes its existence to three important factors:

(a) The presence of a granite basement immediately beneath the area containing free haematite.

(b) The formation of open fault structures by periodic movement along the edge of the Ennerdale Shelf.

(c) The presence of a reactive limestone cover providing a repository for the iron-bearing ore fluids.

8. The concept of an homogeneous granite source provides a satisfactory explanation for the regional distribution of mineralization and the uniform nature of the mineralogy and ore geochemistry. It also accounts for the development of orebodies beneath more than 100 ft. of St. Bees Shale in contradiction to the breccia/shale hypothesis. In terms of previous theories the model is basically "ascensionist" with a provision for local recirculation as determined by the hydrological system in the host rocks.

9. The main phase of mineralization is considered to have taken place in the middle or late Trias following isostatic readjustment and faulting in the basement in response to denudation and sedimentary loading in the adjacent Permo-Triassic basins.

ACKNOWLEDGEMENTS

The work for this thesis was carried out during the tenure of a N.E.R.C. research studentship award, without which the work would not have been possible.

I wish to thank Professor G. M. Brown for the unrestricted use of research facilities in the Department of Geology, and my supervisors Mr. R. Phillips and Dr. D. M. Hirst for their help and encouragement during the work. Special thanks are also due to my fellow research students, particularly Dr. G. Gale and Dr. M. J. Reeves, for their constructive ideas and discussions. Dr. J. G. Holland is thanked for his initial instruction in X-ray fluorescence spectrography.

I am especially indebted to Professor M. H. P. Bott for his kindness in providing the basic gravity data for the Lake District and his guidance in using the "GRAVN" computer programme.

Finally I should like to express my sincere thanks to the British Steel Corporation for allowing access to their underground workings at the Haile Moor and Beckermet Mines, and to Mr. P. Greenwood and Dr. C. Nicholas for their many discussions on the West Cumberland haematites.

REFERENCES

ADLER, I 1966: X-ray emission spectrography in geology. Methods in Geochemistry and Geophysics, Vol. 4 Elsevier Publ. Co., New York.

AMES, L. L., 1961A: Anion metasomatic replacement reactions. Geochim Cosmochim. Acta 56, 521-532

AMES, L. L. 1961B: Cation metasomatic replacement reactions. Geochim Cosmochim. Acta 56, 1017-1024

BERNARD, A. & SAMAMA, J. C., 1968: Premiere contribution a l'etude sedimentologique et geochimique du Trias Ardechois. Faculte des Sciences de Nancy, Rapport scientifique de l'Action Concertee 63 FR 073

BOTT, M. H. P., 1964: Gravity measurements in the north-eastern part of the Irish Sea. Quart. J. Geol. Soc. Lond. 120, 369-396.

BROOKS, F. A., 1960: Trace and minor elements in the Woodbine Subsurface waters of the East Texas Basin. Geochem. Cosmochin Acta 20, 199-214

BROWN, P. E., MILLER J. A. & SOPER N. J., 1964: Age of the principal intrusions of the Lake District. Proc. Yorks. Geol. Soc. 34, 331-342

CHAYES, F., 1960: Gen. correlations between variables of constant sum. J. Geophys. Res. 48, 4185-4193

CHAYES, F., 1970: On deciding whether trend surfaces of progressively higher order are meaningful. Bull. Geol. Soc. Amer. 81, 1273-1278.

CHUKHROV, F. V., 1973: Mineral Deposita 8. 138 - 147

CLARK, L., 1963: Geology and petrology of the Ennerdale granophyre, its metamorphic aureole and associated mineralization. Unpublished Ph. D. thesis, University of Leeds.

COLLEPARDI, M., MASSIDDA, L. & ROSSI, G. 1972: Aging of iron oxide gels. Trans. Inst. Min. Metall. 81, C 43-46

DAVIDSON, C. F., 1966: Some genetic relationships between ore deposits and evaporites. Trans. Inst. Min. Metall. 75, B216-225

DAYSH, G. H. J. & WATSON, E. M., 1951 Cumberland: A survey of industrial facilities. The Cumberland Development Council Ltd.

DIXON, E. E. L. & SMITH, B., 1927: The origin of the Cumberland haematites. Summ. Prog. Geol. Sum. G. B., 23-36

DOVETON, J. H. & PARSLEY, A. J., 1970: Experimental evaluation of trend surface distortion induced by inadequate data-point distribution. Trans. Inst. Min. Metall. 79. B 197-207

DUNHAM, K. C. & ROSE, W. C., 1941: Geology of the iron-orefield of South Cumberland and Furness. Geol. Surv. G. B. Wartime Pamphlet No. 16.

FIRMAN, R. J., 1953: Metamorphism and metasomatism around the Shap and Eskdale granites. Unpublished Ph. D. thesis, University of Durham.

FIRMAN, R. J., 1960: The relationship between joints and fault patterns in the Eskdale granite (Cumberland) and the adjacent Borrowdale Volcanic Series. Quart. J. Geol. Soc. Lond. 116, 317-347.

FOLKMAN, J., 1969: Gravity survey over the Boundary Fault in West Cumberland. Unpublished M. Sc. thesis, Univ. of Durham.

GARRELS, R. M., 1960: Mineral equilibria at low temperature and pressure. Harper & Bros., New York.

GOODCHILD, J. G., 1889: Some observations upon the mode of occurrence and the genesis of metalliferous deposits. Proc. Geol. Assoc. 11, 45-69

GRIGOREV, D. P., 1967: Genetictypes of reniform aggregates, pp 43-50, Metacolloids in Endogenic Deposits, ed. Lebedev, L. M. Plenum Press, New York.

GUNDLACH, H. STOPPEL, D. & Strubel, G., 1972: The hydrothermal solubility of barite. 24th Int. Geol. Congr., Proc. Symp. Sect. 10, 219-229

HARBAUGH, J. W. & MERRIAM, D. F., 1968: Computer applications in stratigraphic analysis. Wiley & Sons, New York.

HEM, J. D., 1960: Restraints on dissolved iron composed by bicarbonate redox potential and pH. U. S. Geol. Surv. Water-Supply Paper 1459-B, 33-55

ICKES, E. L., 1924: Recent exploration for petroleum in the United Kingdom. Trans. Amer. Inst. Min. Metall. Engrs. 70, 1053-1075

INESON, P. R., 1967: Trace element geochemistry of wallrock alteration in the Pennine orefields and Cumberland ironfield. Unpublished Ph. D. thesis, Univ. of Durham.

INGERSON, E., 1947: Liquid inclusions in geological thermometry. Amer. Mineral. 32, 375-388

JAMES, H. L., 1966: Chemistry of the iron-rich sedimentary rocks. Data of Geochemistry, Chap. W., U. S. Geol. Surv. Prg. Paper 440-W

KENDALL, J. D., 1873: Haematite deposits of Whitehaven and Furness. Colliery Guardian 28, 157, 230 and 374

KENDALL, J. D., 1875: Haematite deposits of Whitehavenand Furness. Trans. Manch. Geol. Soc. 13, 231

KENDALL, J. D., 1876: Haematite in the Silurians. Quart. J. Geol. Soc. Lond. 32, 180-183

KENDALL, J. D., 1879: Haematite deposits of West Cumberland. Trans. Fed. Inst. Min. Mech. Engrs. (N. Eng. Inst) 28, 109 - 154

KENDALL, J. D., 1881: Haematite deposits of West Cumberland (supp paper) Trans. Fed. Inst. Min. Mech Engrs. (N. Eng. Inst) 30, 27 - 30

KENDALL, J. D., 1882: Haematite deposits of Furness. Trans. Fed. Inst. Min. Mech Engrs. (N. Eng. Inst) 31, 211-237

KENDALL, J. D., 1893: The iron ores of Gt. Britain and Ireland, Lond.

KENDALL, J. D., 1920: Review of Memoir Geol. Surv. G. B. Vol. 8 - Iron Ores." Mining Mag. 22, 58-62

KENDALL, J. D., 1920: The distribution of ore in depth. Mining Mag 22 282-286

KENDALL, J. D., 1921: Genesis of the Cumberland iron ores. Mining Mag. 24, 96-96

KENDALL, J. D., 1929: The origin of the Cumberland haematite. Mining Mag. 40, 141

KRUMBEIN, W. C. & GRAYBILL, F. A., 1965: An introduction to statistical models in geology. International Series in the Earth Sciences, McGraw Hill, New York.

LACHENBRUCH, A. H., 1970: Crustal temperatures and heat production - implications of the linear heat flow relation. J. Geophys. Res. 75, 3291-3300

LE MAITRE, W., 1968: Chemical variation within and between volcanic rock series - a statistical approach. J. Petrol 9, 220-252

LIEBHAFSKY, H. A., PFEIFFER, H. G., WINSLOW, E. H., & ZERMANY, P. D., 1960: X-ray Absorption and Emission in analytical chemist: Wiley & Sons, New York.

LLEWELLYN, P. G. & STABBINS, R., 1968: Lower Carboniferous evaporites and mineralization in the east and central Midlands of Gt. Britain. Trans. Inst. Min. Metall. 77, B170-173

LLEWELLYN, P. G. MAHMOUD, S. A. & STABBINS, R., 1968: Nodular anhydrite in Carboniferous limestones, West Cumberland. Trans. Inst. Min. Metall. 77, B18-25

MASON, B., 1958: Principles of Geochemistry (2nd Ed) Wiley & Sons N.

McDONALD, W., 1925: West Cumberland haematite deposits. Iron & Coal Trades Rev. 110.

MILLER, R. L. & KAHN, J. S., 1962: Statistical analysis in the geological sciences. Wiley and Sons, New York.

MITCHELL, G. H., 1956: The geological history of the Lake District. Proc. Yorks. Geol. Soc. 30, 407-463

MOSELEY, F. & AHMED, S. M., 1967: Carboniferous joints in the north of England and their relation to earlier and later structures. Proc. Yorks. Geol. Soc. 38, 61-90

NORISH, K. & CHAPELL, B. W., 1967: X-ray fluorescence spectrography, pp 161-214 Physical Methods in Determinative Mineralogy, ed. Zussman, J. Academic Press.

O'LEARY, M, LIPPERT, R. H. & SPITZ, O. T., 1966: Fortram IV and map programme for computation and plotting of trend surfaces for degrees 1 through 6. Computer Contrib. 3, State Geol. Surv., Univ. Kansas

OLIVER, R. L., 1961: The Borrowdale Volcanic and associated rocks of the Scafell area, English Lake District. Quart. J. Geol. Soc. Lond. 117, 377-417

PUCHELT, H, 1967: Zur Geochemie des Bariums in exogenen Zyklus. Springer-Verlag.

RANKAMA, K. & SAHAMA, Th. G., 1955: Geochemistry. Univ. Chicago Press.

RASTALL, R. H., 1906: The Buttermere and Ennerdale granophyre Quart. J. Geol. Soc. Lond. 62, 253-274

REEVES, M. J., 1971: Geochemistry and Minerology of British Carboniferous seatearths from northern coalfields. Unpublished Ph. D. thesis, University of Durham.

ROEDDER, R. E., 1962: Ancient fluids in crystals. Scient. Amer. October.

ROEDDER, R. E., 1971: Metastability in fluid inclusions. Soc. Min. Geol. Japan, Spec. Issue 3, 327-334

ROEDDER, R. E., 1972: Composition of fluid inclusions. Data of Geochemistry, Chap. JJ., U. S. Geol. Surv. Prof. Paper 440-JJ

ROSE, W. C. C., 1937: Borrowdale Volcanic Series, pp 21-40. Gosforth District, Mem. Geol. Surv. G. B.

SASS, J. H., 1971: The Earth's heat and internal temperatures, pp 81-87 Understanding the Earth, ed. Gass, I. G., Smith P. J. and Wilson R. C. L., Artemis Press.

SCHNELLMANN, G. A., 1947: The West Coast haematite bodies. Mining Mag. 76, 137 -

SIMPSON, A., 1968: The Caledonian history of the north-eastern Irish Sea region and its relation to surrounding areas. Scot. J. Geol. 4, 135-163

SMITH, B., 1919: Haematites of West Cumberland, Lancashire and the Lake District. Spec. Rep. Mineral Resources 8, Mem. Geol. Surv. G. B.

SMITH, F. G., & KIDD, D. J., 1949: Haematite - goethite relations in neutral and alkaline solutions under pressure. Amer. Mineral 34, 403-412

SMITH, F. G., 1953: Historical development of inclusion thermometry. Univ. Toronto Press.

SOLOMAN, M., 1966: Origin of barite in the North Pennine orefield. Trans. Inst. Min. Metall. 75, B230-231

SOPER, N. J., 1970: Three critical localities on the junction of the Borrowdale volcanic rocks with the Skiddaw slates in the Lake District. Proc. Yorks. Geol. Soc. 37, 461-493

SORBY, H. C., 1858: On the microscopical structure of crystals, indicating the origin of minerals and rocks. Quart. J. Geol. Soc. Lond. 14, 453-500

SPENCER, D., 1966: Factors affecting element distribution in a Silurian graptolite band. Chem. Geol. 1, 221-249

SYLVESTER-BRADLEY, P. C. and FORD, T. D., 1968: The geology of the East Midlands. Leicester Univ. Press.

TEMPLETON, C. C., 1960: Solubility of barium sulphate in sodium chloride solution from 25°C to 95°C. Chem. Engr. Data 5, 514 - 516

TROTTER, F. M., 1945: The origin of the West Cumbrian haematites. Geol. Mag. 82, 67 - 80

TURNER, F. J. & VERHOOGAN, J., 1960: Igneous and metamorphic petrology. International Series in the Earth Sciences, McGraw Hill New York.

VISTELIUS, A. B. & FULLER, C. R., 1969: On the origin of variation in the composition of granite rocks of Chile and Bolivia. J. Int. Ass. Math Geol. 1, 113-116

WEST, I. M. BRANDON, A. & SMITH, M., 1968: On tidal flat evaporitic facies in the Visean of Ireland. J. Sed. Petrol 38, 1079-1093

WHITE, D. E. HEM, J. D. & WARING, G. A. 1963: Chemical composition of subsurface waters. Data of Geochemistry, Chap. F., U. S. Geol. Surv. Prof. Paper 440-F

YERMAKOV, N. P., 1965: Research on the nature of mineral-forming solutions. International Series of Monographs in Earth Sciences 22, Pergamon Press.

APPENDIX I

GRAVITY INTERPRETATION OF THE BASEMENT STRUCTURE, WEST CUMBERLAND

Introduction

Earlier work by Folkman (1969) in the Gosforth area had indicated a continuation at depth of the Ennerdale granophyre west of the Boundary Fault. This prompted the author to investigate the gravity pattern in the Egremont-Frizington area of the West Cumberland orefield for a similar structure because of a suspected geochemical relationship between haematite mineralization and the Eskdale granite. It was thought that zones of mineralization may reflect a proximity to areas of concealed "granite" in the basement.

To test this hypothesis a series of five carefully chosen profiles across the northern section of the orefield were examined (Fig. 3). Using accepted rock densities and a realistic regional gradient, the contribution to the residual anomaly by the Carboniferous/Permo-Triassic cover was mathematically removed. This enhanced the density contrasts in the Lower Palaeozoic basement and allowed a series of two-dimensional "best-fit" models to be calculated for each of the profiles. For the West Cumberland orefield they indicated a concealed shelf of "granite" extending west of the exposed granophyre and bounded by steep well defined margins which were coincident with the zones of maximum mineralization in the overlying limestones.

This work could not have been undertaken without the encouragement and advise of Prof. Bott and the unrestricted use of his own unpublished gravity data for the Lake District.

Method

Extensive use was made throughout of the computer programme

"GRAVN" written by Bott for calculating the gravity effect of two-dimensional bodies infinite in the "y" direction. The programme operates by evaluating the vertical component of gravitational attraction of one or more such bodies with specified density contrasts at field points above the level of the topmost part of the bodies. To prevent the solution matrix from becoming unstable the profiles were extended several kms. eastwards across the central part of the main Eskdale anomaly. The computation was described by three sequential steps:-

Step 1. Subtraction of the Bouguer anomaly from the regional gradient to give a residual anomaly.

The regional gradient was taken to be 0.2 mgals/km., rising to the NW and having a values of 32-35 mgals over the coast. This was in general agreement with the marine geophysical surveys in the Irish Sea and the values adopted by Bott (1964) and Folkman (1969). Figures 33, 34 and 35 show the regional and Bouguer components of the gravity field along profiles 2, 3 and 4, and display the important flexuring of the steep gradient associated with the western margin of the Eskdale-Ennerdale complex.

Step 2. Refinement of the residual anomaly by removing the contribution from the overlying Carboniferous/Permo-Triassic sediments.

The contributions were calculated (GRAVN) from geological cross-sections constructed along the profiles. Rock densities were taken from various published sources and are listed in Table 8. Isopachytes for the Carboniferous succession in the Whitehaven Coalfield were not available and it proved impossible to remove the cover reliably beyond a zone 2-3 miles west of the Skiddaw/Carboniferous junction. Data for profile 4 was taken directly from Folkman's Bouguer map corrected for post-Borrowdale Volcanic Series sediments. As expected only the low density

FIGURE 33

BOUGUER AND REGIONAL COMPONENTS OF THE GRAVITY FIELD ALONG PROFILE 2

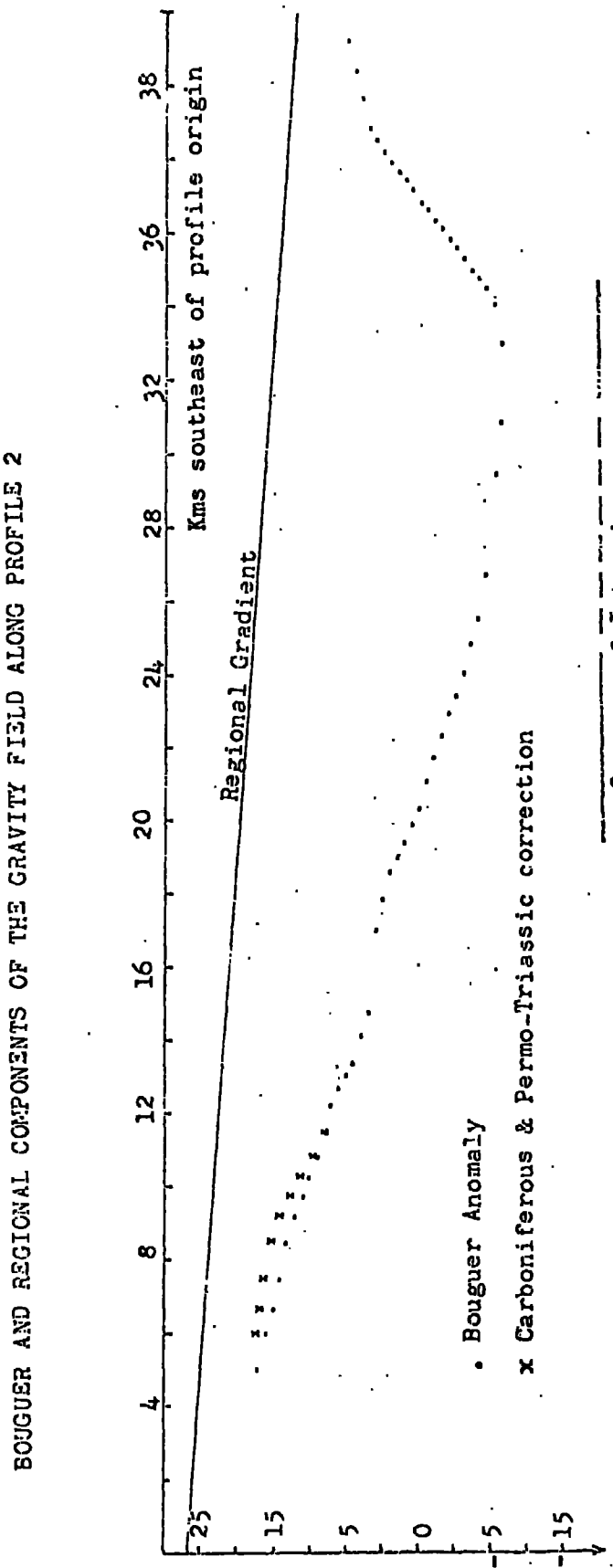

FIGURE 34

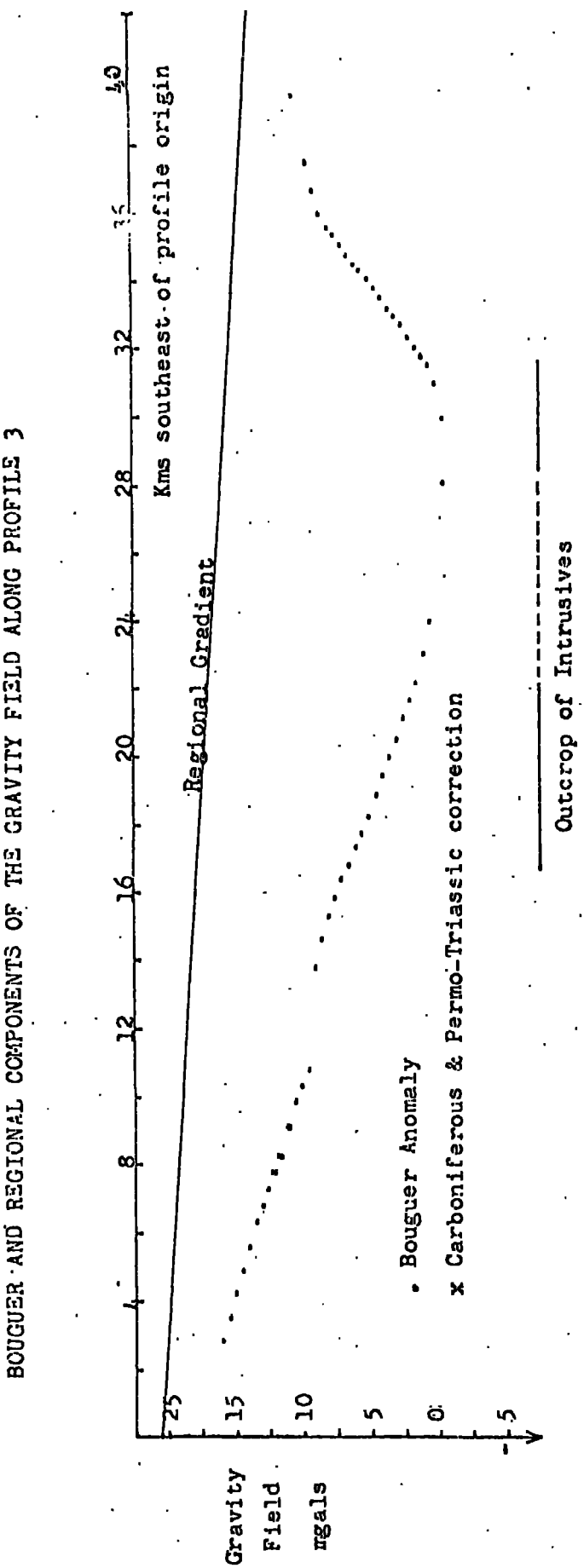
BOUGUER AND REGIONAL COMPONENTS OF THE GRAVITY FIELD ALONG PROFILE 3
Kms southeast of profile origin
0
4
8
12
16
20
24
28
32
36
40
Regional Gradient
Bouguer Anomaly
x Carboniferous & Permo-Triassic correction
Outcrop of Intrusives
Gravity Field mgals
25
15
10
5
0
-5

FIGURE 35

BOUGUER AND REGIONAL COMPONENTS OF THE GRAVITY FIELD ALONG PROFILE 4

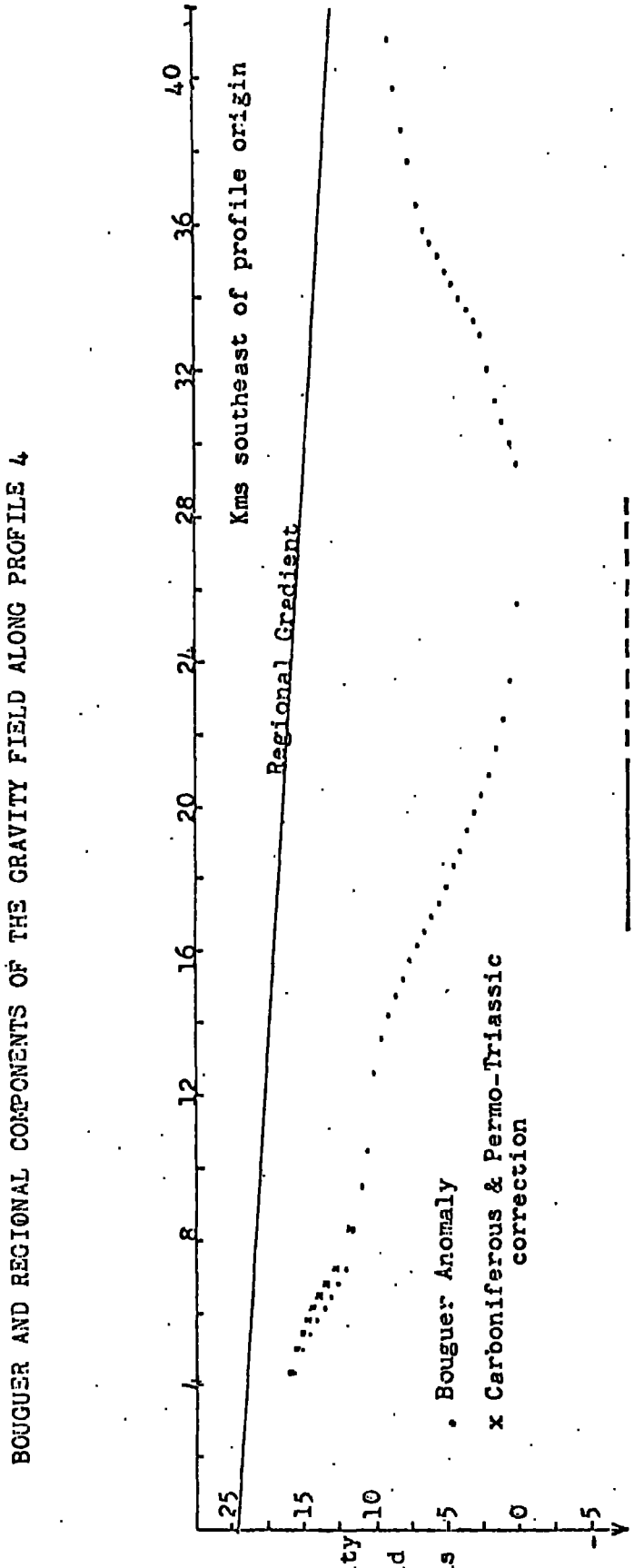

ADOPTED ROCK DENSITIES USED IN THE GRAVITY INTERPRETATION

	Density (grms/cc)		Source
St. Bees Sandstone	2.36		Folkman (1)
Brockram	2.65		Domzalski (5)
Carboniferous sandstone +shale	2.48	weighted mean	Masson-Smith (2)
Carboniferous limestone +shale	2.67	weighted mean	Bell (3)
Borrowdale Volcanic Series	2.74		Bott & Masson-Smith (4)
Skiddaw Slate Series	2.73		Domzalski (5)
Ennerdale granophyre	2.66		Folkman (1)

(1) Folkman 1969: Unpublished M.Sc. thesis, University of Durham
(2) Masson-Smith 1957: Unpublished Ph.D thesis, University of Cambridge
(3) Bell 1959: Unpublished M.Sc. thesis, University of Durham
(4) Bott & Masson-Smith 1957: Quart. J. geol.Soc. Lond., 113, 93- 117
(5) Domzalski 1955: Geophys.Prosp., Hague, 3, 254-7

Permo-Triassic sediments provided any significant contribution to the residual anomalies (e.g. Fig. 35).

Step 3: Calculation and comparison of theoretical and observed anomalies.

In the third and last step, anomalies due to different theoretical models were computed and compared with the observed anomalies until field point residuals were a minimum. The resulting "best-fit" models shown in figures 36 and 37 are compatible with the geological evidence and provide an explanation for the origin and distribution of haematite mineralization in the West Cumberland area.

Interpretation:

Three dimensionally the models describe a shallow concealed shelf of "granite" extending westwards from the exposed granophyre beneath a cover of Palaeozoic sediments. The shelf is bounded to the northwest by a steeply dipping margin (60^{o}-70^{o}) trending N65^{o}E as positioned by profiles 1, 2, 3 and 4. To the southwest the interpretation is less unambiguous, but by combining profile 5 with the isogal trends near Egremont a similar margin can be identified striking E45^{o}S. For convenience these structures have been named the "Ennerdale Shelf", "Coal Fault Line" and "Egremont Line" respectively and are shown in figure 6. Depths to the top of the shelf are only approximate since they are dependent upon the values chosen for the regional background and density contrasts. However, given the general geological and regional constraints a depth of 2-3 kms to the top of the shelf is not unrealistic. Fortunately the position of the margins is largely independant of the above parameters and the values given are a true representation of sub-vertical density surfaces.

In calculating the models, satisfactory fits could only be achieved

FIGURE 36

MODELS OF THE BASEMENT FOR PROFILES 1 AND 2

PROFILE 1

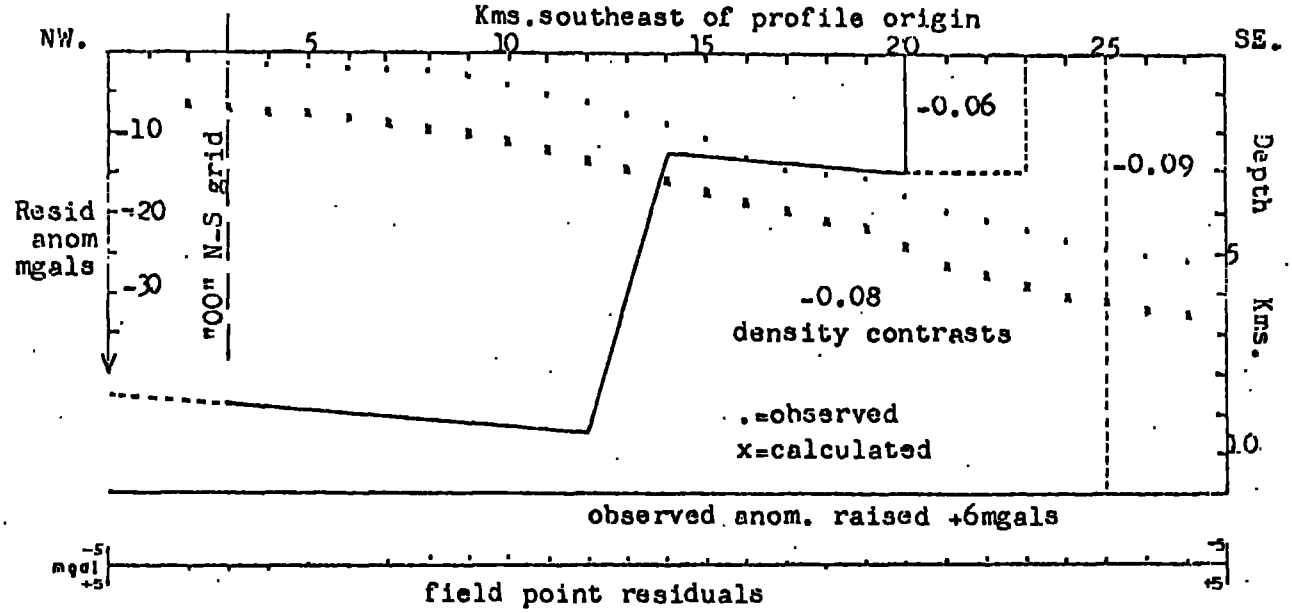

PROFILE 2

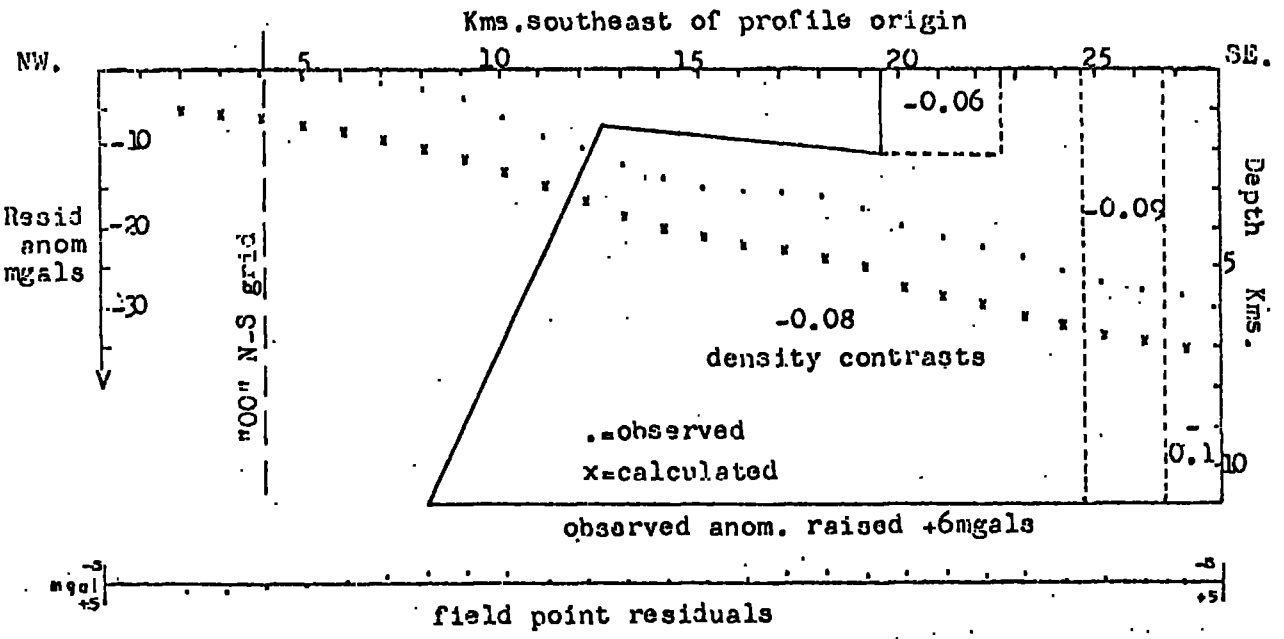

FIGURE 37

MODELS OF THE BASEMENT FOR PROFILES 3 AND 4

PROFILE 3

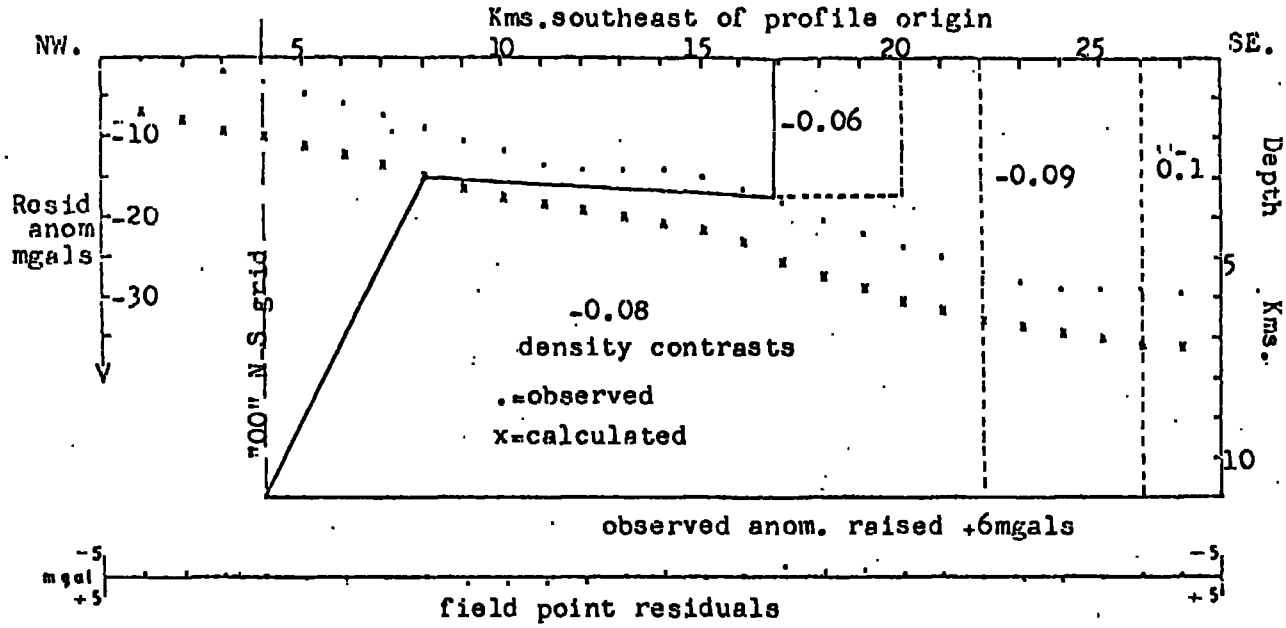

PROFILE 4

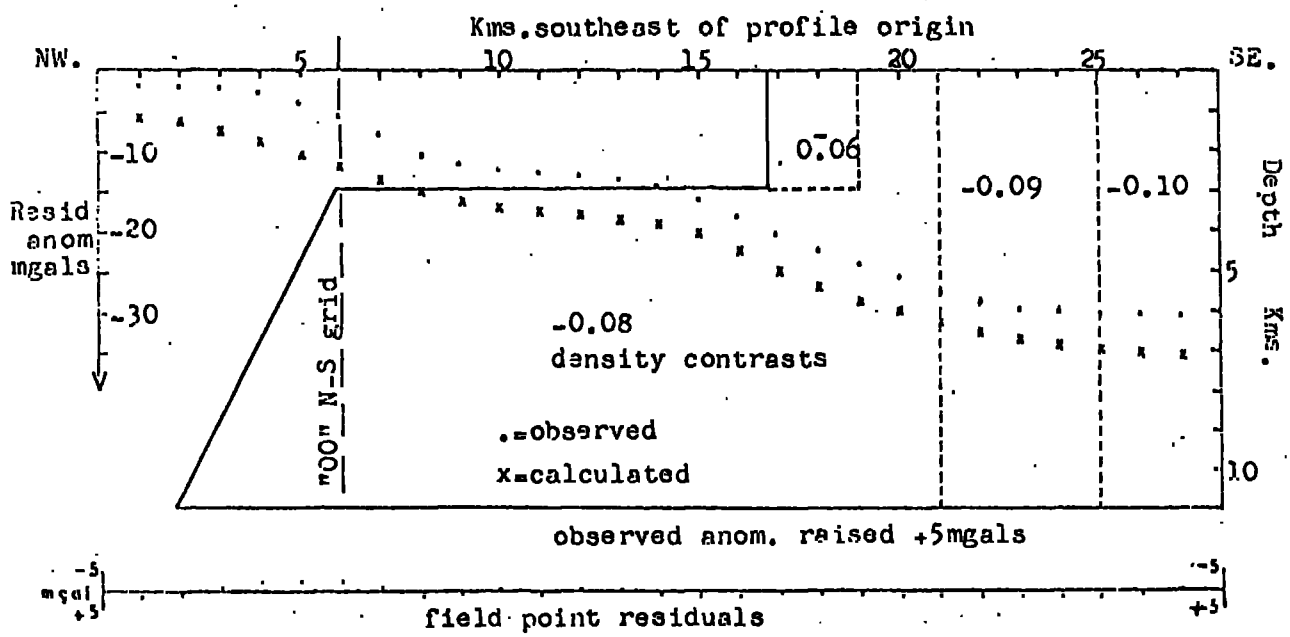

FIGURE 37 contd.

MODEL OF THE BASEMENT FOR PROFILE 5

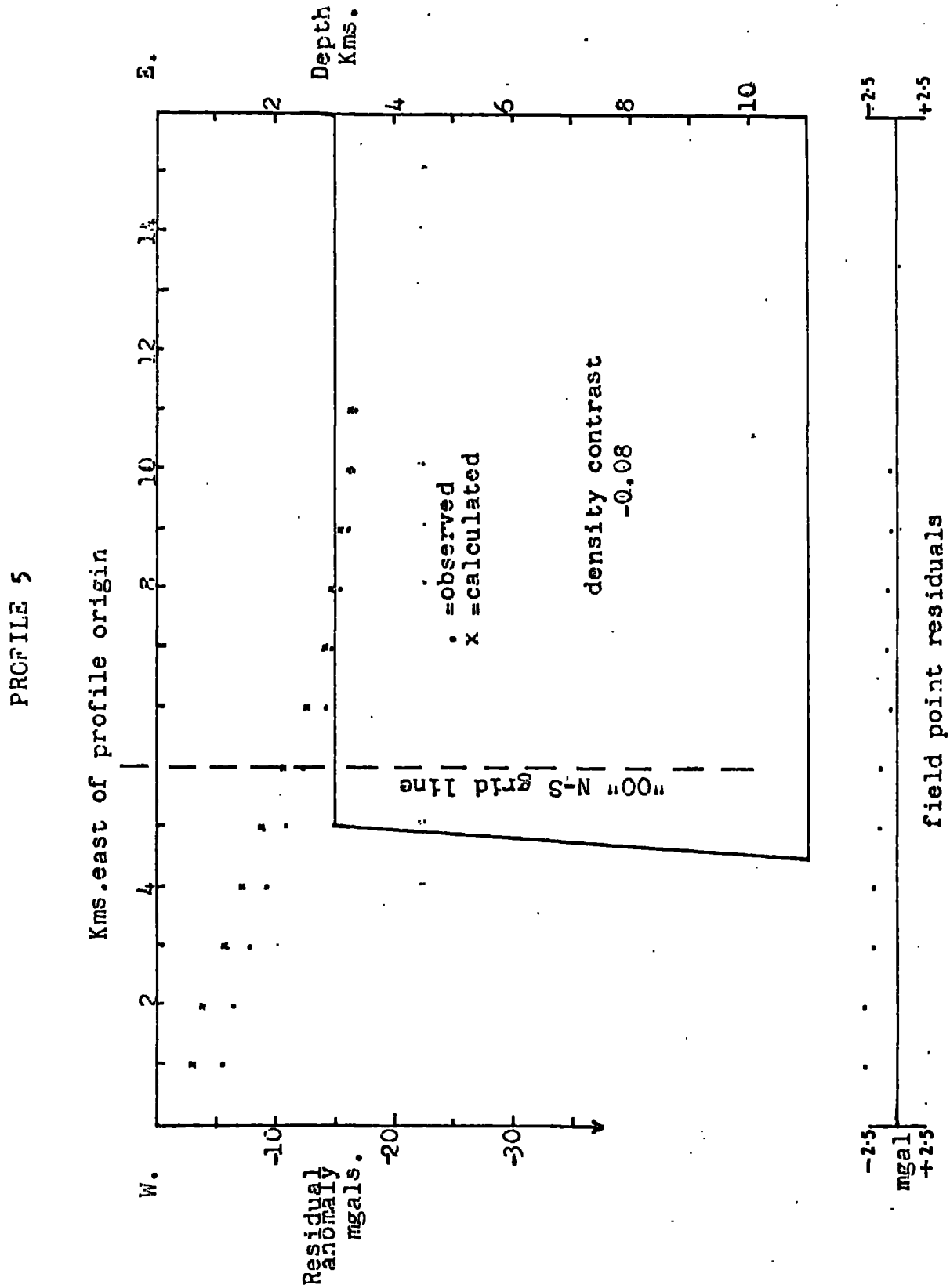

by assuming a progressive decrease in the density contrast within the "granite" from - 0.10 over the Eskdale granite to - 0.08 and -06 over the Ennerdale granophyre.

(e.g. On profile 3 between field points 17 to 22 kms the change in density contrast - 0.16 to - 0.08 coincides with the outcrop of the Ennerdale granophyre).

The persistence of internal density contrasts to at least 10-11 kms indicates the existence of separate intrusive bodies thus confirming the work of Folkman (1969) and Clark (1963).

Positive residuals at the western end of profile 1 are probably related to an undercompensation for the Carboniferous cover. Similarly an over-compensation for the Permo-Triassic sediments on profile 5 would account for the unexplained negative residuals.

APPENDIX II

SAMPLE LOCATION AND GEOCHEMICAL DATA

TABLE A.1. GRID REFERENCES AND GEOLOGICAL SETTING FOR HAEMATITE ORE SAMPLES

Key

CL-WC	Carboniferous limestone, West Cumberland
CL-MF	" " , Millom-Furness
BVS	Borrowdale Volcanic Series
SSS	Skiddaw Slate Series
G	Eskdale Granite
Gp	Ennerdale Granophyre
R	Metasomatic replacement deposit
V	Vein deposit (sensu stricto)

SAMPLE SITE	GRID REF.	HOST ROCK	FORM OF OREBODY
1	NY 079217	CL-WC	R
2	" 076201	"	"
3	" 078201	"	"
4	" 078203	"	"
5	" 076202	"	"
6	" 074205	"	"
7	" 081193	"	"
8	" 073182	"	"
9	" 064175	"	"
10	" 061183	"	"
11	" 061168	"	"
12	" 058167	"	"
13	" 054172	"	"
14	" 057171	"	"
15	" 056170	"	"
16	" 055171	"	"
17	" 053175	"	"
18	" 052177	"	"
19	" 047178	"	"
20	" 048175	"	"
21	" 049172	"	"
22	" 052163	"	"
23	" 051164	"	"

TABLE A.1. cont.

SAMPLE SITE	GRID REF.	HOST ROCK	FORM OF OREBODY
24	NY 051163	CL-WC	R
25	" 050165	"	"
26	" 050166	"	"
27	" 049167	"	"
28	" 048166	"	"
29	" 045166	"	"
30	" 047165	"	"
31	" 046166	"	"
32	" 046170	"	"
33	" 042171	"	"
34	" -42170	"	"
35	" -41171	"	"
36	" 039173	"	"
37	" 040174	"	"
38	" 039174	"	"
39	" 037169	"	"
40	" 035169	"	"
41	" 037166	"	"
42	" 036165	"	"
43	" 347107	BVS	V
44	" 342098	"	"
45	" 282070	"	"
46	" 269039	"	"
47	" 171158	Gp	"
48	" 154169	"	"
49	" 151170	"	"
50	" 135170	SSS	"
51	" 089186	"	"
52	" 090186	"	"
53	" 091187	"	"
54	" 093188	"	"
55	" 095188	"	"
56	" 099191	"	"
57	" 097187	"	"

TABLE A.1. contd.

SAMPLE SITE	GRID REF.	HOST ROCK	FORM OF OREBODY
58	NY 096186	SSS	V
59	SD 227924	BVS	"
60	" 213903	"	"
61	NY 184014	G	"
62	" 184014	"	"
63	SD 118904	"	"
64	NY 175013	"	"
65	" 167008	"	"
65A	" 168007	"	"
66	SD 147986	"	"
67	" 100978	"	"
68	" 178998	"	"
69	" 179997	"	"
70	" 180996	"	"
71	" 178996	"	"
73A	NY 036164	CL-WC	R
74	" 036162	"	"
75	" 036161	"	"
76	" 037160	"	"
77	" 036159	"	"
78	" 037158	"	"
79	" 038158	"	"
80	" 036152	"	"
81	" 038157	"	"
82	" 037157	"	"
83	" 036156	"	"
84	" 033161	"	"
85	" 035157	"	"
86	" 029158	"	"
87	" 029157	"	"
88	" 030157	"	"
89	" 033156	"	"
90	" 028154	"	"
91	" 029153	"	"
92	" 017153	"	"

TABLE A.1. contd.

SAMPLE SITE	GRID REF.	HOST ROCK	FORM OF OREBODY
93	NY 018144	CL-WC	R
94	" 016139	"	"
94A	" 018145	"	"
95	" 015141	"	"
96	" 014142	"	"
97	" 013144	"	"
98	" 013146	"	"
99	" 013147	"	"
100	" 014148	"	"
101	" 015148	"	"
102	" 008142	"	"
103	" 012143	"	"
104	" 008145	"	"
105	" 011145	"	"
106	" 012146	"	"
107	" 016152	"	"
108	" 016151	"	"
109	" 007140	"	"
110	" 007141	"	"
111	" 006144	"	"
112	" 006139	"	"
113	" 001138	"	"
114	" 006135	"	"
115	" 004134	"	"
116	" 000133	"	"
117	NX 997129	"	"
118	" 997125	"	"
119	" 998124	"	"
120	" 998123	"	"
121	" 997123	"	"
122	" 995120	"	"
123	" 995122	"	"
124	" 995121	"	"
125	NY 000125	"	"
126	" 002123	"	"

TABLE A.1. contd.

SAMPLE SITE	GRID REF.	HOST ROCK	FORM OF OREBODY
127	NY 003127	CL-WC	R
128	" 003126	"	"
129	" 011135	"	"
130	" 008131	"	"
131	" 006131	"	"
132	" 005131	"	"
133	" 008128	"	"
134	" 008129	"	"
135	" 010128	"	"
136	" 011129	"	"
137	" 005128	"	"
138	" 004119	"	"
139	" 007118	"	"
140	" 009119	"	"
141	" 011120	"	"
142	" 010120	"	"
143	" 009120	"	"
144	" 010122	"	"
145	" 012125	"	"
146	" 003107	"	"
147	" 012110	"	"
148	" 005112	"	"
149	" 016105	"	"
150	" 022104	"	"
151	" 021105	"	"
152	" 023105	"	"
153	" 025105	"	"
154	" 018101	"	"
155	" 097178	SSS	V
156	" 097179	"	"
157	" 093178	"	"
158	" 087178	"	"
159	" 084181	"	"
160	" 084182	"	"
161	" 080187	"	"

TABLE A. 1. contd.

SAMPLE SITE	GRID REF.	HOST ROCK	FORM OF OREBODY
162	NY 085183	SSS	V
163	" 086175	"	"
164	" 084146	"	"
165	SD 139814	CL-MF	R
166	" 177826	"	"
168	" 266768	"	"
169	" 264768	"	"
170	" 262768	"	"
171	" 264761	"	"
172	" 265759	"	"
173	" 260759	"	"
174	" 259760	"	"
175	" 266746	"	"
176	" 259747	"	"
177	" 255745	"	"
178	" 256750	"	"
179	" 258754	"	"
180	" 255754	"	"
181	" 254754	"	"
182	" 253750	"	"
183	" 253748	"	"
184	" 253746	"	"
185	" 254745	"	"
186	" 251745	"	"
187	" 251741	"	"
188	" 244743	"	"
189	" 240731	"	"
190	" 238734	"	"
191	" 228736	"	"
192	" 240739	"	"
193	" 238738	"	"
194	" 241744	"	"
195	" 246745	"	"
196	" 249747	"	"

TABLE A. 1. contd.

SAMPLE SITE	GRID REF.	HOST ROCK	FORM OF OREBODY
197	SD 248748	CL-MF	R
198	" 247749	"	"
199	" 250750	"	"
200	" 251750	"	"
201	" 248754	"	"
202	" 247755	"	"
203	" 248756	"	"
204	" 247757	"	"
205	" 242757	"	"
206	" 242758	"	"
207	" 240759	"	"
208	" 240760	"	"
209	" 243772	"	"
210	" 246769	"	"
211	" 245770	"	"
212	" 246766	"	"
213	" 244766	"	"
214	" 244765	"	"
215	" 245766	"	"
216	" 244759	"	"
217	" 248770	"	"
218	" 247771	"	"
219	" 248766	"	"
220	" 249765	"	"
221	" 250764	"	"
222	" 253764	"	"
223	" 253763	"	"
224	" 254764	"	"
224A	" 250766	"	"
225	" 255764	"	"
226	" 255764	"	"
227	" 255762	"	"
228	" 256761	"	"
229	" 258762	"	"
230	" 258763	"	"
231	" 082046	BVS	V

TABLE A.2. GRID REFERENCES FOR GRANITE SAMPLES

SAMPLE NO.	GRID REF.	INTRUSIVE	ROCK TYPE
G.1	SD 142981	Eskdale	Pink variety
G.2A	" 165989	"	" " (haematized)
G.2B	" 165989	"	" "
G.3	" 150995	"	" "
G.4	NY 169003	"	" "
G.5	" 190010	"	" "
G.6	" 152018	"	" "
G.7	" 131005	"	" "
G.9	" 140042	Ennerdale	Main phase
G.10	" 150053	"	" "
G.14	" 111001	Eskdale	Pink variety(haematized)
G.26	SD 133907	"	Grey "
G.27	" 112944	"	" "
G.28A	" 115992	"	Pink " (haematized)
G.28B	" 115992	"	" "
G.29A	NY 163004	"	" " (haematized)
G.29B	" 163004	"	" "
G.29C	" 163004	"	" "
LD 264	" 123147	Ennerdale	Main phase
LD 265	" 135144	"	" "

TABLE A.3. GRID REFERENCES FOR PLACES MENTIONED IN THE TEXT AND NOT ILLUSTRATED

LOCALITY	GRID REFERENCE
Barrowmouth	NX 096158
Beckfoot Quarry	NY 166004
Birker Moor	SD 166006
Blea Tarn	NY 293044
Bleng River	NY 083043
Bootle	SD 108882
Boot	NY 176011
Border End	NY 225020
Brantrake	SD 148987
Brothers Water	NY 403126
Burnmoor Tarn	NY 184044
Chapel Hill	SD 107977
Cleator Moor	NY 009150
Clews Gill	NY 133158
Clints Mine	NY 004120
Crag Fell	NY 095146
Crossgill Mine	NY 033158
Crowgarth Mine	NY 016152
Dalegarth	NY 170002
Devoke Water	SD 157972
Eel Crags	NY 190207
Eskdale Green	NY 142001
Eskett Mine	NY 055167
Esk Pike	NY 237075
Gillfoot Park Mine	NY 004112
Gosforth	NY 067036
Grassmoor	NY 174204
Great Barrow	NY 185013
Green Hole	NY 236058
Haile Moor Mine	NY 042088
Hardknott	NY 225015
Harter Fell	SD 218997
Havercroft	NY 080222
Helder Mine	

TABLE A.3. contd.

LOCALITY	GRID REFERENCE
Ingwell	NX 995148
Kepple Crag	SD 196998
Kink Beck	NY 045124
Kirksanton	SD 140807
Knockmurton Fell	NY 095191
Little Urswick	SD 263736
Long Pike	NY 224084
Middle Kinmont	SD 116905
Millyeat	NY 025178
Mockerkin	NY 090232
Nethertown	NX 990075
Orebank House	NY 000135
Orgill	NY 002107
Pallaflat	NX 995123
Plumpton	SD 312785
Red Gill	NY 130168
Red Tarn	NY 268038
Rowrah	NY 057185
Salter Mine	NY 058169
Scafell	NY 215073
Scale Force	NY 150170
Snavy Beck	NY 082228
Sourmilk Gill	NY 171159
Stainton Ground	SD 227923
Stank	SD 233704
Stanley Gill	SD 177996
Thwaites	NY 055128
Tongue Gill	NY 347107
Ullcoats	NY 024103
Wasdale Head	NY 195092
Water Crag	SD 155974
Whitcham	SD 132824
Woodend	NY 009130
Wrynose	NY 260022
Whyndham Mine	NY 003126

TABLE A4 ANALYSES OF MASSIVE ORES, WEST CUMBERLAND OREFIELD

• samples rejected at the 0.01 sig. level by L.D.F.A. (log_{10} data)

Sample No	As	Mn	Ba	Sr	Rb	Pb	Cu	Ni	Zn	Zr	Y	Si	Al	Fe	Mg	Ca	Ti
1	17	5043	15	5	1	2	1	9	28	1	6	33.09	0.22	26.95	1.27	2.52	12
• 2-1	29	728	1	6	8	6	12	6	3	1	6	2.56	0.24	65.09	0.11	0.75	2
3-3	15	24	4	6	1	2	10	9	3	1	1	6.89	0.18	60.27	0.11	0.10	7
4	35	6269	2	3	11	1	17	5	1	1	2	3.20	0.20	58.07	0.30	3.68	4
• 4-1	37	9555	4	14	1	13	11	10	3	1	7	3.62	0.18	52.86	0.83	5.54	2
5-2	28	46	24	3	1	4	22	1	1	3	6	5.50	0.21	63.26	0.10	0.16	10
5-8	17	77	1	2	1	9	12	15	3	4	7	2.68	0.21	66.13	0.04	0.23	10
6-1	20	22	18	4	3	1	8	2	5	5	9	4.09	0.17	64.99	0.08	0.05	7
6-3	10	4	1	5	1	1	1	8	1	21	6	10.56	0.15	55.58	0.08	0.04	8
• 8-1	299	402	441	35	1	72	10	113	8	9	9	11.60	0.39	45.82	0.16	0.14	104
9-5	43	1776	11	7	2	5	16	10	6	8	75	8.56	0.41	45.18	0.32	2.59	63
10	84	222	81	3	1	4	4	1	15	4	4	11.94	0.33	49.26	0.03	0.09	25
• 10-2	96	277	70	10	1	13	3	16	25	6	4	8.47	0.38	49.84	0.04	0.13	27
11-1	47	217	18	4	1	12	2	7	24	8	3	11.02	0.34	54.80	0.07	0.26	31
11-2	16	59	1	2	1	1	21	1	1	8	7	9.10	0.28	55.07	0.05	0.05	15
13	84	636	58	4	4	11	50	6	5	16	15	12.55	0.41	51.82	0.29	0.62	128
13-1	185	174	19	10	4	9	14	2	4	5	7	3.16	0.29	63.93	0.11	0.12	53
14-2	136	1498	26	4	1	19	11	10	5	4	11	2.89	0.30	61.37	0.87	2.47	22
• 14-3	144	61	19	3	3	20	17	13	1	1	7	5.56	0.21	62.31	0.21	0.14	9
• 15-1	83	1324	71	9	7	13	16	4	2	5	16	1.88	0.25	59.73	0.29	4.57	15
15-9	107	1023	42	12	14	14	18	7	4	1	5	3.05	0.17	61.39	0.52	1.30	16
16-23	157	92	9	6	1	7	13	4	2	5	9	9.67	0.24	53.25	0.04	0.09	18
• 17-1	156	109	69	10	5	9	2	1	8	1	5	1.42	0.36	66.31	0.05	0.37	48
• 17-7	260	115	18	7	1	21	8	1	8	5	3	2.50	0.33	64.06	0.04	0.16	34
• 18-1	33	8	6	1	1	10	14	1	2	1	3	1.25	0.16	70.98	0.11	0.03	1
• 18-3	39	1717	20	7	6	4	6	8	1	10	7	2.83	0.21	71.06	1.33	2.44	15

TABLE A4 continued

Sample No	As	Mn	Ba	Sr	Rb	Pb	Cu	Ni	Zn	Zr	Y	Si	Al	Fe	Mg	Ca	Ti
19	27	175	25	1	1	1	10	8	1	1	1	5.35	0.21	60.01	0.03	0.07	9
19-4	37	403	2	5	1	5	17	5	2	3	11	3.85	0.29	71.49	0.09	0.08	7
20-2	38	318	9	6	1	7	12	20	3	1	6	7.92	0.42	62.49	0.07	0.11	23
20-3	35	70	10	1	3	21	7	1	1	1	8	5.05	0.42	58.63	0.04	0.12	63
21-1	37	513	43	4	5	7	8	5	5	2	7	2.72	0.40	64.22	0.04	0.09	46
21-14	43	1227	130	2	1	2	12	1	3	1	10	1.88	0.35	67.84	0.29	0.08	26
22-5	33	50	1	6	1	1	14	14	4	10	5	2.02	0.22	67.11	0.08	0.09	21
22-6	22	11	1	1	2	1	8	7	1	1	1	6.73	0.16	60.76	0.23	0.03	2
23-2	75	330	24	7	6	8	13	8	7	7	9	7.38	0.37	55.10	0.15	0.15	59
23-13	45	108	27	2	1	7	12	11	6	2	6	10.55	0.33	52.75	0.06	0.08	14
• 24-1	238	377	18	4	2	18	8	1	17	6	13	0.88	0.21	70.18	0.34	0.37	11
24-4	180	176	1	12	1	14	28	1	3	11	5	4.50	0.18	63.67	0.07	0.15	12
26-27	164	156	4	4	1	24	16	1	2	4	6	3.88	0.19	64.13	0.17	0.22	20
26-38	124	49	55	1	3	66	21	3	64	2	11	3.82	0.14	66.88	0.23	0.04	9
27-1	65	432	93	3	1	7	7	4	2	1	3	9.97	0.22	52.94	0.31	0.52	17
• 27-3	390	423	8	12	6	67	19	14	10	1	11	1.36	0.28	68.94	0.04	0.09	30
• 28-8	282	4511	5	5	1	13	13	8	7	1	14	1.43	0.31	67.27	0.15	0.63	23
29-10	137	81	41	2	1	18	10	8	23	3	3	3.89	0.22	65.15	0.04	0.05	13
• 29-11	145	94	5	5	4	10	11	7	5	1	1	4.98	0.20	64.42	0.13	0.05	8
30-2	138	54	24	7	1	12	17	1	1	4	4	3.47	0.19	64.39	0.04	0.06	29
• 30-3	181	46	30	1	4	10	9	1	3	3	5	9.44	0.16	58.50	0.03	0.04	7
• 32-1	158	103	32	8	2	11	16	3	15	6	5	2.72	0.20	66.81	0.05	0.08	9
32-14	78	65	40	5	3	34	13	2	4	7	2	6.13	0.17	61.98	0.05	0.12	22
33-2	141	612	32	5	6	11	16	7	7	12	10	7.55	0.28	55.45	0.19	1.75	146
33-4	236	539	5	9	3	19	7	1	5	11	7	3.75	0.29	62.47	0.17	0.89	61
• 34-2	193	218	41	5	3	7	15	10	3	9	14	2.22	0.37	66.81	0.11	0.07	26
34-4	105	189	3	9	4	16	7	5	4	9	14	10.59	0.23	51.74	0.04	0.11	24

TABLE A4 continued

Sample No	As	Mn	Ba	Sr	Rb	Pb	Cu	Ni	Zn	Zr	Y	Si	Al	Fe	Mg	Ca	Ti
• 35	197	176	39	10	5	16	5	1	2	14	11	2.79	0.26	63.93	0.03	0.22	34
35-2	157	992	5	6	2	52	14	10	3	10	8	5.86	0.23	65.14	0.11	0.32	43
• 36-10	169	265	13	12	2	13	16	8	4	1	8	6.52	0.23	63.49	0.19	0.22	13
36-11	138	271	54	6	1	24	12	12	1	4	3	5.67	0.19	59.51	0.12	0.18	12
• 37-8	117	160	61	10	1	7	1	8	6	2	3	11.85	0.20	48.65	0.16	0.19	22
38-15	106	838	31	11	1	14	18	4	5	1	9	5.28	0.21	58.92	0.52	1.16	18
38-19	166	43	71	6	1	17	10	1	9	9	10	2.33	0.26	64.33	0.08	0.08	48
• 39-1	56	247	44	5	6	10	12	1	3	2	5	2.07	0.36	63.81	0.03	0.10	12
39-2	110	347	6	9	2	31	22	7	5	1	7	2.42	0.20	66.12	0.04	0.27	17
• 40-3	141	57	1	4	2	16	21	9	3	1	5	1.78	0.21	63.20	0.04	0.09	19
40-4	145	226	128	11	5	50	16	7	1	8	10	1.57	0.32	66.73	0.06	0.09	38
41-1	57	153	4	4	4	15	11	5	2	1	6	9.75	0.23	52.95	0.14	0.11	14
41-10	35	66	28	1	1	9	14	1	1	3	6	5.87	0.18	62.55	0.04	0.05	2
42-33	182	18	30	1	1	25	16	10	2	3	9	2.78	0.20	65.98	0.15	0.06	16
42-50	91	57	1	3	3	22	11	3	3	4	1	4.18	0.15	63.86	0.04	0.04	14
73A-2	151	79	38	1	1	25	1	1	1	4	7	4.39	0.35	61.99	0.03	0.12	55
• 73A-17	202	146	23	5	4	28	10	4	1	4	10	4.61	0.28	60.74	0.04	0.14	47
74-2	105	68	39	5	4	9	4	1	3	3	2	6.64	0.18	58.86	0.28	0.09	14
74-3	240	169	21	1	1	20	17	5	10	4	11	1.78	0.26	68.29	0.24	0.08	22
76-4	164	57	9	2	4	11	18	3	3	6	5	2.82	0.29	64.15	0.03	0.08	35
76-15	220	52	28	1	1	9	5	1	22	1	6	3.54	0.20	63.54	0.03	0.07	40
77-1	144	66	21	4	2	11	10	13	2	26	8	14.46	0.20	45.15	0.15	0.06	32
78-4	84	79	14	1	2	12	22	5	7	2	1	2.47	0.19	66.66	0.19	0.05	11
78-10	221	98	17	5	1	1	4	10	5	2	3	2.95	0.15	64.61	0.18	0.04	14
80-2	97	260	27	1	4	2	11	1	32	2	5	2.57	0.22	65.79	0.24	0.47	49
80-8	100	98	23	1	4	23	14	3	5	7	7	1.84	0.22	67.66	0.20	0.13	55
83-2	100	362	17	1	9	12	8	4	12	5	10	3.30	0.23	64.24	0.20	0.23	10
• 83-4	81	113	12	1	1	16	2	1	3	1	3	7.99	0.16	58.35	0.04	0.05	1

TABLE A4 continued

Sample No	As	Mn	Ba	Sr	Rb	Pb	Cu	Ni	Zn	Zr	Y	Si	Al	Fe	Mg	Ca	Ti
• 83-5	117	133	1	1	1	11	11	1	3	6	11	1.92	0.23	68.61	0.04	0.06	2
• 84-2	184	354	18	2	1	61	13	3	7	3	13	2.39	0.26	64.90	0.06	0.10	14
84-4	154	95	30	3	1	1	15	7	8	5	17	1.81	0.25	67.42	0.04	0.08	49
• 85-5	252	215	20	8	1	24	13	1	7	10	21	1.39	0.41	69.77	0.04	0.11	54
• 85-6	358	221	22	2	1	10	17	5	7	3	1	1.33	0.41	66.56	0.03	0.17	20
• 86-3	85	439	28	1	4	24	6	9	4	17	5	4.40	0.25	58.38	0.07	0.09	10
• 86-6	200	608	25	4	1	8	16	2	3	12	92	1.26	0.37	63.66	0.03	2.40	32
87-1	75	741	51	6	1	9	25	27	3	12	8	2.33	0.41	62.20	0.10	0.41	54
• 88-3	131	334	35	7	1	18	11	7	9	35	5	3.88	0.33	61.13	0.10	0.07	11
• 90-2	137	455	5	6	1	41	9	3	7	7	7	2.11	0.32	61.74	0.10	2.18	11
• 90-3	148	52	6	1	6	9	13	1	16	1	5	1.91	0.28	68.29	0.10	0.09	5
91-5	90	125	15	5	3	22	8	8	1	6	9	12.59	0.24	51.35	0.03	0.12	19
• 91-9	167	226	14	4	5	39	10	5	3	2	6	7.61	0.22	54.72	0.14	0.14	12
92-3	107	440	8	4	1	1	13	1	6	8	1	2.20	0.29	66.32	0.04	0.23	17
92-7	250	288	11	5	1	12	13	4	22	2	5	0.92	0.30	67.34	0.07	0.24	22
93-2	124	908	29	7	1	10	9	1	1	7	1	0.44	0.21	67.54	0.06	0.11	48
94-2	64	31	7	5	1	5	12	5	1	2	4	10.96	0.17	58.62	0.15	0.06	5
94A-2	81	52	12	10	2	15	3	20	5	6	1	5.44	0.21	62.28	0.03	0.06	26
94A-6	41	19	13	1	1	1	10	5	1	5	9	8.96	0.17	59.80	0.08	0.06	8
95-4	195	1255	17	1	1	1	17	9	1	1	7	6.43	0.17	58.86	0.56	1.23	4
96-3	195	1529	22	4	1	16	2	2	4	15	9	1.69	0.36	65.78	0.35	1.33	143
• 96-11	262	592	15	2	3	5	1	3	5	3	6	1.39	0.28	66.45	0.07	1.37	9
97-1	97	47	8	2	2	8	12	5	1	5	3	4.02	0.21	62.11	0.05	0.05	13
98-5	144	60	8	2	1	9	30	1	6	9	9	2.29	0.24	65.71	0.07	0.09	15
• 98-10	144	53	11	1	3	21	1	6	5	3	2	1.97	0.22	67.03	0.26	0.06	17
99-5	332	1065	24	25	2	18	23	5	11	6	2	1.16	0.37	64.70	0.17	2.23	49
99-12	77	19	15	3	3	1	12	9	6	1	6	6.60	0.22	58.16	0.04	0.10	25

TABLE A4 continued

Sample No	As	Mn	Ba	Sr	Rb	Pb	Cu	Ni	Zn	Zr	Y	Si	Al	Fe	Mg	Ca	Ti
100-2	35	14	14	3	1	6	8	5	3	4	4	8.28	0.20	57.76	0.22	0.05	6
100-10	55	35	24	1	1	10	31	1	10	2	1	8.42	0.24	56.78	0.07	0.10	27
•101-3	387	28	1	7	4	21	21	10	1	4	3	3.82	0.20	63.22	0.13	0.10	21
102-1	68	2187	104	2	1	6	22	14	4	1	6	7.12	0.28	57.35	0.07	0.08	33
102-8	98	511	52	1	1	26	23	23	1	4	1	6.29	0.27	57.89	0.06	0.07	27
•103-2	448	243	6	7	1	61	21	3	20	5	8	1.53	0.37	70.65	0.04	0.34	45
103-4	400	721	30	1	1	44	9	5	13	17	10	1.85	0.37	65.88	0.17	1.06	70
104-1	112	25	70	2	1	16	16	1	8	4	1	5.19	0.31	62.61	0.04	0.05	37
•104-11	360	410	122	3	2	19	20	1	10	4	4	1.51	0.27	64.60	0.03	0.90	36
105-5	61	252	1	10	2	2	20	16	3	6	4	0.85	0.21	65.88	0.08	0.86	11
105-7	48	20	12	6	3	3	17	3	7	1	8	0.62	0.23	68.20	0.03	0.06	18
•106-1	284	131	37	6	3	41	9	7	8	2	2	4.47	0.19	64.44	0.13	0.05	28
106-7	74	114	19	1	4	39	17	6	8	1	23	6.34	0.17	59.90	0.08	0.12	11
107-3	228	45	1	1	1	14	16	1	3	1	4	4.53	0.21	60.81	0.11	0.10	19
•108-1	408	187	4	1	2	34	9	13	4	6	10	4.10	0.22	62.96	0.14	0.07	7
108-5	88	93	3	5	6	13	30	59	11	3	7	1.96	0.21	67.50	0.19	0.27	6
109-2	65	73	292	3	7	7	14	1	4	1	5	0.44	0.21	67.54	0.06	0.11	51
•109-3	94	190	37	4	3	29	7	8	6	11	5	0.20	0.22	68.07	0.03	0.42	14
110-1	47	18	133	1	1	7	2	11	8	4	1	1.38	0.24	67.22	0.04	0.06	38
110-6	94	152	53	6	16	3	23	2	11	6	3	0.43	0.39	68.36	0.07	0.73	115
111-1	214	102	46	9	1	43	15	15	3	4	10	10.17	0.19	52.61	0.24	0.06	25
111-2	14	21	8	3	1	1	17	3	1	3	7	5.28	0.20	62.67	0.05	0.06	5
112-3	115	26	29	3	1	4	19	8	9	5	3	0.51	0.20	68.76	0.04	0.09	11
112-4	68	19	9	1	1	1	17	4	13	3	7	2.17	0.18	67.27	0.23	0.06	30
113-6	61	11	1	3	1	10	17	1	4	1	6	1.40	0.14	68.83	0.23	0.04	1
113-8	242	75	10	2	1	1	20	15	1	7	5	12.19	0.20	48.90	0.22	0.13	11
114-2	157	285	880	16	1	20	14	4	4	1	7	2.69	0.26	62.94	0.19	1.56	115

TABLE A4 continued

Sample No	As	Mn	Ba	Sr	Rb	Pb	Cu	Ni	Zn	Zr	Y	Si	Al	Fe	Mg	Ca	Ti
• 114-6	185	157	58	6	2	8	19	7	4	1	4	3.36	0.20	65.60	0.16	0.09	13
115-1	74	26	1	4	1	2	21	25	1	2	4	1.11	0.15	68.75	0.11	0.07	7
115-3	70	29	2	5	1	55	22	9	6	2	4	0.23	0.19	70.01	0.06	0.07	12
116-3	231	292	9	7	4	1	12	7	8	10	9	1.33	0.44	66.88	0.23	1.18	82
• 116-6	131	25	1	1	5	13	7	12	1	2	3	0.43	0.21	69.52	0.03	0.05	17
117-3	521	8	1	1	1	7	11	6	8	2	1	1.51	0.28	68.19	0.27	0.07	21
117-13	171	66	1	5	1	8	7	5	8	8	9	3.07	0.24	65.36	0.23	0.05	13
• 118-2	138	77	39	3	2	13	8	2	15	5	5	1.02	0.30	66.32	0.04	0.09	19
118-8	70	27	69	8	2	3	17	3	1	1	4	1.46	0.21	69.00	0.16	0.05	17
119-2	92	275	10	10	1	10	16	3	7	5	5	1.89	0.19	67.80	0.16	0.25	14
119-10	74	329	16	4	1	4	1	8	7	1	4	7.81	0.18	58.01	0.19	0.38	31
• 120-3	70	153	25	4	9	7	13	3	1	3	1	12.84	0.16	49.66	0.20	0.04	5
120-6	320	1009	50	20	1	71	18	17	16	1	19	0.80	0.43	67.88	0.25	0.10	8
121-1	81	650	44	20	4	6	17	12	8	3	3	2.35	0.42	64.29	0.23	0.99	73
121-2	130	405	34	6	1	14	12	6	10	1	3	2.88	0.42	64.16	0.16	0.34	38
122	277	496	240	7	2	8	25	13	5	3	14	2.64	0.29	65.80	0.18	0.08	59
123-2	60	21	1	1	1	1	19	24	1	1	1	13.56	0.17	52.87	0.06	0.04	9
123-6	30	106	14	1	1	20	14	8	1	1	1	8.08	0.17	60.02	0.03	1.05	8
• 124-1	384	461	54	8	1	17	32	12	16	1	4	1.09	0.25	70.27	0.22	0.08	8
• 125-1	115	107	14	3	2	6	16	1	6	3	4	1.83	0.21	67.75	0.23	0.43	4
• 125-3	110	406	34	7	3	22	7	3	9	4	8	0.89	0.23	68.77	0.08	1.01	30
• 126-2	138	104	18	6	1	15	8	4	6	4	4	0.66	0.25	68.80	0.03	0.11	25
• 126-5	125	225	11	4	5	7	5	1	6	10	1	0.27	0.22	69.54	0.03	0.06	19
• 127-1	155	850	51	6	1	15	8	1	15	5	2	0.29	0.27	67.23	0.03	0.41	28
• 127-2	300	400	29	5	2	18	11	13	10	1	6	6.71	0.24	56.99	0.10	0.14	9
128-3	154	104	8	6	2	5	11	1	7	1	3	0.34	0.28	69.04	0.03	0.06	46
• 128-4	191	1097	70	15	3	12	16	3	1	7	10	1.03	0.23	68.83	0.22	0.07	33
129-5	200	103	5	7	1	24	9	8	18	10	7	3.46	0.30	65.97	0.19	0.10	21
[illegible]	[illegible]	[illegible]	48	6	3	4	10	17	1	22	6	9.40	0.21	55.56	0.21	0.15	105

TABLE A4 continued

Sample No	As	Mn	Ba	Sr	Rb	Pb	Cu	Ni	Zn	Zr	Y	Si	Al	Fe	Mg	Ca	Ti
130-3	120	14	41	2	7	15	13	4	4	7	7	3.00	0.33	64.79	0.03	0.11	100
130-6	58	104	8	3	1	10	15	1	4	1	9	2.59	0.22	65.41	0.19	0.47	33
• 131-1	257	515	45	10	2	45	48	6	9	2	6	0.92	0.22	68.04	0.04	0.60	26
• 131-3	82	343	18	3	2	1	1	1	2	3	5	1.81	0.17	65.22	0.06	1.40	6
132-6	82	35	4	3	1	6	15	23	1	1	3	4.91	0.27	62.87	0.03	0.05	23
132-14	207	90	1	5	8	21	9	1	7	9	6	4.29	0.36	61.85	0.04	0.12	46
133-1	180	46	1	3	1	36	21	1	5	2	5	4.23	0.21	62.66	0.06	0.08	17
133-6	182	35	1	3	1	6	3	9	12	1	4	0.35	0.24	69.15	0.08	0.10	22
134-1	58	37	19	6	4	13	24	6	7	10	7	3.65	0.20	64.53	0.09	0.05	5
135	130	93	974	28	3	8	11	1	2	10	7	12.17	0.18	51.12	0.05	0.33	148
• 135-4	164	68	31	16	1	27	13	12	1	1	5	9.82	0.24	52.07	0.04	0.14	8
• 136-1	94	167	8	5	2	1	1	1	2	4	4	3.19	0.24	63.51	0.04	0.07	15
136-3	22	22	10	1	1	1	7	48	2	3	5	10.21	0.16	53.97	0.13	0.05	5
• 137-10	367	295	4485	137	3	17	54	42	15	14	13	1.17	0.44	64.36	0.07	0.12	582
• 138	48	31	19	31	5	18	25	2	7	1	5	3.48	0.14	67.06	0.09	0.06	4
138-4	27	64	18	1	1	4	11	9	3	1	1	6.80	0.14	63.11	0.17	0.04	1
139-8	100	84	19	3	3	7	12	1	6	12	6	1.58	0.30	67.20	0.04	0.13	109
139-11	71	74	6	4	4	17	5	3	9	9	8	2.33	0.25	66.27	0.04	0.13	13
141-4	84	586	11	2	1	60	14	12	1	7	7	11.02	0.29	52.29	0.08	0.77	72
141-7	121	517	11	1	1	2	22	5	6	4	2	8.44	0.19	54.59	0.04	0.81	17
142-1	74	724	23	2	1	6	17	8	11	1	3	1.66	0.18	66.73	0.04	1.24	11
142-2	110	259	10	3	1	16	16	9	6	4	4	1.31	0.15	70.12	0.26	0.30	21
143-1	114	208	9	6	3	7	21	9	1	1	5	3.35	0.20	64.63	0.17	0.20	19
• 143-2	205	326	37	12	1	17	18	11	6	6	8	1.11	0.28	64.70	0.03	1.90	28
• 144-2	225	348	23	14	4	73	21	9	7	6	6	1.06	0.30	67.80	0.08	0.88	43
144-3	224	50	7	4	1	19	21	4	5	5	8	1.16	0.24	71.57	0.04	0.04	29
145	140	60	3	1	1	9	2	1	5	4	10	3.86	0.21	63.54	0.03	0.05	22
145-6	277	93	10	4	1	58	95	4	14	5	13	4.04	0.25	64.52	0.11	0.16	45

TABLE A4 continued

Sample No	As	Mn	Ba	Sr	Rb	Pb	Cu	Ni	Zn	Zr	Y	Si	Al	Fe	Mg	Ca	Ti
146-1	168	88	19	4	2	32	20	3	31	12	5	2.13	0.27	68.23	0.04	0.11	37
146-2	128	1	2327	1007	1	14	37	12	7	30	6	1.01	0.49	46.99	0.08	3.73	2252
147-6	241	63	39	9	6	4	15	1	1	8	2	5.92	0.26	56.32	0.06	0.08	38
147-8	174	17	5	1	1	15	13	4	2	1	4	7.01	0.16	59.88	0.04	0.04	9
148-1	164	521	75	8	1	1	13	5	17	4	2	10.12	0.22	53.19	0.11	0.73	50
148-6	130	504	93	10	1	6	11	2	6	12	7	2.85	0.21	63.51	0.22	0.54	24
149-4	102	90	26	3	1	3	15	9	1	,7	3	14.77	0.19	44.39	0.04	0.73	68
• 149-6	91	58	105	7	1	14	2	16	2	4	6	7.65	0.20	57.06	0.08	1.06	19
150-8	185	85	241	22	3	10	19	3	1	4	10	11.34	0.16	54.23	0.14	1.07	54
150-16	412	172	45	12	2	18	23	6	10	12	9	3.75	0.32	62.32	0.04	0.43	74
• 151	282	690	132	3	1	19	12	, 5	2	4	10	3.78	0.21	64.49	0.07	0.13	26
151-7	108	203	72	7	1	4	9	3	6	5	11	5.15	0.38	58.90	0.04	0.90	38
• 152-2	270	35	16	6	1	16	9	8	1	1	3	3.41	0.15	67.73	0.04	0.06	9
152-3	222	58	810	26	3	12	29	2	11	4	5	2.53	0.23	60.72	0.04	0.19	111
153	87	42	78	4	1	8	4	4	1	10	5	11.53	0.15	54.12	0.06	0.07	23
154-4	230	33	11	15	1	1	12	5	6	4	2	5.15	0.21	62.93	0.04	0.05	19
154-6	95	23	69	4	1	5	19	4	1	23	2	7.83	0.16	61.19	0.03	0.05	13

TABLE A5 ANALYSES OF BOTRYOIDAL ORES, WEST CUMBERLAND OREFIELD

Sample No	As	Pb	Cu	Ni	Zn	Y	Mn	Ba	Sr	Rb	Zr	Ti	Si	Fe	Al	Ca	Mg
5-3	102	44	4	1	2	7	228	55	26	6	3	11	1.50	69.33	0.30	0.21	0.13
9-13	82	23	17	6	2	9	1994	23	10	1	5	1	0.42	65.31	0.37	2.65	0.04
• 12-5	95	43	1	1	1	-	357	23	6	-	-	53	1.91	67.91	0.34	0.16	0.11
• 16-12	362	37	11	3	8	11	714	1536	20	7	1	186	1.01	68.91	0.18	0.63	0.20
17-11	828	49	6	1	4	10	2114	152	22	1	14	18	2.13	63.19	0.35	1.82	0.49
23-14	654	34	4	1	4	1	290	36	7	5	8	2	1.73	67.96	0.32	0.09	0.09
28-3	1017	58	13	14	2	31	1392	37	7	3	4	9	1.05	68.73	0.23	1.18	0.38
• 32-20	369	19	16	13	3	9	142	1	9	5	1	7	1.03	69.62	0.26	0.09	0.13
35-6	182	41	7	1	1	3	344	267	14	6	6	12	1.45	68.40	0.27	0.12	0.09
• 38-19	895	37	14	8	7	11	307	54	12	3	12	103	0.91	67.81	0.21	0.08	0.04
39-1	985	58	22	1	12	5	764	57	7	5	1	103	0.51	68.67	0.27	0.11	0.03
42-30	1528	54	1	6	8	6	729	1935	17	1	4	25	1.49	67.15	0.32	0.71	0.09
76-1	344	46	13	7	7	4	122	11	7	9	1	5	0.60	68.40	0.27	0.08	0.03
• 76-3	481	42	12	4	7	8	123	15	7	3	3	12	0.77	68.38	0.23	0.59	0.22
77-1	552	47	5	6	23	14	200	27	6	1	7	3	1.36	69.74	0.18	0.04	0.09
78-2	283	51	1	3	6	2	269	39	5	3	1	4	1.55	68.82	0.25	0.21	0.16
81-2	348	86	18	10	12	13	1176	23	15	1	1	5	0.53	67.28	0.22	1.17	0.03
81-8	543	72	19	10	13	8	360	24	8	6	4	7	0.72	68.28	0.26	0.08	0.03
84-6	867	63	7	7	9	1	513	33	8	1	1	3	1.30	70.37	0.29	0.16	0.10
94A-7	308	72	1	7	7	3	363	41	31	4	9	33	1.81	67.78	0.34	0.14	0.11
95-1	348	57	6	4	10	5	230	25	15	13	3	3	1.83	67.20	0.40	0.16	0.13
104-29	241	33	1	7	3	1	229	87	6	3	5	1	1.34	68.44	0.22	0.11	0.10
105-6	413	40	9	10	1	15	559	35	31	3	5	5	1.56	65.58	0.29	1.75	0.03
107-1	392	28	20	14	8	9	194	1	7	7	1	1	1.07	70.34	0.14	0.04	0.08
115-7	418	40	4	6	4	1	248	33	10	3	10	7	1.30	69.75	0.29	0.16	0.08
117-4	600	52	1	1	10	1	344	15	8	8	1	1	1.39	69.22	0.34	0.15	0.13
119-4	222	44	1	1	5	2	506	18	25	2	9	2	1.46	67.96	0.30	0.92	0.11

• samples rejected at the 0.01 sig. level by L.D.F.A. ($\log_{10}$ data)

TABLE A5 continued

Sample No	As	Pb	Cu	Ni	Zn	Y	Mn	Ba	Sr	Rb	Zr	Ti	Si	Fe	Al	Ca	Mg
132-2	252	37	7	1	1	2	97	35	5	6	1	2	1.36	68.70	0.24	0.12	0.16
137	454	57	14	6	12	15	500	3137	116	3	14	351	1.01	65.13	0.57	0.13	0.07
140-1	538	71	22	11	12	12	878	14	15	3	4	15	0.72	65.63	0.28	2.07	0.03
150-18	603	39	4	1	5	4	302	500	17	1	4	8	1.37	66.76	0.27	0.71	0.06
152-4	870	55	10	5	3	7	938	1240	36	4	13	17	1.47	66.91	0.27	0.55	0.11
232	1443	50	7	4	6	6	295	1440	50	2	2	17	1.30	67.91	0.29	0.14	0.04

TABLE A 6 ANALYSES OF ORES FROM VEINS IN THE LOWER PALAEOZOICS

	As	Mn	Ba	Sr	Rb	Pb	Cu	Ni	Zn	Zr	Y	Si	Al	Fe	Mg	Ca	Ti
Massive Haematites from veins in the Skiddaw Slate Series (pseudomassive)																	
51-1	132	923	1	4	6	29	13	13	7	1	5	2.32	0.38	66.64	0.04	0.04	26
51-3	534	2098	28	8	2	126	1	33	32	2	13	1.09	0.63	67.02	0.03	0.04	8
52-14	51	48	1	10	1	4	30	24	4	4	14	0.87	0.19	69.31	0.04	0.04	7
53-3	47	65	1	1	1	5	35	2	7	4	7	0.16	0.13	70.27	0.13	0.04	1
53-4	69	60	1	7	1	8	21	4	4	1	13	0.83	0.18	69.09	0.11	0.03	1
54-2	63	3170	53	4	7	64	16	10	7	2	11	1.14	0.34	70.01	0.27	0.04	30
54-9	45	1666	29	5	3	15	21	10	1	2	2	1.01	0.28	70.39	0.20	0.03	18
55-1	269	1294	70	7	5	43	18	11	11	2	12	3.55	0.44	62.57	0.07	0.06	14
56-2	285	119	10	4	6	27	24	33	2	3	12	1.00	0.34	68.73	0.44	0.06	6
57-2	110	1384	24	4	3	20	15	8	3	1	10	1.96	0.41	67.03	0.04	0.03	6
57-3	260	394	22	2	4	18	23	13	5	4	9	1.22	0.46	67.70	0.05	0.04	39
58-7	191	943	1	3	2	25	44	12	12	1	11	1.73	0.36	68.52	0.29	0.04	1
158-4	244	1600	8	9	1	50	23	7	10	1	39	0.90	0.43	69.25	0.03	0.04	2
158-9	100	607	13	6	1	32	14	4	9	3	20	5.31	0.32	61.28	0.03	0.06	5
159-9	95	3526	166	2	1	27	4	13	14	4	9	1.03	0.44	67.53	0.14	0.04	45
159-14	101	4100	18	5	7	8	32	33	10	1	9	2.22	0.36	67.64	0.08	0.03	3
160-2	186	292	5	6	1	18	18	46	7	6	9	0.97	0.31	70.41	0.19	0.04	1
160-3	120	347	2	8	1	22	15	10	5	7	32	1.56	0.25	68.43	0.28	0.03	1
161-3	150	1209	18	6	1	47	16	11	7	1	12	1.37	0.44	68.49	0.04	0.03	32
162	95	279	25	3	3	17	9	9	6	1	16	2.28	0.30	64.90	0.03	0.05	3
162-2	153	679	100	11	2	19	12	12	7	1	18	1.74	0.46	66.24	0.03	0.04	14
163-2	814	3285	20	7	9	290	21	57	18	4	12	1.59	0.51	63.37	0.89	2.06	28
Botryoidal Haematites from veins in the Eskdale granite																	
63-3	2024	1275	1	21	8	60	16	20	10	3	28	1.03	0.46	67.46	0.03	0.09	76
63-8	1437	866	48	11	1	55	14	12	11	1	6	0.43	0.20	69.85	0.03	0.06	12
64-19	1231	405	35	12	7	475	11	26	106	4	12	0.69	0.34	68.30	0.03	0.06	7
71-7	1480	6733	1	28	7	431	13	17	103	8	29	1.88	0.30	53.93	4.35	6.07	1

TABLE A6 continued

	As	Mn	Ba	Sr	Rb	Pb	Cu	Ni	Zn	Zr	Y	Si	Al	Fe	Mg	Ca	Ti
Massive Haematites from veins in the Eskdale granite (pseudomassive)																	
48-4	112	410	39	4	9	30	18	3	3	6	15	3.08	0.69	62.93	0.06	0.04	50
61-3	92	607	13	1	3	11	10	11	4	5	15	6.61	0.23	59.41	0.10	0.06	8
61-33	32	4679	27	4	1	6	1	7	3	38	16	27.77	0.12	31.29	4.48	4.22	3
64-17	415	281	25	4	1	124	32	7	31	13	13	1.16	0.36	70.14	0.27	0.05	1
64-19	110	113	19	5	15	14	79	6	7	12	25	5.35	0.54	58.28	0.03	0.08	32
65-11	590	345	36	10	3	107	83	15	70	18	3	1.08	0.36	71.06	0.18	0.06	6
65-27	1088	362	25	16	4	174	142	18	117	19	10	1.28	0.42	66.18	0.03	0.07	8
65A-3	1355	990	19	10	1	297	24	12	97	13	19	1.50	0.48	65.57	0.04	0.11	18
66-1	753	426	6	14	5	160	36	12	126	17	18	2.21	0.44	67.14	0.10	0.05	6
66-4	715	402	26	10	2	178	23	6	82	13	13	1.89	0.39	67.53	0.04	0.04	13
68-4	163	342	14	3	3	20	35	11	23	4	9	4.02	0.36	61.33	0.10	0.07	10
68-21	1095	741	23	13	8	497	66	5	92	6	21	1.89	0.38	68.93	0.15	0.08	1
69-7	1056	603	13	12	2	207	43	20	99	4	12	10.65	0.31	52.63	0.03	0.09	11
69-20	1112	317	1	8	1	249	29	20	97	17	8	3.35	0.27	65.49	0.03	0.07	11
70-1	397	407	1	6	5	68	35	6	40	4	11	0.54	0.39	67.26	0.03	0.24	5
70-3	95	132	2	7	6	14	12	4	8	1	6	5.25	0.42	57.19	0.03	0.20	5
Massive Haematites from veins in the Borrowdale Volcanics Series (pseudomassive)																	
44-4	85	464	75	1	20	19	9	3	13	50	57	5.17	1.01	58.28	0.08	0.09	164
44-10	61	236	95	7	20	18	18	6	14	26	13	5.96	0.99	57.80	0.08	0.07	190
45-1	115	199	3	5	13	17	9	8	7	10	25	9.51	0.50	53.19	0.13	0.12	30
45.21	166	382	36	6	12	8	10	5	7	18	29	8.34	0.80	54.95	0.26	0.07	66
46	119	447	1	9	4	10	11	17	5	4	9	5.73	0.49	60.35	0.08	0.08	86
[illegible]	106	263	2	8	5	21	5	1	6	11	9	1.85	0.06	66.66	0.03	0.10	103
[illegible]	153	438	1	11	1	27	12	11	5	10	5	11.36	0.26	46.54	0.20	0.46	10
[illegible]	233	631	17	7	1	9	4	15	2	4	8	14.28	0.20	50.49	0.03	0.45	9

TABLE A7 ANALYSES OF MASSIVE ORES, MILLOM-FURNESS OREFIELD

Sample No	As	Mn	Ba	Sr	Rb	Pb	Cu	Ni	Zn	Zr	Y	Si	Al	Fe	Mg	Ca	Ti
168	28	221	3	1	1	1	8	4	8	9	1	3.13	0.37	61.31	0.06	1.37	116
168-15	34	48	1	8	3	6	15	1	4	9	1	2.79	0.36	63.26	0.05	0.19	89
170-1	37	151	1	4	1	1	15	13	8	17	5	4.23	0.34	61.20	0.15	0.51	181
170-2	29	229	7	1	1	1	9	4	8	12	3	3.75	0.32	61.23	0.04	0.53	94
171-1	29	735	1	10	1	3	1	15	5	3	1	1.46	0.26	58.23	0.03	5.42	24
171-8	42	589	7	3	1	11	7	7	5	6	4	3.11	0.22	57.81	0.04	4.34	20
172-10	60	930	29	23	1	13	16	36	6	206	5	8.03	0.48	45.11	0.08	2.49	402
173-1	66	1296	10	2	1	7	13	3	5	14	6	1.32	0.44	57.79	0.03	5.60	154
173-4	76	1026	22	2	3	15	12	6	9	10	4	1.34	0.31	59.80	0.04	4.48	71
174-22	140	297	8	1	1	14	8	10	3	8	4	5.02	0.29	59.98	0.04	0.09	77
174-25	122	228	5	4	1	2	14	11	6	12	12	8.26	0.22	52.86	0.12	0.32	35
175-1	27	141	16	1	10	16	18	5	14	4	2	0.94	0.26	69.38	0.04	0.55	5
176	37	1223	33	3	2	7	23	11	2	1	1	5.36	0.19	59.08	0.05	0.07	13
176-10	53	70	14	2	1	15	24	8	1	3	10	1.13	0.30	68.93	0.05	0.07	16
177-2	68	584	32	1	1	2	24	14	4	2	6	0.34	0.32	69.13	0.11	0.07	6
178-1	2130	4149	114	19	1	430	1	114	158	2	20	0.53	0.30	43.96	0.03	9.22	22
179-8	42	1063	37	6	4	35	51	1	10	8	3	1.30	0.41	69.60	0.04	0.15	55
179-18	48	752	24	1	1	1	23	5	9	16	3	0.43	0.31	66.78	0.03	1.19	101
180-4	25	96	17	2	2	6	27	28	6	43	16	2.96	0.36	63.84	0.12	0.10	222
180-6	23	40	7	1	14	15	14	1	6	26	2	0.57	0.25	57.65	0.03	0.07	93
181-2	1007	307	5	9	2	200	21	27	67	17	5	1.75	0.25	68.36	0.11	0.06	23
181-5	513	514	13	4	2	156	21	14	21	6	3	1.63	0.22	66.39	0.04	1.28	5
183-5	30	4636	41	11	1	13	15	17	1	4	9	1.27	0.27	28.68	0.14	5.01	6
184-3	36	477	9	3	1	10	7	4	7	3	4	0.82	0.22	65.56	0.04	3.35	10
186-1	36	2456	48	14	1	4	12	6	1	1	8	1.51	0.28	47.53	0.09	5.63	9
187-2	410	428	13	5	1	75	6	19	63	6	1	8.09	0.22	54.45	0.03	2.04	13
188-2	21	46	2	1	1	5	1	1	1	5	3	3.76	0.21	63.05	0.11	0.11	30
189-4	178	138	8	1	1	23	10	6	11	3	6	0.76	0.22	71.36	0.07	0.04	3

TABLE A7 continued

Sample No	As	Mn	Ba	Sr	Rb	Pb	Cu	Ni	Zn	Zr	Y	Si	Al	Fe	Mg	Ca	Ti
191-1	35	77	14	1	1	3	15	1	8	5	1	1.41	0.24	66.94	0.10	0.07	10
191-9	26	45	19	1	1	6	17	1	2	4	5	1.24	0.27	68.82	0.08	0.08	14
192-1	42	98	2	3	1	14	17	1	6	28	3	3.92	0.29	60.06	0.04	0.19	151
192-15	45	41	1	1	1	2	16	3	8	26	1	3.29	0.27	63.43	0.04	0.27	93
193-9	25	150	19	2	4	8	14	4	8	5	2	3.13	0.21	66.37	0.09	0.09	3
194-2	73	1007	10	7	1	49	18	6	13	19	25	1.43	0.57	67.85	0.08	0.22	159
194-3	118	7767	117	12	1	99	28	9	27	11	39	2.60	0.26	65.55	0.07	0.17	22
196-15	63	362	1	3	2	23	10	6	3	17	12	1.27	0.35	67.81	0.05	0.11	49
196-27	25	94	1	1	1	1	10	1	7	11	5	3.55	2.29	63.00	0.04	0.31	62
197-3	55	111	1	6	1	7	8	1	7	23	8	2.42	0.27	64.81	0.04	0.06	82
197-5	51	111	1	1	1	16	10	15	10	18	6	2.46	0.25	64.94	0.10	0.05	57
198-1	54	785	1	9	1	1	1	3	6	13	5	1.00	0.34	66.40	0.04	2.00	77
198-10	73	1326	10	1	2	6	18	4	9	3	1	1.17	0.37	60.95	0.05	4.50	69
199-2	95	1095	8	9	1	16	15	28	1	25	5	2.54	0.42	52.40	0.03	6.69	110
199-5	50	1837	33	10	1	3	1	8	1	4	13	4.27	0.42	48.25	0.08	5.88	88
200-2	107	229	1	1	1	10	22	4	1	2	4	0.57	0.21	67.88	0.03	0.51	4
200-9	469	704	1	10	1	60	24	31	28	6	5	3.94	0.26	61.28	0.05	2.07	23
202-10	1523	332	2	8	1	62	14	38	32	4	10	0.90	0.22	71.32	0.04	0.22	14
203-1	823	663	3	7	1	33	72	29	120	7	1	0.31	0.30	68.61	0.03	0.34	3
204-9	12	24	4	1	1	3	8	7	5	5	2	3.84	0.23	64.31	0.10	0.07	54
204-10	20	26	1	1	1	4	11	6	6	2	2	5.67	0.24	59.71	0.07	0.16	33
205-1	83	360	1	1	1	6	4	27	9	10	1	3.36	0.29	62.91	0.23	0.56	68
205-7	137	240	1	5	2	17	50	19	18	15	9	3.41	0.44	62.58	0.19	0.78	381
206-12	103	54	2	4	2	3	3	6	6	9	5	4.44	0.37	61.07	0.04	0.12	111
206-15	108	145	1	6	2	3	1	6	12	15	3	4.77	0.28	59.35	0.07	0.29	88
207-9	1114	470	9	6	1	478	26	36	119	2	5	2.29	0.29	62.23	0.16	2.22	1
208-2	43	7035	159	1	1	13	11	6	15	67	6	1.32	0.33	69.01	0.16	0.06	205

TABLE A7 continued

Sample No	As	Mn	Ba	Sr	Rb	Pb	Cu	Ni	Zn	Zr	Y	Si	Al	Fe	Mg	Ca	Ti
208-4	60	170	4	1	3	2	31	2	8	15	3	2.48	0.31	64.37	0.13	0.31	137
209-1	92	192	1	1	1	14	19	1	10	4	3	1.77	0.32	66.07	0.11	1.11	48
209-9	40	939	17	2	1	1	13	1	15	13	1	0.86	0.28	62.46	0.06	4.30	81
210-5	56	49	17	7	4	11	4	28	5	5	6	16.57	0.16	52.01	0.10	0.05	4
210-7	121	71	1	2	4	198	67	12	4	7	8	1.69	0.30	64.78	0.10	0.06	38
211-20	82	240	21	1	1	19	15	51	23	2	4	4.12	0.37	65.08	0.04	0.07	44
212-2	20	6	13	3	1	11	2	16	1	1	1	10.20	0.18	50.47	0.04	0.48	33
214-10	915	2312	62	6	3	245	30	40	86	9	8	0.62	0.40	67.74	0.03	0.09	17
215-1	93	77	14	3	1	9	11	4	2	40	3	9.25	0.49	54.73	0.13	0.09	778
216-1	56	373	8	1	1	4	7	2	9	2	4	1.13	0.21	62.09	0.19	4.49	33
217-2	57	117	43	4	1	9	17	8	5	2	10	5.60	0.34	57.88	0.19	0.06	67
217-3	73	1689	7	6	2	22	20	7	4	17	2	1.68	0.37	61.25	0.67	3.20	238
219-3	64	411	84	3	1	13	15	13	10	12	9	7.28	0.36	55.98	0.23	0.06	157
220-2	54	102	4	8	1	13	11	8	10	6	16	1.19	0.33	70.48	0.04	0.07	76
220-4	75	439	12	1	1	5	8	40	8	8	8	1.24	0.24	70.02	0.09	0.05	28
221-3	85	218	29	8	1	9	11	13	9	10	23	1.60	0.33	66.18	0.03	0.07	106
222-1	101	139	99	28	1	28	23	14	4	5	9	3.74	0.29	64.19	0.07	0.07	115
222-16	256	231	1	9	2	27	12	17	14	7	10	1.54	0.40	66.13	0.13	0.11	44
223-2	63	77	7	1	1	2	1	11	1	8	4	10.08	0.26	52.38	0.08	0.06	130
223-3	48	36	5	1	1	9	9	10	2	8	3	11.17	0.20	52.58	0.04	0.05	93
224-3	130	461	95	1	1	21	12	8	9	9	17	1.66	0.38	67.18	0.06	0.08	110
224A-1	118	265	444	4	1	38	12	10	15	9	18	2.91	0.43	62.00	0.03	0.10	178
225-5	478	216	10	2	1	179	16	73	70	9	4	2.70	0.30	66.55	0.20	0.08	48
226-1	17	26	18	1	1	12	4	9	4	1	4	8.77	0.22	55.31	0.07	0.07	15
227-1	52	784	1	7	4	1	20	9	7	1	1	2.73	0.23	65.98	0.12	0.37	24
227-6	272	220	1	6	1	27	11	3	7	6	6	2.74	0.22	66.70	0.08	0.07	31
228-3	223	479	9	6	1	15	16	1	6	12	7	3.50	0.21	62.75	0.03	0.42	104
229-1	33	93	1	1	1	7	8	7	3	8	4	2.58	0.26	63.94	0.07	0.05	25
230-5	142	540	1	5	1	14	20	11	14	3	1	1.83	0.30	62.50	0.05	1.57	42
230-11	45	409	9	2	2	6	19	5	6	3	4	4.19	0.30	25.59	0.06	0.11	34

TABLE A8 ANALYSES OF BOTRYOIDAL ORES, MILLOM-FURNESS OREFIELD

Sample No	As	Mn	Ba	Sr	Rb	Pb	Cu	Ni	Zn	Zr	Y	Si	Al	Fe	Mg	Ca	Ti
212	1589	320	1	14	1	62	19	7	17	1	5	0.96	0.19	70.05	0.04	0.22	5
213-2	2665	363	1	18	1	86	8	9	24	9	3	1.00	0.23	69.09	0.04	0.07	5
214-13	3398	816	20	14	1	104	17	8	31	4	2	0.33	0.23	68.67	0.03	0.08	13
215-1	1343	159	1	8	6	40	17	13	10	1	4	1.30	0.29	68.42	0.04	0.05	34
215-4	4424	806	43	65	3	162	16	5	39	7	7	0.96	0.28	69.14	0.04	0.26	29
219-2	1127	781	26	10	2	64	7	5	14	1	5	0.35	0.17	68.33	0.05	0.06	14
221-4	883	165	1	7	1	49	4	10	9	2	9	0.32	0.15	69.32	0.03	0.05	9
224-2	849	206	7	7	1	74	32	77	9	3	3	0.68	0.30	67.85	0.03	0.52	12
225	712	307	1	8	2	47	6	7	10	5	2	0.95	0.16	69.95	0.06	0.42	1
228-4	1268	816	22	7	1	75	14	11	30	4	10	1.02	0.21	66.97	0.04	1.87	9

ANALYSES OF THE GRANITE SAMPLES

Sample No	SiO_2 %	Al_2O_3 %	Tot. Fe %	MgO %	CaO %	Na_2O %	K_2O %	TiO_2 %	MnO %
G.1	76.42	15.20	2.12	0.35	0.38	3.35	5.17	0.24	0.00
G.2A	77.91	15.22	1.29	0.10	0.09	3.53	5.30	0.12	0.00
G.2B	76.32	15.01	1.61	0.08	0.13	3.63	5.20	0.13	0.04
G.3	75.72	15.03	1.95	0.27	0.45	3.33	5.02	0.21	0.03
G.4	77.36	14.97	1.30	0.13	0.14	3.91	5.10	0.12	0.01
G.5	75.59	15.36	2.21	0.32	0.29	3.32	4.98	0.23	0.03
G.6	76.39	15.15	2.30	0.26	0.29	3.40	5.16	0.21	0.02
G.7	77.77	14.56	1.99	0.23	0.19	3.36	5.00	0.19	0.03
G.9	75.79	14.46	1.49	0.37	0.23	8.29	0.03	0.24	0.02
G.10	75.29	15.06	1.15	0.68	0.30	8.34	0.15	0.29	0.01
G.14	78.13	15.06	0.55	0.16	0.13	3.41	5.13	0.10	0.00
G.26	66.11	15.68	5.25	1.59	2.34	3.23	4.82	0.67	0.14
G.27	66.77	16.63	5.20	1.49	1.49	3.15	4.29	0.72	0.18
G.28A	67.35	12.69	0.87	0.20	0.00	2.87	4.22	0.10	0.00
G.28B	75.85	15.20	2.02	0.24	0.15	3.57	4.96	0.16	0.03
G.29A	77.82	15.15	0.82	0.16	0.11	3.53	5.41	0.13	0.00
G.29B	76.68	14.95	1.68	0.12	0.27	3.61	4.92	0.12	0.01
G.29C	78.78	15.12	0.74	0.17	0.21	3.72	5.08	0.13	0.00
L.D.264	74.15	14.86	1.13	0.48	1.15	3.25	0.00	0.38	0.02
L.D.265	73.28	14.93	1.52	0.49	1.04	3.07	0.13	0.48	0.03

TABLE A9

TABLE A9 continued

Sample No	Ba ppm	Zr ppm	Y ppm	Sr ppm	Rb ppm	Zn ppm	Cu ppm	Ni ppm	As ppm	Pb ppm
G.1	195	126	27	42	343	50	2	7	1	29
G.2A	1	78	27	13	526	14	2	5	4	12
G.2B	9	83	26	8	493	73	3	6	6	21
G.3	119	121	27	37	364	28	4	5	10	20
G.4	9	82	28	21	453	19	1	5	1	15
G.5	146	132	34	26	387	51	4	8	38	20
G.6	120	113	19	34	382	22	1	7	1	22
G.7	79	105	25	23	390	34	3	6	12	19
G.9	1	184	25	55	8	1	1	2	1	4
G.10	1	170	31	73	16	13	1	4	1	9
G.14	130	63	21	26	382	7	2	3	1	8
G.26	916	255	30	226	140	45	30	10	2	11
G.27	795	282	50	258	207	104	30	9	12	34
G.28A	88	83	22	33	368	17	1	3	2	10
G.28B	53	96	30	28	358	41	3	3	35	17
G.29A	60	85	21	35	414	5	1	4	3	7
G.29B	71	79	20	16	450	20	1	4	11	8
G.29C	60	85	24	38	405	5	1	5	22	12
L.D.264	1	349	36	91	5	4	1	3	1	6
L.D.265	1	346	53	82	10	5	1	4	1	5